The Natural and Industrial Cycling of Indium in the Environment

by

Sarah Jane O'Connell White

B.A., Princeton University (2002)

Submitted to the Department of Civil and Environmental Engineering
in partial fulfillment of the requirements for the degree of

Doctor of Philosophy in the field of Environmental Chemistry

at the

MASSACHUSETTS INSTITUTE OF TECHNOLOGY

June 2012

Author .....
Department of Civil and Environmental Engineering
May 4, 2012

Certified by .....
Harold F. Hemond
William E. Leonhard Professor of Engineering
Professor of Civil and Environmental Engineering
Thesis Supervisor

Accepted by .....
Heidi M. Nepf
Chair, Departmental Committee for Graduate Students

The Natural and Industrial Cycling of Indium in the Environment

by

Sarah Jane O'Connell White

Submitted to the Department of Civil and Environmental Engineering
on May 4, 2012, in partial fulfillment of the
requirements for the degree of
Doctor of Philosophy in the field of Environmental Chemistry

Abstract

Indium is an important metal whose production is increasing dramatically due to new uses in the rapidly growing electronics, photovoltaic, and LED industries. Little is known, however, about the natural or industrial cycling of indium or its environmental behavior. Industrial emissions of indium are already larger than natural emissions. A review of the literature suggests that metal smelting and coal burning are the primary industrial sources of indium to the environment, while releases from the semiconductor and electronics industries are small at present. This scenario may change with the rapid growth of indium use in the electronics and semiconductor industries.

Studies were conducted on indium cycling in the atmosphere, indium deposition to a peat bog over the past century, and indium behavior in a creek influenced by acid mine drainage. Atmospheric indium concentrations in the northeastern United State vary from <0.7 to 8 pg/m^3, with significant differences geographically and temporally. Atmospheric back trajectories, correlation of indium to other metals in these samples, and receptor modeling suggest that the highest indium concentrations come from nonferrous smelters in the north, while lower concentrations are seen in air traveling from the midwestern US. Fluxes of indium to Thoreau's Bog in Concord, MA, began increasing in the early 1900s, well before indium was used significantly in industry, and are likely the result of emissions from nonferrous smelting and coal combustion. Fluxes peaked in the 1970s, and have been decreasing until the present, likely reflecting the advent of particulate emissions controls in the US and Canada. Acid-mine drainage contributes indium concentrations 10^4 times higher than natural freshwaters to Mineral Creek, Colorado, and all of this indium exists in the dissolved phase. During an experimental raising of the pH of this system, essentially all of the indium associates with the particulate phases, primarily due to sorption to iron-oxides.

Knowledge of the anthropogenic and natural cycling of indium can lead to a greater understanding of the environmental impacts and human health effects of this metal. With further study, this understanding may lead to pollution prevention, and allow informed decision making about indium's use, handling, and disposal.

Thesis Supervisor: Harold F. Hemond
Title: William E. Leonhard Professor of Engineering
Professor of Civil and Environmental Engineering

Acknowledgments

Thanks to my advisor, Harry Hemond. I admire his insatiable curiosity, enthusiasm for science, dedication to his students' research and development as scientists, and his understanding that it is important to pursue some of the many wonderful diversions outside of research that life provides. I have learned a great deal from him, both about science and life, and will strive to follow the example that he has set.

I am indebted to my committee members, Phil Gschwend and Ed Boyle. Phil strives every day to make the world a tangibly better place. I hope to someday teach, learn, and argue with as much passion as he does. This project was his brainchild, and I am thankful for his foresight and guidance from the very beginning. I thank Ed for teaching me about trace-metal analysis, for giving so generously of his lab space, materials, expertise, and time, and for embracing my project and helping it to grow.

I had many sources of funding that made this project possible, including a National Science Foundation Grant, an MIT Earth Systems Initiative Linden Graduate Fellowship, an MIT Energy Initiative Martin Family Graduate Fellowship for Sustainability, an MIT Earth Systems Initiative Ignition Grant, and support from the SRC/Sematech Engineering Research Council for Environmentally Benign Semiconductor Manufacture. Additionally, undergraduates who worked on this thesis were funded by MIT's Undergraduate Research Opportunities Program and the MIT Energy Initiative Martin Family Society funding for undergraduate research.

I was lucky enough to collaborate with many amazing researchers during the course of this thesis, including Katie Walton-Day, Rob Runkel, Briant Kimball, Andrea Foster, Cynthia Hines, Ajay Somani, Duane Boning, Paudely Zamora, Patricia Burkhart, Vicky Diadiuk, Tim Yeakley, and Mansooreh Dehghani. Alan Shiller has been helpful in locating interesting samples for indium measurements, and is a fellow connoisseur of strange and interesting metals. I am grateful to those who provided me with samples and data, including Daniel Pedersen, John Durant, Lynn Salmon, Dominic Cianciarelli, Ed Sholkovitz, and Bill Linak. I am also indebted to the many people who helped me with field work, including Amy Mueller, Charu Varadharajan, Desiree Plata, Dave Kuo, Hanan Karam, Jennifer Apell, and Robin Zhao.

My previous advisors and mentors, Satish Myneni and Carol Kumamoto, gave me research experiences that inspired me to pursue a Ph.D, and provide me with continued support and inspiration.

I was lucky enough to work with many amazing undergraduates during my graduate work. Katherine Orchard, Maria Duaime, Carrie Keach, Laurie Kellndorfer, and Fatima Hussain were great colleagues to have in the lab, taught me a great deal about research and mentorship, and contributed a substantial amount to this thesis.

I developed an outreach exhibit about the life-cycle of metals in consumer electronics during my dissertation. I could not have done this without the help of Kathy Vandiver, Ingrid Chaires, and the many volunteers who helped to present the exhibit.

I am indebted to the members of Supergroup, who taught me what it means to ask the tough questions, and always pushed me to make my work better. In addition to providing intellectual and scientific rigor, Supergroup members have been great friends, and bake celebratory cakes that rival any I've ever seen. Thanks to Charu Varadharajan, Matt Orosz, Amy Mueller, Schuyler Senft-Grupp, Irene Hu, Loretta Fernandez, Desiree Plata, Xanat Flores-Cervantes, Dave Kuo, Dave Griffith, Patricia Tcaciuc, Elizabeth Finn, Jenn Apell, Daniel Prendergast, Jordon Hemingway, Eben Cross, James Hunter, Anthony Carrasquillo, Kelly Daumit, Sean Kessler, Becca Neumann, Hanan Karam, Mason Stahl, and Ben Scandella. John MacFarlane was a life saver on more than one occasion. His generosity, expertise, and good humor were invaluable.

The Boyle lab: Rick Kayser, Jong-Mi Lee, Jess Fitzsimmons, Gonzalo Carrasco, and Simone Moos, welcomed me into their lab, and shared their time, talents, and trace-metal-grade acid. I appreciate their generosity and friendship.

Parsons is an amazingly welcoming community that I do not expect I'll find many other places in my career. I thank the people who keep things running and give freely of their time and energy: Sheila Frankel, Vicki Murphy, Jim Long, Gayle Sherman, and Joanne Batziotegos. Thanks also to everyone in building 1 whose behind-the-scenes work is indispensable.

I have had a great group of friends and co-conspirators during graduate school. My office, the208, was a place of great focus as well as amusing diversions. The Quad: Gaj Sivandran, Dave Griffith, and Sean Clarke, provided the right feng shui for finishing a thesis. Becca Neumann is a great friend and has been a source of research inspiration over the years. Anne Thompson, Amy Mueller, and Bec Gianotti are generous, inspiring, and provide wonderful distractions.

Thanks to my parents for instilling in me a love of science, and for being proud of every one of my accomplishments. I have been lucky enough to live in the same city as my brothers and their families for the past 10 years, and to have inherited a supportive and loving extended family. Thanks to Dan, Lise, John, Maren, Eliza, Andrew, MC, Krista, Franklin, Hazel, Becky, Bill, Tyler, and Rina.

I owe the biggest thanks to my husband, Will. Not only has he kept me well-fed and seen me through times of frustration, but he also contributed a great deal to the scientific content of this thesis by asking tough questions, helping with derivations, teaching me Matlab, and contributing ideas to make the work better. I am blessed to have found such an amazing partner, and look forward to the many more adventures that lay ahead.

Contents

List of Figures

List of Tables

Chapter 1

Introduction

The world is on the brink of an energy revolution, in which electrical power—produced, controlled, and transformed in significant part by semiconductor devices—will be increasingly important. New semiconductor manufacturing processes, resulting in lower-cost photovoltaics, more-efficient light-emitting diodes (LEDs), and better power electronics devices (such as have helped to enable large-scale wind power development), are critical to this revolution.

The development of new semiconductors will likely require the use of new materials, potentially in large quantities. A majority of the metals in the periodic table are now being considered for use in research or commercial-scale semiconductor fabrication (Figure 1-1, [David, 2005]). All of these metals come from, and ultimately return to, the environment in various forms, yet little is known about the environmental behavior or toxicology of many of them. Will there be surprises that threaten the environmental sustainability of new technologies, like those in the past that utilized lead and mercury? Can adverse environmental impacts be anticipated? Can industry be proactive, rather than be forced to reactively develop new processes in response to environmental problems and consequent regulations? Given the rapid and compelling growth of new semiconductor material applications, industry and government will benefit from incorporating environmental sustainability information *a priori.*

The study of anthrobiogeochemical cycles, the flow of materials through industry and the environment, may provide a key to the early environmental assessment of new industrial materials. Classically, these two components have been separated, with industrial ecologists

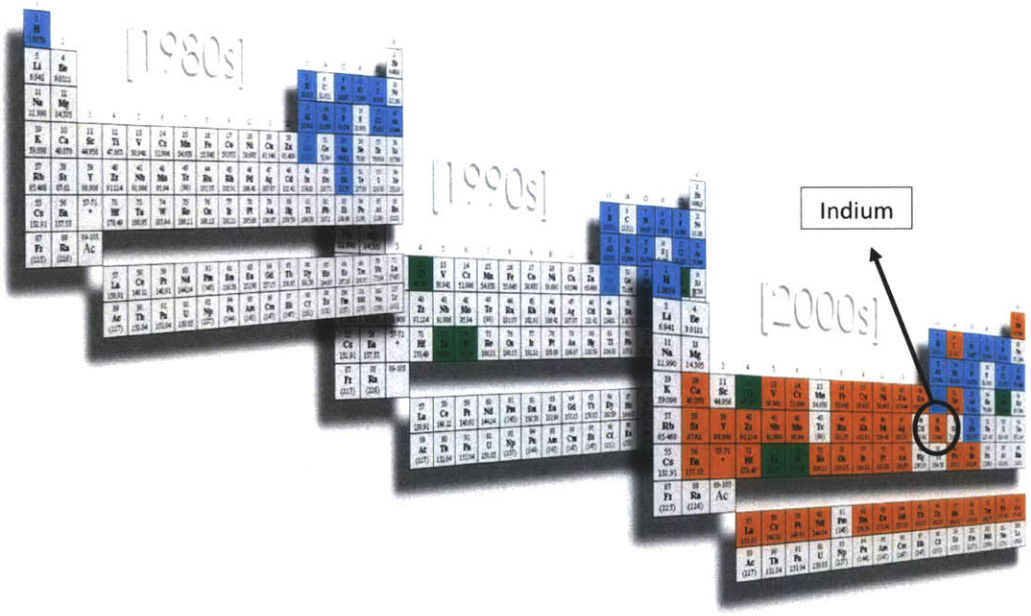

Figure 1-1: While only a dozen elements of the periodic table were used in semiconductor technologies in the 1980s, nearly the whole periodic table was employed in semiconductor technology or research by the 2000s. Figure from David [2005].

focusing on industry and geochemists focusing on the environment. Yet, accounting for both components is critical for a complete understanding of potential environmental impacts. For example, Klee and Graedel [2004] noted that when an element's anthropogenic fluxes, or industrial flows, become comparable to its natural fluxes, it has a high probability of adversely impacting organism and human health, and should be flagged for priority study as a potentially harmful element. Natural cycling includes processes such as weathering, windborne or waterborne transport, volcanism, and biological uptake. The industrial life-cycle of a metal includes mining and smelting, manufacture, the product lifespan, and end-of-life disposal or recycling. To accurately predict the environmental impacts of a particular metal, the entire industrial life-cycle must be evaluated, taking particular care to assess the amount of the metal that escapes from the product stream to the environment in mobile forms. This concept of calibrating to natural fluxes is particularly useful for assessing the impact of metals newly introduced to mass industrial use, for which few of the toxicological and ecotoxicological effects have been established.

In the absence of detailed toxicological studies, the likelihood of adverse effects of elements can be gauged by comparing anthropogenic fluxes and concentrations to natural values [e.g. Nriagu, 1996, Pacyna and Pacyna, 2001, Klee and Graedel, 2004]. In the case of metals, it is suggested that toxicity is most likely to result when the concentrations with which organisms have evolved are suddenly changed. Garrels et al. [1975] have noted that US drinking water standards for a variety of metals linearly correspond to the natural stream concentrations of those metals, suggesting that adverse human health impacts can begin to occur when natural levels are significantly exceeded. Lead and mercury are two examples of metals whose global anthropogenic fluxes significantly exceed their natural fluxes [Klee and Graedel, 2004], and both have come under severe regulatory constraint as a result of demonstrated toxicity (Figure 1-2). A drinking water standard for indium has not been set, but there is already evidence that industrial releases are exceeding natural fluxes.

While evaluations that do not distinguish between scales of flux or speciation of metals are important at the outset of study, it is critical to understand the physical and chemical speciation of a metal in order to thoroughly understand its transport and subsequent bioavailability. For example, Klee and Graedel [2004] consider the total flux of a metal in rivers to be both the dissolved and particle-associated metal. However, the particle-bound metal may be more likely to settle out, and may be less accessible to organisms, than the

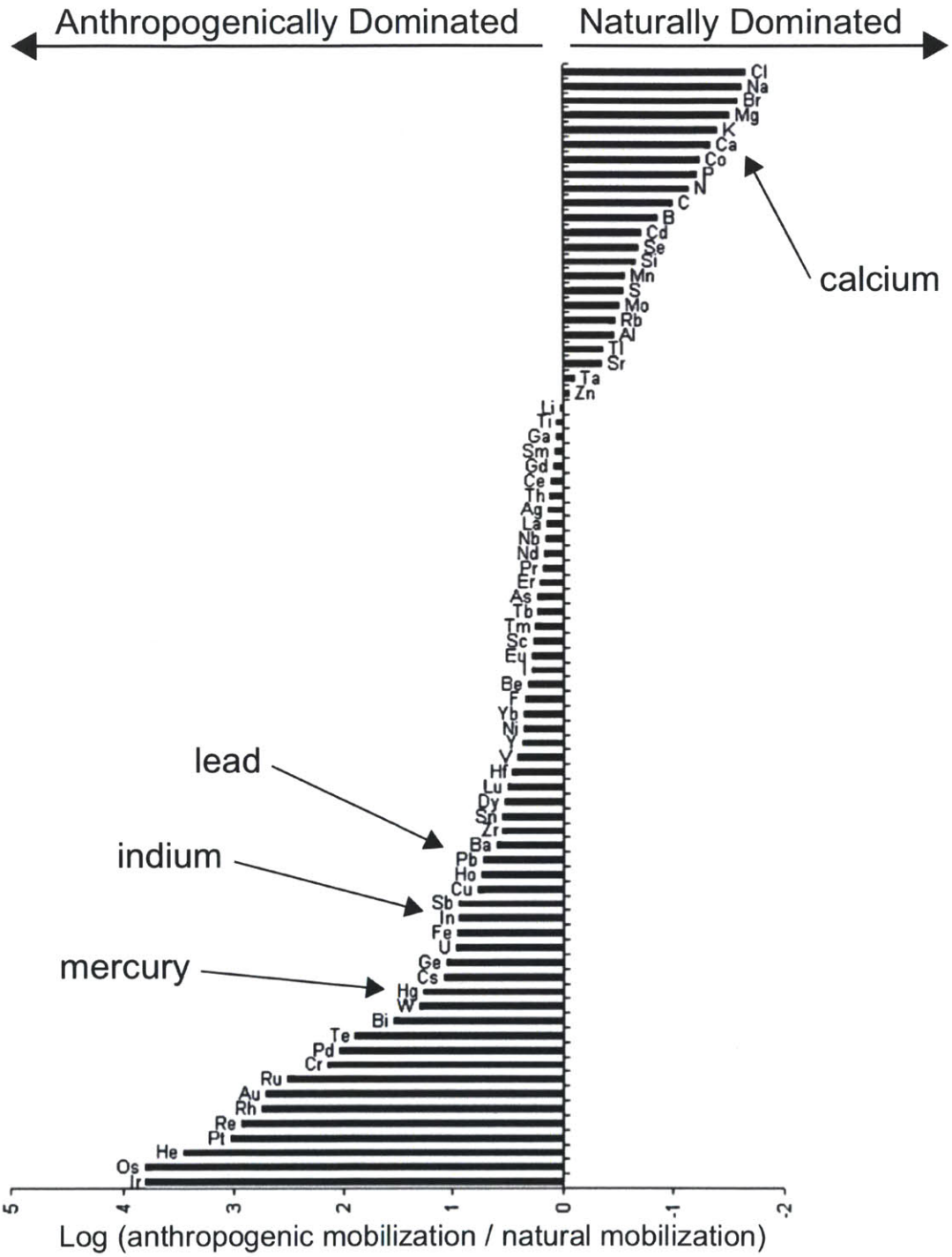

Figure 1-2: Klee and Graedel [2004] suggest that an element can be flagged as potentially harmful when its anthropogenic fluxes significantly exceed its natural fluxes. Figure republished with permission of Annual Reviews, from Klee, R.J., and T.E. Graedel (2004) Elemental Cycles: A Status Report on Human or Natural Dominance. *Annu. Rev. Environ. Resour.* 29:69-107; permission conveyed through Copyright Clearance Center, Inc.

dissolved phase. The particle-bound metal population has differences within it: a metal may behave very differently depending on whether it is bound in the silicate structure or sorbed to the surface. Additionally, the dissolved metal may itself have varying degrees of bioavailability, depending on its complexation and partitioning.

Therefore, one key to understanding the environmental and health impacts of a poorly studied metal is to examine its industrial life cycle in the context of its natural geochemical cycling, with a focus on the chemical and physical forms that it takes. This thesis focuses on the natural and industrial cycling of indium, a metal whose use is increasing rapidly, but whose environmental impacts are poorly understood.

1.1 Indium

World production and industrial usage of indium has increased 10-fold over the past 30 years, and is poised to expand even more dramatically, potentially by several orders of magnitude, over the next 20 years. Yet little is known about indium's environmental behavior or toxicity, both of which are needed to plan carefully for its industrial use, and to evaluate product and process sustainability.

Indium is used in indium tin oxide (ITO) coatings for electronic displays (flat panel, liquid crystal, etc.) [Jorgenson and George, 2005], and in new families of high efficiency photovoltaic cells [Anonymous, 2008] and LEDs [Nakamura et al., 1994]. Considerable increases in these uses are expected in the near future; the LED market grew by 300% between 2001 and 2004 [Whitaker, 2007], and the photovoltaic (PV) market is predicted to grow 1000-fold by 2030 [Hoffmann, 2006]. Novel demands such as ITO electrodes in the catalytic splitting of water may further drive demand for indium [Kanan and Nocera, 2008]. Nano-scale applications of indium also may grow in quantum dot applications [e.g. Ohkouchi et al., 2004], and in flexible displays and solar panels [e.g. Devi et al., 2002]. Thus there is significant potential for massively increased indium use.

Increased industrial use often, but not always, translates into increased environmental concentrations. Increased environmental concentrations of indium have been observed. For example, a 100-fold difference in groundwater concentrations of indium has been observed between a semiconductor industrial park and a neighboring site in Taiwan (9 μg/L versus 0.01 μg/L) [Chen, 2006]. Additionally, there is evidence that acute exposure to indium,

particularly in occupational settings, can cause significant lung toxicity [White and Hemond, 2012, and references therein]. Toxicity from low-level or chronic exposure has been poorly studied [White and Hemond, 2012].

Because of its growing importance in industry, elevated environmental concentrations, and observed toxicity, it will be important to understand indium's potential environmental impacts and human health effects. With this knowledge, detrimental effects may be minimized through careful industrial use, recycling, or substitution.

1.2 Thesis Outline

The main objective of this thesis is to better understand indium's natural and anthropogenic cycling. This includes specific studies to measure how indium's environmental concentrations have changed historically, to characterize atmospheric concentrations of indium and the inputs and outputs that dictate these concentrations, and to determine indium releases from industrial sources, including mining, smelting, and coal combustion.

Chapter 2 is a literature review of the natural and industrial cycling of indium in the environment, the extent of human perturbation to its natural cycling, and what is known about its health effects. It is found that industrial emissions of indium are already larger than natural emissions. Metal smelting and coal burning are the primary industrial sources of indium to the environment, while releases from the semiconductor and electronics industries are small at present. This scenario may change with the rapid growth of indium use in the electronics and semiconductor industries.

Historical atmospheric deposition over the past century was measured in a peat core from Thoreau's Bog, Concord, Massachusetts. Because undisturbed peat cores are difficult to obtain, a novel coring method was developed and is described in **Chapter 3**. The coring method, along with detailed information about dating the core and indium analysis, are presented. Fluxes of indium to this region began increasing at least in the early 1900s, decoupled from its use in industry, which stayed low until the 1980s. This is likely due to emissions from nonferrous smelting, not associated with the production of indium, and from coal combustion. Fluxes peaked in the 1970s, and have been decreasing until the present, likely reflecting the advent of particulate emissions controls in the US and Canada.

Because atmospheric releases are thought to be large but are poorly quantified, and

because inhalation is thought to be an important exposure pathway for indium, **Chapter 4** presents our studies of the cycling of indium in the atmosphere in the northeastern United States. Archived air filter samples from 5 locations from Boston, MA to Rochester, NY were analyzed for indium; concentrations vary from <0.7 to 8 pg/m^3. There are significant differences between samples from different locations and over the course of a year. Atmospheric back trajectories generated with NOAAs Hybrid Single-Particle Lagrangian Integrated Trajectory (HYSPLIT) model suggest that the highest indium concentrations come from the north, potentially from smelting operations, while lower concentrations are seen in air traveling from the midwestern US.

Further work to constrain the source of indium to the atmosphere in the Northeastern United States is presented in **Chapter 5**. Correlations between indium and other metals in the air filter samples studied show that air traveling from the north has a distinct chemical makeup than air traveling from the west, with higher ratios of indium to other metals. Our studies of the composition of particles emitted from two important sources of indium to the atmosphere show that a hydrolometallurgical zinc smelter has indium concentrations 100 times higher than concentrations in coal fly ash. Additionally, we use receptor modeling to test the hypothesis that smelting operations contribute large amounts of indium to the atmosphere in the northeastern United States. The receptor modeling shows that sources high in nonferrous metals (Zn, Pb, Cu) peak on days when air is traveling from the north, suggesting that air from the north is indeed supplying metals associated with nonferrous smelting.

Chapter 6 describes measurements characterizing aqueous releases of indium at an abandoned mining site in Colorado. The acid-mine drainage from this abandoned mining district causes indium concentrations in Mineral Creek, CO, to be 10^4 times higher than natural freshwater concentrations, and all of this indium is in the dissolved phase. During an experimental raising of the pH of this system from 3 to >8, essentially all of the indium associates with the particulate phase. Indium concentrations are 40-70% higher in Fe-oxides collected after the pH modification than in those collected before the experiment, suggesting that sorption to iron-oxides is the primary removal mechanism of indium from this system.

Lastly, **Appendix A** details our attempts to develop an electrochemical technique to separate and pre-concentrate indium from aqueous solution. Because natural aqueous concentrations are lower than the detection limits of presently available analytical instru-

ments, a technique to pre-concentrate indium is critical to its routine measurement. Pre-concentration may also work to separate indium from analytical interferents, which could be important for its analysis.

Chapter 2

The Anthrobiogeochemical Cycle of Indium: A Review of the Natural and Anthropogenic Cycling of Indium in the Environment

Adapted from: White, S.J.O. and H.F. Hemond, The Anthrobiogeochemical Cycle of Indium: A Review of the Natural and Anthropogenic Cycling of Indium in the Environment, *Critical Reviews in Environmental Science and Technology*, 42:155-186, 2012. Reprinted by permission of the publisher, Taylor & Francis Ltd, http://www.tandfonline.com.

2.1 Abstract

Indium is an important metal whose production is increasing dramatically due to new uses in the rapidly growing electronics, photovoltaic, and LED industries. Little is known about the natural or industrial cycling of indium, and toxicological data are incomplete. This review presents the existing state of knowledge of indium's natural and industrial fluxes, chemical behavior, toxicity, and analytical methods by which it is measured. Additionally, it presents evidence of industrial influence on environmental indium concentrations, and seeks

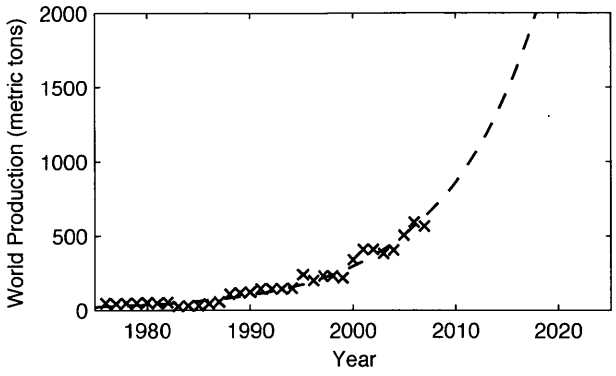

Figure 2-1: Past and potential growth of indium production. Xs denote USGS World Production data [Kelly and Matos, 2008a], and dashed line is a best-fit exponential line, extended to 2025.

to define future research needs that will allow a thorough investigation of the environmental behavior of indium and allow informed decisions about its use, handling, and disposal.

2.2 Introduction

World production and industrial usage of indium has increased 10-fold over the past 30 years ([Kelly and Matos, 2008a], Figure 2-1), and is poised to expand even more dramatically, potentially by several orders of magnitude, over the next 20 years. An extrapolation of historical production indicates a seven-year doubling time. Yet little is known about indium's environmental behavior or toxicity, both of which are needed to plan carefully for its industrial use, and to make decisions about product and process sustainability.

Indium is used in indium tin oxide (ITO) coatings for electronic displays (flat panel, liquid crystal, etc.) [Jorgenson and George, 2005], and in new families of high efficiency photovoltaic cells [Anonymous, 2008] and LEDs [Nakamura et al., 1994]. Considerable increases in these uses are expected in the near future; the LED market grew by 300% between 2001 and 2004 [Whitaker, 2007], and the photovoltaic (PV) market is predicted to grow 1000-fold by 2030 [Hoffmann, 2006]. Novel demands such as ITO electrodes in the catalytic splitting of water may further drive demand for indium [Kanan and Nocera, 2008]. Nano-scale applications of indium also have the potential to burgeon in quantum dot applications [e.g. Ohkouchi et al., 2004], and in flexible displays and solar panels [e.g. Devi et al., 2002]). Thus the potential for massively increased indium use is significant. Increased industrial use often, but not always, translates into increased environmental concentrations.

It is important to understand indium's potential environmental impacts and human health effects—including the impacts of nanomaterials, which typically travel farther and are more bioavailable than macro materials of the same makeup—so that any detrimental effects can be minimized through careful industrial use, recycling, or substitution.

In the absence of detailed toxicological studies, the likelihood of adverse effects of elements can be gauged by comparing anthropogenic fluxes and concentrations to natural values [e.g. Nriagu, 1996, Pacyna and Pacyna, 2001, Klee and Graedel, 2004]). In the case of metals, it is suggested that toxicity is most likely to result when natural concentrations, with which organisms have evolved, are suddenly changed. Garrels et al. [1975] have noted that US drinking water standards for a variety of elements linearly correspond to the natural stream concentrations of those metals, suggesting that adverse human health impacts can begin to occur when natural levels are significantly exceeded. Lead and mercury are two examples of metals whose global anthropogenic fluxes significantly exceed their natural fluxes [Klee and Graedel, 2004], and both have come under severe regulatory constraint as a result of toxicity concerns. Natural stream concentrations of indium are on the order of picomolar ($\sim$0.1 ng/kg). A drinking water standard for indium has not been set, but there is already evidence that industrial releases are exceeding natural fluxes.

Therefore, one key to understanding the environmental and health impacts of a poorly studied metal is to examine its industrial life cycle in the context of its natural geochemical cycling. A metal can be flagged for further detailed study when its anthropogenic fluxes become comparable to its natural fluxes. Natural cycling includes processes such as weathering and subsequent wind or waterborne transport, volcanism, and biological uptake. The industrial life-cycle of a metal includes mining and smelting, manufacture, the product lifespan, and end-of-life disposal or recycling. To accurately predict the environmental impacts of a particular metal, the entire industrial life-cycle must be evaluated, taking particular care to assess the amount of the metal that escapes from the product stream to the environment in potentially mobile forms.

We summarize the existing state of knowledge of indium's chemical behavior and its natural and industrial fluxes. We also address indium's toxicity, review the analytical methods by which indium is measured, and present evidence of industrial influence on environmental indium concentrations. Finally, we seek to define future research needs that will lead to a more thorough understanding of the environmental behavior of indium and

Table 2.1: Indium enrichment in sulfide minerals and tin oxide [Smith et al., 1978]

Mineral Name	Mineral Makeup	Typical Indium Conc. (ppm)	Maximum Indium Conc. (ppm)
Sphalerite	Zinc Iron Sulfide	5–100	5,000
Galena	Lead Sulfide	5–10	100
Boulangerite	Lead Antimony Sulfide	10–50	300
Chalcopyrite	Copper Iron Sulfide	10–50	1,000
Bournonite	Copper Lead Antimony Sulfide	10–50	300
Cassiterite	Tin Oxide	10–50	10,000

allow informed decisions about its use, handling, and disposal.

2.3 Background

2.3.1 Occurrence

In the earth's crust, indium occurs at average concentrations of 52 μg/kg sediment, about the same concentration as silver and mercury, two orders of magnitude less than arsenic, and 3 orders of magnitude less than lead [Wedepohl, 1995, Rudnick and Gao, 2004]. Marine sediments have indium concentrations of 74–120 μg/kg [Matthews and Riley, 1970b], and similar values (20–150 μg/kg) have been seen in a peat core and in lake sediments [Grahn et al., 2006, Steinnes et al., 2003]. Natural waters contain picomolar ($\sim$0.1 ng/kg) concentrations of indium.

Relative to these background concentrations, indium tends to be enriched in sulfide minerals and in tin oxide [Wood and Samson, 2006, Smith et al., 1978]. Typical ore concentrations are 5–100 ppm (Table 2.1).

Zinc and lead-zinc ores are presently the main source of purified indium metal, of which $\sim$600 metric tons were produced in 2007. During processing, indium is typically leached from various zinc and lead-zinc wastes with hydrochloric or sulfuric acid. The largest producer of indium is China, followed by Japan, Korea, Canada and Belgium. [Jorgenson and George, 2005, Alfantazi and Moskalyk, 2003].

Indium is also enriched in fossil fuels. Average indium concentrations in coal are 100 μg/kg, similar to crustal concentratinos. Concentrations in petroleum are typically about 1 μg/kg, but range as high as about 20 mg/kg [Smith et al., 1978].

2.3.2 Chemical behavior

A group III element, indium (atomic number 49) is located below aluminum and gallium and above thallium in the periodic table. It has a full *d* orbital and typically exists in nature as a 3+ ion, although a less-stable 1+ form can exist. Indium is considered a relatively 'hard' ion, tending to complex with hard ligands such as OH^-, F^-, and acetate, but is softer than Al^{3+} and Ga^{3+}, so will also complex with softer ligands such as HS^- and Cl^- [Wood and Samson, 2006].

Based on available data, $In(OH)_3{}^0$ almost always predominates in natural waters, except at very low pH (< 4.5) or very high F^- or Cl^- concentrations [Wood and Samson, 2006]. Organic ligands may also alter this speciation, as evidenced by relatively strong complexation of indium with small organic molecules. For example, indium typically has higher complexation constants for small organic molecules than Cu^{2+}, Pb^{2+}, and Zn^{2+}, but lower than Hg^{2+} [Martell and Smith, 1977]. (Note that Wood & Samson found no information for bicarbonate and carbonate complexes or for indium complexes at elevated temperature or pressure, and did not take into account organic ligands.) Multiple organometallic indium compounds have been synthesized [e.g. Banger, 2006], though to our knowledge none have been found naturally.

Indium's tendency to complex with hydroxide ion suggests that it may adsorb to hydroxide-like surface sites on sinking particles in the ocean [Whitfield and Turner, 1987]. A fractionation study in the Mediterranean has confirmed that indium is heavily associated with the particulate fraction, and is comparable in particle reactivity to aluminum, cesium, thorium, titanium, zirconium, and hafnium [Alibo et al., 1999].

Low concentrations of indium in pristine environments and oceans (pM or ~0.1 ng/kg) suggest that indium and its compounds are extremely insoluble. The low solubility of indium is also predicted theoretically from mineral solubility constants (Table 2.2). Wood and Samson [2006] show that waters in contact with the rare mineral dzhalindite [$In(OH)_3(s)$] would have a maximum concentration of 5 μg/L (~40 nmol/L) at pH 4.5–9 (Figure 2-2), significantly higher than observed ocean and freshwater concentrations (discussed subsequently). This is an upper limit for indium hydroxide solubility; mixed hydroxide phases are more likely to be found in nature and would be less soluble than the pure indium mineral. Sulfide end-members are also important due to indium's chalcophyllic tendencies, but

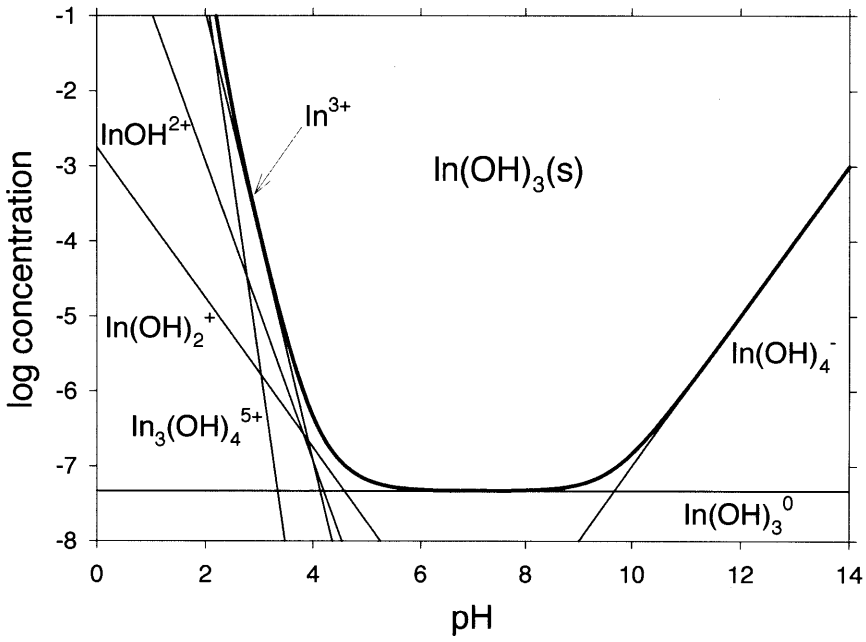

Figure 2-2: Stability diagram for dzhalindite ($In(OH)_3(s)$) at 25°C and zero ionic strength. Reprinted from Wood and Samson [2006] The aqueous geochemistry of gallium, germanium, indium, and scandium. *Ore Geol. Rev.* 28(1), 57-102, with permission from Elsevier.

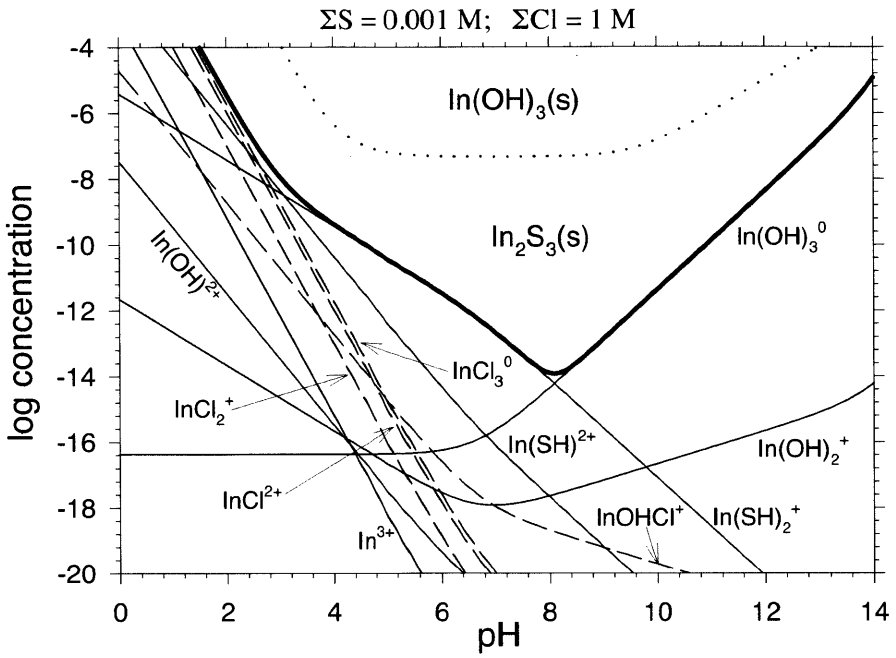

Figure 2-3: Stability diagram for In_2S_3 at 20°C, 1 M total chloride, and 0.001 M total sulfide. Reprinted from Wood and Samson [2006] The aqueous geochemistry of gallium, germanium, indium, and scandium. *Ore Geol. Rev.* 28(1), 57-102, with permission from Elsevier.

the solubility constant for only one indium-sulfide solid, In_2S_3(s), has been studied, and this mineral has not been identified in nature [Wood and Samson, 2006]. Nonetheless, data for this solid suggests that sulfide precipitation is very likely to set an upper bound on indium mobility in anoxic waters; pH 6–8 waters in contact with this particular sulfide mineral are predicted to have a maximum dissolved indium concentration of ~0.1 ng/L (0.9 pmol/L). Chloride complexes do not contribute significantly to the solubility of the indium sulfide mineral phase described above except at pH <3 in most natural waters (Figure 2-3). For more detail regarding indium's aqueous geochemistry, see Wood and Samson [2006].

Indium is considered to be a volatile element [Hinkley and Matsumoto, 2007, Yi et al., 1995, Shaw, 1952, Jorgenson and George, 2005, Palme and Jones, 2004], and appears to be only slightly less volatile than lead, suggesting the potential for long-range transport and participation in gas-phase reactions (Figure 2-4) [Deis, 2009, Geiger et al., 1987]. The temperature range shown encompasses earth surface temperatures, as well as metallurgical processing temperatures (generally ~1000–1800 K [Bodsworth, 1994]).

Table 2.2: Mineral solubility constants for indium compounds

Compound	Solubility constant	Reference
$In(OH)_3$	$K_{sp} = 1.3 \times 10^{-34}$	[Wedepohl, 1995]
	$K_{sp} = 10^{-36.9}$	[Wood and Samson, 2006]
In_2S_3	$K_{sp} \sim 10^{-73.24}$	[Wood and Samson, 2006]
$In_2(CO_3)_3$	$K_{sp} \sim 10^{-15}$	[Wedepohl, 1995]
$InPO_4$	$K_{sp} \sim 10^{-25}$	[Wedepohl, 1995]
	$K_{sp} = 10^{-21.63}$	[Wood and Samson, 2006]

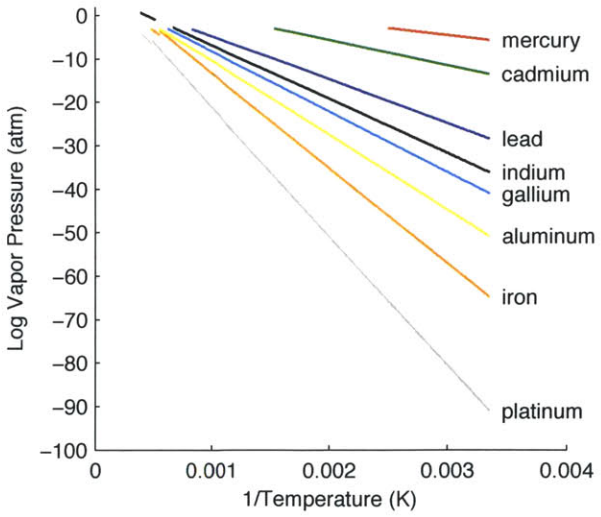

Figure 2-4: Vapor pressure of various metals versus temperature. Data from Geiger et al. [1987] and Deis [2009].

2.3.3 Toxicity

There is considerable evidence suggesting that indium compounds have significant, if not extreme, toxicity. There are no drinking water standards set for indium in the United States, but maximum work-place air exposure limits have been recommended to be 0.1 mg/m^3 (time-weighted average) [NIOSH, 1992, ACGIH, 2007]. It should be noted that this recommended limit is higher than the concentrations of 0.01-0.05 mg/m^3 that have been observed to be associated with lung toxicity in the workplace [Chonan et al., 2007]. Clearly there is a lack of understanding of the safe levels of indium exposure. Additionally, the form that indium takes is extremely important to its toxicity, including its aqueous complexation and its chemical and physical speciation in the atmosphere. Most of the studies discussed subsequently specify only the starting compound used, but not the concentration thought to be 'available' for uptake by organisms (typically thought to be the free ion activity, In^{3+}). For example, at neutral pH, most indium is expected to exist as $In(OH)_3{}^0$, as discussed previously, which can lead to a gross overestimation of the available indium in these experiments. In order to gain a true understanding of the toxicity seen in these studies, more detailed information about the speciation of indium during the experiments must be determined.

Most evidence for indium toxicity to humans has been from occupational inhalation exposure. For example, a 27-year old indium worker was diagnosed with 'interstitial pneumonia consistent with the inhalation of indium tin oxide particles', and died 3 years later despite treatment [Homma et al., 2003]. He had worked with the wet and dry grinding of indium sputtering targets for 3 years. Additionally, his high blood serum levels of indium (290 $\mu g/L$ as compared to the average for healthy males of <0.1 $\mu g/L$) suggest that indium dissolution from indium tin oxide (ITO) particles can cause chronic systemic effects, as evidenced by his emaciation, liver damage, and enlarged spleen. Studies of over 700 workers in Japanese indium factories show that lung damage is found in a significant number of them, and that "inhaled indium could be a potential cause of occupational lung disease" [Homma et al., 2005, Chonan et al., 2007, Hamaguchi et al., 2008, Nakano et al., 2009]. The studies suggest that indium itself is the toxic component of ITO since workers exposed only to indium had similar lung damage as those exposed to ITO, and since exposure to tin oxide produces a different type of damage than exposure to ITO.

In addition to ITO toxicity seen in humans, pulmonary toxicity and reduced weight gain

(suggesting systemic toxicity) have been seen in hamsters [Tanaka et al., 2002]. Pulmonary toxicity has also been shown for other compounds, such as indium arsenide (InAs) [Tanaka, 2004, Tanaka et al., 1994, Yamazaki et al., 2000, Tanaka et al., 2003], indium phosphide (InP) [Uemura et al., 1997, Oda, 1997, Tanaka et al., 2002, Yamazaki et al., 2000], indium chloride ($InCl_3$) [Blazka et al., 1994a,b], and copper indium diselenide ($CuInSe_2$) [Morgan et al., 1997, 1995]. These compounds cause lung inflammation, often accompanied by hyperplasia (increased growth of benign cells), interstitial fibrosis (scarring of tissue between the air sacs), and occasionally by pneumonia (inflammation and filling with fluid) and emphysema (loss of elasticity causing collapsing airways). Oda [1997] showed that physical irritation by particles is not the sole cause of toxicity, since TiO_2 particles produced no lung damage. Additionally, comparative studies with As_2O_3, $NaAsO_3$, As_2Se_3, InP, $InCl_3$, GaAs, AlGaAs, or copper gallium diselenide ($CuGaSe_2$) have suggested that indium itself is a major cause of the toxicity seen [Morgan et al., 1995, 1997, Tanaka, 2004, and references therein]. In nearly all of these cases, pulmonary toxicity was accompanied by reduced weight gain. Notably, tumors developed in the lungs of rats chronically exposed to InP aerosols, and are thought to be due to oxidative stress [Gottschling et al., 2001].

Reproduction has not been shown to be inhibited by exposure to $InCl_3$ [Chapin et al., 1995], but multiple studies have shown that fetal mortality and malformations increase with $InCl_3$ exposure: rats, intravenously [Nakajima et al., 1998, 2000, 2007b, 2008]; rats, orally [Ungvary et al., 2000, 2001]; rabbits, orally [Ungvary et al., 2000]; rat embryos [Nakajima et al., 1999, 2008]; mouse embryos [Chapin et al., 1995]; and hen eggs [Gilani and Alibhai, 1990]. The fetal toxicity of $InCl_3$ is thought to be a direct effect on the fetus (rather than ill effects on the mother) since similar effects are typically seen *in vitro* and *in vivo* [e.g. Nakajima et al., 2008, Chapin et al., 1995]. Several other studies, however, have found no increase in malformations: mice, intravenously [Nakajima et al., 2000]; mice, orally [Chapin et al., 1995]; and rats, orally [Nakajima et al., 1998]. Studies of the testicular toxicity of InAs have shown a range of responses: no toxicity to hamsters [Omura et al., 1996a], reduced sperm count but no histological changes to rats [Omura et al., 1996b], and reduced sperm count along with severe lesions of the testes of hamsters [Omura et al., 2000]. InP showed testicular toxicity [Omura et al., 2000, 2002].

The ecotoxicity of indium appears to depend greatly on the organism exposed (Table 2.3). Onikura et al. [2008] reported the LC50 for $InCl_3$ to several aquatic species, and

Table 2.3: Published measures of acute toxicity for indium compounds. As discussed in the text, these studies do not identify the 'available' indium concentrations used (typically thought to be the free ion activity, In^{3+}), and may therefore underestimate the toxicity observed. LD50: Lethal dose 50, dose at which 50% of organisms die; IC: Inhibitory Concentration; TC: Toxic Concentration (based on growth rate, not mortality); EC: Effective Concentration; MTC: Microbial Toxic Concentration, essentially EC50; TEC: (Threshold Effect Concentration) as indicated by significant cell viability reduction.

Compound	Species	Acute Toxicity Measure	Value	Reference
$InCl_3$	Mice, intravenous	LD50	12.5 mg/kg	[Castronovo and Wagner, 1973]
$InCl_3$	Mouse fibroblast cells	TC50	2300 μM	[Schmalz et al., 1997]
$InCl_3$	Hamster kidney cells	TC50	2110 μM	[Schmalz et al., 1997]
$InCl_3$	Human gingival fibroblasts	TC50	4200 μM	[Schmalz et al., 1997]
In_2O_3	Mice, intravenous	LD50	0.3 mg/kg	[Castronovo and Wagner, 1973]
$In(NO_3)_3$	Rats, intraperitoneal	LD50	5.55 mg/kg	[Adamson et al., 1975]
$InCl_3$	*Americamysis bahia*	LC50	30.48 mg/L	[Onikura et al., 2008]
$InCl_3$	*Brachionus plicatilis*	LC50	24.42 mg/L	[Onikura et al., 2008]
$InCl_3$	*Artemia salina*	LC50	51.00 mg/L	[Onikura et al., 2008]
$InCl_3$	*Sillago japonica*	LC50	> 20 mg/L	[Onikura et al., 2008]
ITO (nano-material)	*Hydra attenuata* (invertebrate)	EC50	Very toxic (0.1–1 mg/L)	[Blaise et al., 2008]
ITO (nano-material)	*Pseudokirchneriella subcapitata* (alga)	IC50	Toxic (1–10 mg/L)	[Blaise et al., 2008]
ITO (nano-material)	11 microbial species (MARA assay)	MTC ($\sim$ EC50)	Harmful (10–100 mg/L)	[Blaise et al., 2008]
ITO (nano-material)	*Thamnoplatyurus platyurus* (invertebrate)	LC50	Harmful (10–100 mg/L)	[Blaise et al., 2008]
ITO (nano-material)	Photosynthetic enzyme complexes (PECs) from spinach	IC20	Harmful (10–100 mg/L)	[Blaise et al., 2008]
ITO (nano-material)	*Vibrio fischeri* (bacteria)	IC25	Not Toxic (>100 mg/L)	[Blaise et al., 2008]
ITO (nano-material)	trout primary hepatocyte cells	TEC	Not Toxic (>100 mg/L)	[Blaise et al., 2008]
$InCl_3$	Tilapia larvae	LC50	170 μM	[Lin and Hwang, 1998]
$In(NO_3)_3$	*Vibrio fischeri* (bacteria)	EC50 at 24 hr	0.06 mM	[Zurita et al., 2007]
$In(NO_3)_3$	*Chlorella vulgaris* (alga)	EC50 at 24 hr	0.68 mM	[Zurita et al., 2007]
$In(NO_3)_3$	*Daphnia magna* (cladoceran)	EC50 at 24 hr	0.28 mM	[Zurita et al., 2007]
$In(NO_3)_3$	PLHC-1 fish cell line	EC50 at 24 hr	5.9 mM	[Zurita et al., 2007]

show for comparison that thallium, a relatively toxic metal, is significantly more toxic than indium in some cases and significantly less toxic in others. Another study showed that ITO as a nanomaterial ranged from very toxic (LD50 of 0.1–1 mg/L) to not toxic (LD50 >100 mg/L), depending on species [Blaise et al., 2008]. For comparison, ITO displayed among the highest toxicity seen in the study, along with $CuZnFe_2O_3$, $NiZnFe_2O_3$, and Ho_2O_3. Three-day-old tilapia larvae showed an LC50 to $InCl_3$ of 170 μM (37.6 mg/L), ~1000x higher (less toxic) than for Cd [Lin and Hwang, 1998]. $In(NO_3)_3$ was found to be harmful to several aquatic species, in the order from most to least toxic: *Vibrio fisheri* > *Daphnia magna* > *Chlorella vulgaris* > PLHC-1 fish cells [Zurita et al., 2007]. In a study of several metals' effects on soil bacteria, indium inhibited growth of soil bacteria, but had no effect on soil dehydrogenase activity, which is a measure for soil respiration and therefore a proxy for antimicrobial activity in soils [Murata et al., 2005].

The lifetime of indium in the body varies depending on route of exposure. Van Hulle, 2005 showed that InAs is almost entirely excreted in feces within 72 hours. Castronovo and Wagner [1973] find that, when $InCl_3$ or In_2O_3 are injected into the tail veins of mice, they are excreted in two fractions—one having a half-life of ~2 days, the other having a half-life of 69–74 days. Evidence from occupational exposure suggests that inhaled indium has a long lifetime in the human body, since workers exposed at the time of study show similar blood serum concentrations to those formerly exposed (median time since exposure = 4.6 yr) [Chonan et al., 2007].

Several studies point to the inhibition of heme synthesis (by direct or indirect inhibition of the delta-aminolevulinic acid dehydratase (ALAD) enzyme) as a mechanism of indium toxicity [Conner et al., 1993, 1995, Fowler et al., 2005, Rocha et al., 2004][Van Hulle, 2005]. Rocha et al. [2004] show that In^{3+} competes with Zn^{2+} for the ALAD enzyme binding site, since the enzyme activity is rescued upon addition of excess zinc. They suggest that In^{3+} can additionally inhibit ALAD activity by oxidizing methionine groups, as evidenced by the partial rescue of enzyme activity upon addition of glutathione, a reducing agent. It is also possible that rather than acting as a reductant, glutathione is acting to complex indium, making it less available for competition with Zn.

Thus it is evident that indium toxicity is a significant concern. Toxic effects, including one death, have been observed in humans after occupational exposure and in numerous animal studies. Pulmonary toxicity has been found and studied most, though evidence has

also been found for system and specific organ toxicity, carcinogenesis, and teratogenicity. Ultimately, the extent of toxic and ecotoxic effects will depend upon the activity of indium, its physical and chemical form, and the chemical conditions of the particular environment. Chronic toxicity is poorly studied, but is likely more important than acute toxicity due to the low natural concentrations of indium.

2.3.4 Analytical techniques

Indium concentrations in environmental samples have been measured in many ways, including by neutron activation analysis [e.g. Matthews and Riley, 1970a,b], atomic absorption spectrophotometry [e.g. Tuzen and Soylak, 2006, Minamisawa et al., 2003], hydride generation with atomic absorption detection [Busheina and Headridge, 1982, Yan et al., 1984, Castillo et al., 1988, Liao and Li, 1993, Matusiewicz and Krawczyk, 2007], thermal ionization mass spectrometry [e.g. Chow and Snyder, 1969, Yi et al., 1995], anodic stripping voltametry [Paolicchi et al., 2004], and inductively coupled plasma-mass spectrometry (ICP-MS) [e.g. Alibo et al., 1998, Orians and Boyle, 1993, Steinnes et al., 2003, Grahn et al., 2006]. Colorimetric detection [Mizuguchi et al., 2004] and immunoassays [Chakrabarti et al., 1994] have also been utilized. The most common technique for environmental samples, where indium exists at trace concentrations, is ICP-MS.

Even using ICP-MS, measurements of natural waters typically require sample preconcentration in order to be within a detectable range. Additionally, this step is important for removing other ions and dissolved organic matter, which can interfere with many analyses. Preconcentration has been carried out in three main ways: (1) solvent extraction [e.g. Alibo et al., 1998]; (2) ion-exchange [e.g. Matthews and Riley, 1970a,b, Orians and Boyle, 1993, Tuzen and Soylak, 2006]; and (3) coprecipitation [e.g. Ueda and Mizui, 1988, Minamisawa et al., 2003]. Often these are followed with an evaporation step; evaporation alone is typically not feasible because it can result in a complicated matrix that interferes with the analytical technique.

The most widely-used concentration technique for environmental samples has been a solvent extraction technique that consists of chelation by HDEHP (bis(2-ethylhexyl) hydrogen phosphate) and H_2MEHP (2-ethylhexyl dihydrogen phosphate), extraction into heptane, then back extraction with HCl [Alibo et al., 1998]. Also used are ion-exchange schemes, including cation exchange using 8-hydroxyquinoline [e.g. Orians and Boyle, 1993, Moham-

mad et al., 1993] or Chelex-100 [e.g. Orians and Boyle, 1993], and anion exchange at either high pH [e.g. Chow and Snyder, 1969] or high chloride concentration [e.g. Matthews and Riley, 1970a]. Coprecipitation is less widely-used, but schemes such as precipitation with hafnium-hydroxide [Ueda and Mizui, 1988] or chitosan [Minamisawa et al., 2003] have been employed.

It is important to use trace-metal-clean techniques for indium analyses, including acid washing all sample bottles and labware and using plastic labware (typically low-density polyethylene (LDPE), high-density polyethylene (HDPE), or polypropylene (PP)) to prevent both loss and contamination of the sample from sorption to/desorption from container walls. As long as concentrations are high compared to blanks, and blanks are sufficiently low, we have found that background levels of indium in our laboratory are low enough that positive pressure hoods and ultra-pure acids are not necessary in all cases. However, rigorous quality control is important to ensure that measurements are not influenced by contamination. Indium contamination has been proposed, for example, to dominate ocean measurements made in 1969 [Chow and Snyder, 1969], prior to the adoption of trace-metal clean techniques [Amakawa et al., 1996].

Although rarely documented in the literature, there are potentially serious analytical interferences for indium. It is often unclear in published data whether interferences were taken into consideration but were minor or were unintentionally ignored; thus we suggest that care be taken in the interpretation of literature values. As discussed above, complex matrices with high ion content (such as seawater) are very difficult to measure with any of the available analytical techniques without a prior step to separate indium from the matrix. This is also true when dealing with marine or estuarine sediments having high salt concentrations. In our own studies we have seen systematic underestimates for graphite furnace atomic absorption (GFAA) measurements of indium in saline, anoxic sediments; in addition to salt interferences, it is possible that sulfides contribute to this interference. For GFAA, it is important to use a matrix modifier, typically palladium, sometimes combined with tartaric acid, tungsten, or molybdenum, to get consistent results [e.g. Acar et al., 1999, 2000, Shan et al., 1985]. While the use of matrix modifiers allowed Acar et al. [1999, 2000] to measure elevated concentrations (50 ppb) of indium in seawater without pre-concentration, we have been unable to measure natural concentrations in complicated matrices without a pre-concentration step.

When using ICP-MS for indium analysis, care must be taken to account for several significant interferences, including those from ^{113}Cd (12.2% of Cd) and $^{97}Mo^{16}O^{+}$ (9.56% of Mo) at Indium-113, and ^{115}Sn (0.34% of Sn) at Indium-115. These are typically corrected for by monitoring another isotope of the interfering element (e.g. ^{111}Cd and ^{117}Sn) and using the natural isotopic ratio to subtract the interfering isotope's signal. However, this correction is best carried out if the overall correction is small, and in some cases is difficult because there is not another isotope free of interferences (e.g. Mo). Mass resolution in excess of 40,000 would be needed to resolve these interferences; otherwise, assumptions must be made about whether it is possible to ignore the probable interferent contribution.

Despite these problems, reproducible measurement methods have been developed for many sample types. Available data are presented subsequently.

2.4 Indium's Anthrobiogeochemical Cycle

There is much that is unknown about the reservoir concentrations and natural and industrial fluxes of indium (Figure 2-5). In general, reservoir concentrations are better known than are fluxes within and between the reservoirs. As can be seen, most of the industrial fluxes of indium are not yet known.

While Figure 2-5 does not distinguish between scales of fluxes, we will consider three spatial scales of a metal's anthrobiogeochemical cycle: (1) the global, atmospheric scale, classified as gases and aerosols resulting in long-range transport; (2) the regional scale, classified as settleable particles released to the atmosphere and resulting in short-range transport; and (3) the local scale, classified as waterborne releases resulting in transport within a watershed. The recognition of scales is important because different transport mechanisms are required to distribute metals at each scale. Transport in turn is critically dependent on the physical and chemical form of a metal [Hemond and Fechner-Levy, 2000].

2.4.1 Atmospheric Cycling

Measured atmospheric concentrations of indium have ranged from 53 fg/m^3 at the South Pole to 43.3 ng/m^3 near the Bunker Hill lead smelter in Kellogg, Idaho [Smith et al., 1978, Maenhaut and Zoller, 1977, Ragaini et al., 1977]. The reservoir value of 0.2 t in Figure 2-5 is based on the South Pole number, and is thus a lower bound, particularly since industrial

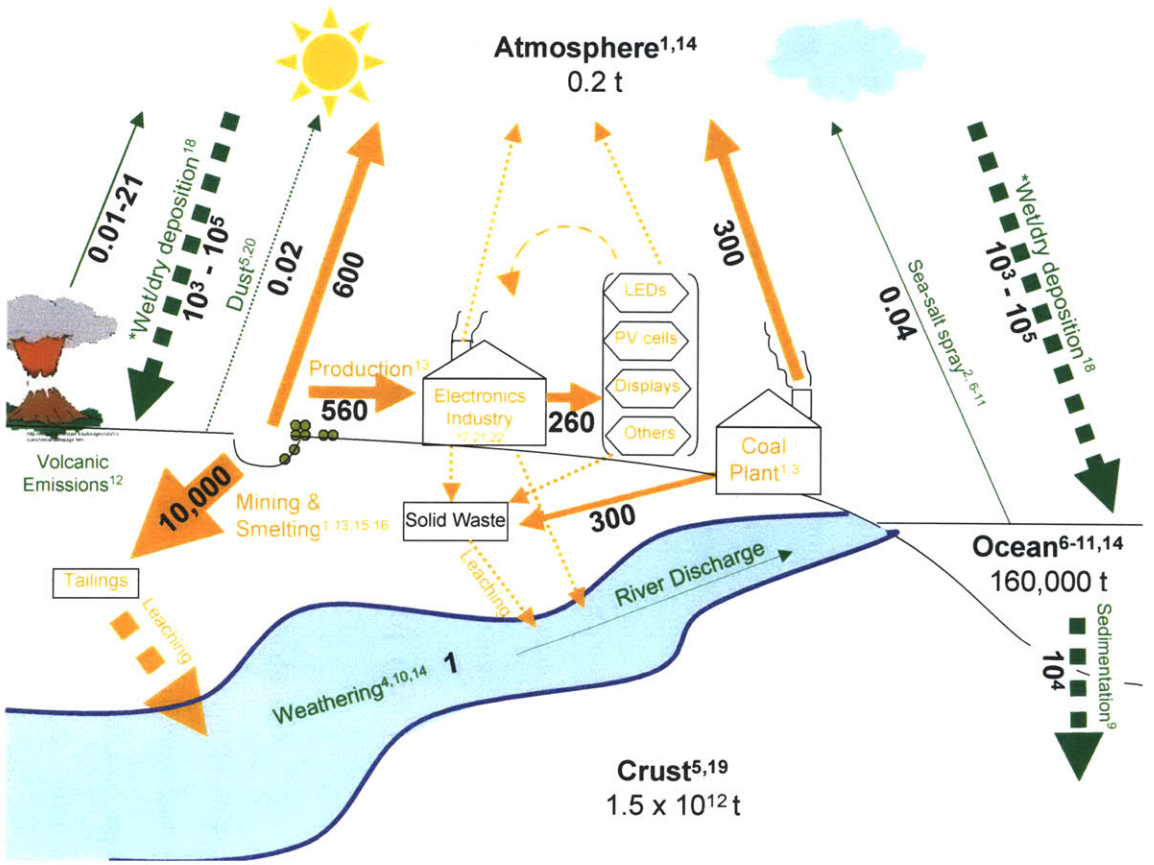

Figure 2-5: Indium's anthrobiogeochemical cycle, 2007. Reservoir units = metric tons; Flux units = metric t/yr; Solid arrow = relatively well-known flux; Dashed arrow = unknown flux; Green arrow = natural flux; Orange arrow = anthropogenic flux; Arrow width = approximate relative magnitude. *Due to the method of estimation, wet/dry deposition fluxes may include both natural and industrial sources. 1) Smith et al. 1978; 2) Klee & Graedel 2004; 3) EIA 2008; 4) Nozaki et al. 2000a; 5) Rudnick & Gao 2004; 6) Obata et al. 2004; 7) Obata et al. 2007; 8) Amakawa et al. 1996; 9) Matthews & Riley 1970 a & b; 10) Alibo et al. 1998; 11) Alibo et al. 1999; 12) Matsumoto & Hinkley 2001; 13) USGS 2008a; 14) Garrels et al. 1975; 15) USGS 2008b; 16) USGS 2008c; 17) Zamora, 2008; 18) Extrapolated from Steinnes et al. 2003, Grahn et al. 2006, and unpublished data from authors; 19) Fairbridge [1972]; 20) Hinkley & Matsumoto 2001; 21) Tolcin 2009; 22) Yeakley 2009.

emissions may presently contribute higher amounts of indium than they did prior to 1975, the year the measurement was taken.

Inputs to the atmosphere

Natural inputs to the atmosphere include dust, ocean sea-spray, and volcanic emissions. Estimates of rock and soil dust flux to Antarctica [Hinkley and Matsumoto, 2001] and the average crustal indium concentration (52 μg/kg; [Rudnick and Gao, 2004]) lead to an estimate of a global indium dust flux of ~0.02 t/yr (Figure 2-5). This should be considered a lower bound; the flux density may be highest near regional sources such as deserts. Ocean sea spray is estimated to be of the same order of magnitude as the dust flux (~0.04 t/yr) (Figure 2-5), based on a mean value for indium of 1 pmol/L in seawater, average salinity of 0.035%, and an annual production of sea-salt aerosols of 10–11.7 x 10^{15} g/yr (method and aerosol estimates from Klee and Graedel [2004]). Matsumoto and Hinkley [2001] have suggested that volcanic emissions provide a significant global flux of indium, based on Antarctic ice core levels of 0.006 to 0.34 pg/g (ppt), higher than expected from only dust and sea-salt spray. This corresponds to a global volcanic flux of ~0.01–21 t/yr (Figure 2-5) (calculated using data from Matsumoto and Hinkley [2001]). This is supported by an estimate of worldwide volcanic emissions of indium of 14 t/yr [Hinkley et al., 1999]. Hinkley et al. [1994] suggest that indium concentrations in volcanic emissions are higher than in the crust or ocean due to fractionation of the more volatile elements. Also interesting to note is that, according to this ice core, indium concentrations have varied substantially over the past 73,000 years, but were generally lower in the past 10,000 years than in earlier times. This could be further indication that volcanic degassing has at times contributed substantially to indium concentrations in the atmosphere.

Industrial inputs to the atmosphere result from fossil fuel combustion, mining and smelting, semiconductor and electronics manufacture, and incineration. Coal burning releases approximately 600 tons of indium annually (based on average indium concentrations in coal of 0.1 ppm [Smith et al., 1978] and world coal use [EIA, 2008]), of which approximately 50% is released to the atmosphere (Figure 2-5) [Smith et al., 1978, and references therein]. This calculated value may be significantly lower if modern environmental controls are taken into account. Additionally, while the total release is well-known, the distribution between fly-ash and bottom-ash is uncertain. The indium concentration in NIST standard 1633: Coal Fly

Ash is not certified, but has been measured at ~0.2 mg/kg [Roelandts and Gladney, 1998]. Petroleum use contributes a negligible amount of indium to the atmosphere compared to the release from coal [Smith et al., 1978][EIA, 2008].

Pacyna and Pacyna [2001] estimate that 45 tons of indium were released to the atmosphere by non-ferrous smelting in 1995, and while there is controversy about the accuracy of this estimate, the potential is recognized for large releases of indium to the atmosphere from mining and subsequent metal refining processes. In addition to the dust generated in the mining process, there may be substantial dust releases during transport of the concentrate after roasting, during the roasting process itself, and even from aeolian erosion of tailings ponds [Lottermoser, 2007]. In addition, pyrometallurgy and hydrometallurgy result in atmospheric emissions, dusts, and fumes [Lottermoser, 2007]. The estimate for mining and smelting emissions to the atmosphere of ~600 t/yr in Figure 2-5 is based on the Smith et al. [1978] estimate that 10% of indium extracted with zinc ore is lost to the atmosphere during processing. There is large uncertainty in this estimate; emissions from copper or tin mining are not included, nor are the effects of modern-day environmental controls.

Global releases from semiconductor and electronics manufacture are presently small compared to those from coal burning and from mining and smelting. Indium used in semiconductors is either part of the base substrate or is deposited via a form of physical vapor deposition (PVD). PVD techniques are also widely used to deposit indium tin oxide for flat panel displays and solar cells [e.g. Singh et al., 2005, Zhou, 2005]. Chemical vapor deposition processes are infrequently used for indium [Zamora, 2008]. The most probable point of atmospheric release is during the production of indium phosphide and indium arsenide substrates, and of indium sputtering targets for use in deposition, particularly in the grinding and polishing steps [Diadiuk, 2008]. In fact, the cases cited above of illness and death associated with the grinding of ITO sputtering targets [Homma et al., 2003, 2005, Chonan et al., 2007, Nakano et al., 2009] resulted from exposure to high factory air concentrations (10–50 $\mu g/m^3$) [Chonan et al., 2007], suggesting the potential for release to the environment. Additionally, elevated mean atmospheric concentrations (10 ng/m^3) have been found near a large semiconductor industrial park in Taiwan, compared to mean concentrations of 5 ng/m^3 in a nearby urban area [Chen, 2007], although errors are not reported for these values in order to confirm that they are significantly different between sites. Despite the potential for release, the total amount of indium produced and sent to

the semiconductor and electronics industries is estimated to be 20 times less than what is released to the environment from mining and smelting; therefore, present-day semiconductor and electronics releases are necessarily small in comparison. However, this may not be true under possible future conditions of a 100- or 1000-fold expansion of production of indium-containing devices.

Atmospheric releases from finished electronics and semiconductor products are probably small compared to the fluxes discussed above. Indium may be released through the use of products such as zinc oxide in tire rubber, or leaded gasoline, due to indium's tendency to exist as an impurity in zinc, lead, tin, copper, cadmium, and arsenic materials [e.g. Smith et al., 1978]. At the end of product life, incineration may release indium to the atmosphere. Measurements above an urban refuse incinerator in 1976 revealed a contribution of 0.013 ng In/m^3 to the local atmosphere, a significant fraction of the 0.03 to 0.06 ng In/m^3 concentrations commonly observed in urban air [Greenberg, 1976, Greenberg et al., 1978b]. Greenberg and colleagues [1976, 1978b] also revealed that most indium from incinerators was associated with respirable particles (<0.2 μm). At the time Greenberg and colleagues' studies were conducted, most indium was thought to come from impurities in iron, lead, zinc, and tin products. It would be useful to revise this number considering the large mass of new products that contain indium. While such emissions are currently thought to be small in comparison to mining/smelting, this also could change as more indium-containing semiconductors and electronics are disposed and incinerated.

Outputs from the atmosphere

The main outputs from the atmosphere are wet and dry deposition. Neither have been measured for indium, but total wet plus dry deposition may be inferred in two ways. First, sediment and peat cores can be used to derive sedimentation rates, from which one can infer atmospheric deposition. Assumptions must be made about the fraction of indium falling on the watershed that is transported to the sediments, and whether there are local watershed inputs. Records obtained from ombrotrophic bogs simplify the situation because such bogs only receive atmospheric inputs. The total deposition values given in Figure 2-5 (land plus water deposition ~2,000–400,000 t/yr) encompass a wide range because they are extrapolated from three different systems ([Grahn et al., 2006, Steinnes et al., 2003], our own work) with varying assumptions. Wet plus dry deposition must also reflect the total input of

indium to the atmosphere, assuming a steady-state atmospheric model. Based on Figure 2-5, total inputs to the atmosphere are ~1,000 t/yr. This is the same order of magnitude as the lower estimate of deposition cited above, but two orders of magnitude less than the upper estimate. Additionally, the residence time of indium in the atmosphere implied by Figure 2-5 is short (~1–100 minutes), partially due to the lower-bound value calculated for the atmospheric reservoir, but partially because the wet and dry deposition estimates may also reflect regional deposition, resulting in shorter overall atmospheric residence times than expected. Clearly there is much to be learned regarding actual atmospheric deposition rates.

2.4.2 Ocean Cycling

Indium concentrations in the ocean range from 0.05 to 4.5 pM (0.006 to 0.5 ng/L), depending on location [Obata et al., 2004, 2007, Amakawa et al., 1996, Matthews and Riley, 1970a,b, Alibo et al., 1998, 1999]. The lowest concentrations have been measured in the semi-enclosed seas near Japan [Obata et al., 2007] and the South Australian Basin in the Antarctic Circumpolar Region, where there is little atmospheric input [Obata et al., 2004]. It is also possible that these measurements are low due to a more stringent filtration step during sample collection (0.04 μm rather than 0.45 μm). North Pacific concentrations are ~0.1 pM and have a depth profile characteristic of conserved elements [Amakawa et al., 1996]. North Atlantic values are higher (0.6–2.7 pM) and have distinctly different depth profiles, one being a profile characteristic of scavenged elements [Matthews and Riley, 1970a,b] and the other being a concave upward profile in which concentrations increase from the surface to depth [Alibo et al., 1999]. The Matthews data [1970a, 1970b] may be less reliable because they were taken prior to the advent of rigorous trace-metal-clean techniques, but the difference in depth profiles may also be due to differences in sample location. Mediterranean waters have a profile characteristic of conserved elements, with an average concentration of 4 pM [Alibo et al., 1999]. Other measurements in the eastern Indian Ocean and the southeast Asian Seas typically show profiles characteristic of conserved elements, between 0.5-2.5 pM and with varying features depending on location [Obata et al., 2004].

Chow & Snyder's [1969] ocean measurements are thought to be contaminated [Amakawa et al., 1996]. Other ocean measurements that are thought to be contaminated or that represent the measurement of clearly polluted waters are referenced in Smith et al. [1978]

and are not included here.

As is the case for other particle-reactive (scavenged) elements such as aluminum and thorium, indium concentrations are higher in the Atlantic than in the Pacific, and higher still in the Mediterranean. But the interoceanic variability for indium (~6–16x different) is much higher than for other elements except aluminum [Alibo et al., 1999]. As mentioned previously, a fractionation study in the Mediterranean has confirmed that indium is heavily associated with the particulate fraction, and is comparable in particle reactivity to aluminum, cesium, thorium, titanium, zirconium, and hafnium [Alibo et al., 1999]. This suggests residence times close to the 100–200 year residence time estimated for aluminum [Alibo et al., 1999, Orians and Bruland, 1985].

Inputs to the ocean

Inputs to the ocean include wet and dry deposition resulting from natural and anthropogenic sources, as well as riverine inputs and benthic sources. The river flux of ~1 t/yr given in Figure 2-5 is calculated using dissolved concentrations (0.28 pM) from an area in Thailand assumed to be pristine [Alibo et al., 1998, Nozaki et al., 2000a]. It is unclear, however, how closely the Thai rivers represent global freshwater background concentrations, or how indium's chemical behavior affects this flux. Industrial areas may also contribute a larger flux. There have been additional studies that show decreases in estuarine indium concentrations in excess of that expected from dilution, suggesting that riverine inputs to the ocean may be smaller than the total of riverine fluxes [Alibo et al., 1998, Nozaki et al., 2000b]. Although not all data are clearly supportive of this claim, several data sets clearly show that end-member mixing cannot entirely explain estuarine indium concentrations (e.g. the Thai river data from Alibo et al. [1998] and the Japanese river data from Nozaki et al. [2000b]). The removal could be due to flocculation or biological removal by filter feeders.

The flux estimate calculated above is 100x smaller than the riverine flux of 100 t/yr estimated by Klee and Graedel [2004]. This is due to the fact that our estimate only takes into account dissolved indium concentrations, rather than those associated with particles, since dissolved concentrations are more mobile and more 'available' to organisms. This overestimation of natural fluxes by Klee and Graedel means that the ratio of anthropogenic to natural fluxes that they have calculated could be 100x too low. Additionally, the free ion activity, In^{3+}, may be more appropriate than the total dissolved species to consider, since

the free ion is thought to be the important species in terms of uptake by organisms. The complexation of indium in natural waters must be better understood in order to determine more specific bioavailability and to truly understand the natural flux values that should be considered.

Alibo et al. [1999] assert that aeolian dust is probably the main natural source of indium to the oceans, based on elevated surface concentrations in some depth profiles [e.g. Matthews and Riley, 1970a,b], and on the absence of additional known significant sources of indium to the oceans other than riverine transport. The estimate above for a global indium dust flux of ~0.02 t/yr does not necessarily support this assertion, however. Additionally, indium to aluminum ratios in the ocean are 1–2 orders of magnitude higher than typical crustal ratios [Alibo et al., 1999]. Since aluminum is also believed to be mainly supplied by dust, and differential solubility of aluminum and indium is unlikely to account for all of the difference, indium either has a significant input source other than dust, or is removed more slowly than previously estimated [Obata et al., 2007]. Volcanic fluxes could be significant at times, as discussed previously. There are no reports in the literature of benthic sources, but researchers have hypothesized that they could be significant [Obata et al., 2004, 2007]. Additionally, industrial inputs to the atmosphere are significant, and therefore may be significant sources of indium to the ocean.

Outputs from the ocean

Sedimentation and sea-salt spray are the main outputs from the ocean, processes that could also differ between indium and aluminum. In fact, Obata et al. [2004, 2007] contend that indium is longer-lived than previously thought, supported by the fact that indium concentrations tend to be more homogeneous than aluminum concentrations. One can estimate a sedimentation rate for indium of 10^4 t/yr (Figure 2-5), based on an assumed sedimentation rate of ~1 mm/yr, an average ocean sediment concentration of 0.1 mg indium/kg sediment [Matthews and Riley, 1970b], and the ocean-covered surface area of the earth of $\sim 3.6 \times 10^8$ km^2. This is well within the range of sedimentation rates for indium of 10^3–10^5 t/yr, based on the steady-state assumption that inputs to the ocean must equal outputs. As mentioned above, sea-salt spray is estimated to be ~0.04 t/yr.

2.4.3 Freshwater Cycling

The few studies of indium in rivers show dissolved concentrations of 0.1–0.4 pM for Thai rivers and at least an order of magnitude higher (1.0–15.0 pM) for the Japanese rivers studied [Alibo et al., 1998, Nozaki et al., 2000a,b]. In all cases, concentrations decreased toward the sea as the rivers transitioned to estuaries and salinity increased. Though the study size is small, higher riverine concentrations appear to correlate with more densely populated and industrialized areas [Alibo et al., 1998, Nozaki et al., 2000a,b]. There have been no published lake or wetland measurements. Our own measurement of indium concentrations in a Massachusetts lake is 1.5 pM, close to measurements by other groups for a low-salinity river in a populated area [Alibo et al., 1998, Nozaki et al., 2000a,b]. While interferences are expected to be small in this sample, they were not quantified; therefore this measurement is best regarded as an upper bound.

Inputs to freshwaters

Chemical weathering provides the background concentration of indium in rivers. As noted above, the river flux of ~1 t/yr given in Figure 2-5 is calculated using dissolved river concentrations from an area in Thailand assumed to be pristine [Alibo et al., 1998, Nozaki et al., 2000a], so this flux also represents the amount of indium released annually by weathering.

Local anthropogenic inputs to freshwaters include coal burning, mining and smelting, semiconductor and electronics manufacture, and incineration. Of the approximately 300 tons of indium that remains in bottom ash from coal burning annually [Smith et al., 1978][EIA, 2008], an unknown amount of this leaches into freshwaters when the bottom ash is landfilled, stored in waste ponds, or recycled in materials such as cement, asphalt, and backfill. Fly ash can also be trapped and either landfilled or put into waste ponds, and therefore could also release indium to freshwaters via leaching.

The local release of metals from mining and smelting has been shown to occur for many elements [e.g. Douay et al., 2008, Mighall et al., 2002, Sterckeman et al., 2002]. Boughriet et al. [2007] have shown high indium concentrations (up to ~75 mg/kg) in river sediments near smelters. This can be caused by short range atmospheric transport, the leaching of tailings by natural waters, the production and leaching of slags and residues by metallurgy, and by the specific chemistry of the waste stream and the degree of influence of acid mine

drainage [Lottermoser, 2007]. One may estimate a flux of ~10,000 t/yr to tailings (Figure 2-5), based on the total amount of indium extracted from the earth with zinc and lead ores, minus the amount produced for industry and the amount released to the atmosphere [Kelly and Matos, 2008a, Smith et al., 1978] This may be an underestimate since indium is also enriched in copper and tin ores, which are not accounted for here. It is unknown how much of this indium leaches into freshwaters.

Because indium is a byproduct of primary metal mining (primary metals being those such as Zn, Pb, or Cu, that exist as a primary ore rather than an inclusion), its releases from mining and smelting are distinct from primary metal releases. The environmental release of a metal from mining/smelting is often considered to be the total produced as purified metal and sent to industry [e.g. Klee and Graedel, 2004]. Yet, as shown in Figure 2-5, this amount is far smaller than the amount that is extracted from the earth but not produced for market, instead being lost to the atmosphere or water. Calculations suggest that only 5% of the indium extracted from the earth due to zinc and lead mining is actually produced as indium metal (data from [Kelly and Matos, 2008a,b,c, Smith et al., 1978]). If the 5% production value is taken to be the flux to the environment, as has been done in prior published comparisons [e.g. Klee and Graedel, 2004], the anthropogenic total flux from mining could be underestimated by as much as 20 times. Because it is produced as a byproduct, this also means that indium has likely been released to the environment for hundreds of years, much longer than it has been used in industry, and that new demand by the semiconductor and electronics industries, although increasing production of such a metal, might actually decrease its overall environmental release by increasing its recovery from mining and smelting wastes.

Semiconductor and electronics manufacture, particularly the production of indium phosphide and indium arsenide wafer substrates and of sputtering targets, may also lead to local environmental releases. Elevated indium levels (9.3 μg/L) have been found in groundwater near a large semiconductor industrial park in Taiwan, compared to a nearby district (0.01 μg/L) [Chen, 2006]. Manufacturing processes may lead to the production of solid and slurry wastes [Diadiuk, 2008]. Deposition processes, while less likely to result in atmospheric releases, do have potential for significant waterborne releases. In particular, physical vapor deposition (PVD) is inefficient and may lead to environmental release; over 55% of the metal is estimated to be lost to the chamber walls in e-beam PVD, the main

process used for indium deposition, and ~30% is estimated to be lost during sputtering, an alternate process for indium deposition [Zamora, 2008, Tolcin, 2009, Nakajima et al., 2007a, and references therein]. Additional indium can be etched away after deposition if the semiconductor wafers and other thin-film devices are to be patterned [Yeakley, 2009]. The metal that is deposited on the walls and other chamber parts either flakes off in pieces that are sent to a reclamation center or are cleaned off using a sand-blasting technique or a chemical wash [Zamora, 2008]. It is unknown whether the indium in the abrasive or in the waste chemicals is reclaimed or released to the environment [Zamora, 2008].

Waterborne releases from electronics and semiconductor products during their lifespan or at the end of their life could result from leaching directly from the product or from its incineration ashes. Finke et al. [1996] performed standard leaching tests on copper indium diselenide (CIS) photovoltaic cells, finding indium concentrations in the leachate as high as 3.2 ppm. This number may be an overestimate, since the leaching tests used were harsh, the solar cells were cut into small pieces after having their glass covers removed, and there are no blanks reported to rule out contamination [Finke et al., 1996]. Incinerator ashes have been measured at 1 mg indium/kg [Greenberg et al., 1978b], but it is unknown how much could leach from the ashes.

Nozaki et al. [2000a,b] hypothesize that elevated dissolved indium in Japanese Rivers comes from medical wastes, by analogy with elevated Gd being attributed to the release of stable $Gd(DTPA)^{2-}$ from medical imaging [Bau and Dulski, 1996]. The primary indium isotope used in medicine is ^{111}In [Harris and Messori, 2002], and the ^{111}In-DTPA complex is used for brain and spinal imaging [Thompson and Orvig, 2003]. While medical release is a potential explanation for elevated Gd, which is used in medicine as a stable isotope [Thompson and Orvig, 2003], radioactive ^{111}In is used, which decays to ^{111}Cd with a half-life of 2.8 days [Deis, 2009] and thus will not persist as indium in the environment. Neither would the starting solution for isotope production contain stable indium since ^{111}In is made by proton capture by silver or cadmium [Macdonald et al., 1975]. Medical releases are therefore not a likely explanation for elevated riverine concentrations of indium.

Outputs from freshwaters

Outputs from freshwaters include transport to the ocean via rivers, aquifer recharge, and sedimentation in lakes and rivers. Transport from rivers to the ocean was calculated above

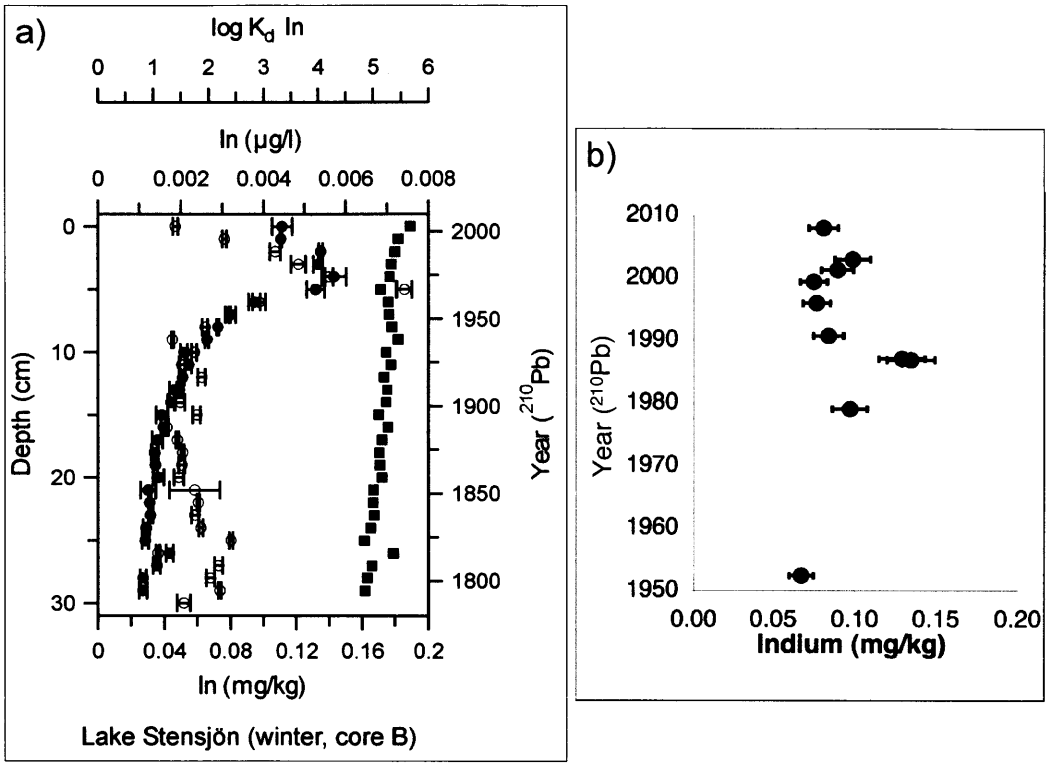

Figure 2-6: Sediment cores showing indium concentrations. A) Data from southern Sweden (Grahn et al. [2006] *J. Environ. Monit.* 8(7): 732-744. Reproduced by permission of the Royal Society of Chemistry.) Closed circles = acid-leachable sediment concentration; open circles = pore-water concentrations; closed squares = solid-water partitioning constant, K_d. B) Author's data from the Charles River, Massachusetts. Circles = acid-leachable sediment concentration.

as ~1 t/yr (Figure 2-5). Recharge to aquifers has not been quantified, and sedimentation can be calculated in a similar way as for ocean sedimentation. Our data and that of Grahn et al. [2006] suggest a mean In sediment concentration of 0.1 mg/kg and lake sedimentation rates of 0.1–1 cm/yr. Combined with assumed sediment densities of 2.5 g/cm^3 [Avnimelech et al., 2001] and a total surface area covered by freshwaters of 2.5 $\times$ 10^6 km^2 [Wetzel, 2001], a freshwater sedimentation flux of 100–1000 t/yr is estimated.

In addition to considering sedimentation as an important natural sink, sediment and peat are also useful historical archives. One high-resolution sediment core shows that indium concentrations have been increasing for at least 150 years prior to 1970, after which they may have actually decreased [Grahn et al., 2006] (Figure 2-6a), and one low-resolution peat

core supports this timeline [Steinnes et al., 2003]. This runs counter to the pattern of increasing indium use in Europe and the United States since 1970 [Grahn et al., 2006, Kelly and Matos, 2008a]. Our preliminary results from a sediment core from the Charles River, Massachusetts, are of similar magnitude and peak shape to the Grahn data (Figure 2-6b). Grahn and colleagues suggest that the higher-than-expected levels prior to 1970 are due to sulfide ore mining in Europe, and that the present decrease, if it is in fact global in scale, may be due to better emission controls. We additionally hypothesize that increasing demand for indium has driven its enhanced recovery from mining waste streams, decreasing its release to the environment and contributing to an actual recent decrease in sediment concentrations.

2.5 Conclusions and Research Needs

Much remains unknown about indium's natural and anthropogenic cycling, but it is clear that indium use will continue to increase rapidly. Anthropogenic fluxes appear to already exceed natural fluxes, flagging indium as an element in need of more study. Additionally, there is evidence that environmental concentrations of indium are already changing as a result of anthropogenic activity.

Semiconductor and electronics manufacture is presently a small contributor to industrial fluxes of indium to the environment; the largest industrial fluxes of indium come from coal burning and mining and smelting. As industrial use increases, however, releases from semiconductor and electronics manufacture may become increasingly important.

There remain a large number of open questions about the environmental releases and behavior of indium. In order to better understand indium's environmental cycling, and what effect indium will have on the environment and human health, research needs include: (1) confirming the magnitude and scale of the mining fluxes of indium, and establishing their link to changing environmental concentrations; (2) establishing the fluxes from semiconductor and electronics manufacture so that potential problems resulting from increases in industrial use can be anticipated and forestalled; (3) determining the toxic effects of low, environmental concentrations of indium, particularly from chronic exposure; and (4) understanding indium's behavior and transport, including organic complexation, vapor phase behavior, and size fractionation of atmospheric releases.

2.6 Acknowledgments

Funding was provided by NSF Grant CBET-0853866, an MIT Earth Systems Initiative Ignition Grant, and the SRC/Sematech Engineering Research Council for Environmentally Benign Semiconductor Manufacture. Additional support was provided by an MIT Earth Systems Initiative Linden Graduate Fellowship and an MIT Energy Initiative Martin Family Graduate Fellowship for Sustainability to S.J.W., and by the William E. Leonhard Professorship to H.F.H. We thank Ajay Somani and Duane Boning at MIT's Department of Materials Science, Paudely Zamora, Patricia Burkhart, and Vicky Diadiuk at MIT's Microsystems Technology Laboratory, and Tim Yeakley at Texas Instruments for information on semiconductor manufacture. We thank Will Fox, Loretta Fernandez, Ed Boyle, and Cynthia Hines for comments on the manuscript and Phil Gschwend for fruitful conversations. Maria Duiame helped with the Charles River sample preparation, Katherine Orchard helped with literature review, and Charuleka Varadharajan, Amy Mueller, Desiree Plata, and Dave Kuo helped with field sampling.

Chapter 3

A Novel Method for Coring Peat

Authors: Sarah Jane O. White, Carrie Keach, Harold F. Hemond

3.1 Introduction

Bogs are important archives of environmental change. Ombrotrophic bogs are particularly useful for tracking historical atmospheric contaminant deposition since they receive only atmospheric inputs, without confounding contributions from surface or groundwater inputs. Bogs are additionally useful because they are less prone to disruption from bioturbation, as may occur in lake or marine sediments. Researchers have successfully reconstructed historical deposition records for metals such as lead [e.g. Lee and Tallis, 1973, Oldfield et al., 1979, Kylander et al., 2009], antimony [e.g. Cloy et al., 2009, 2005] and vanadium [Cloy et al., 2011] using ombrotrophic peat cores.

However, peat can be particularly difficult to core due to its compressibility and the presence of plant roots. Existing corers [e.g. Jowsey, 1966, Cuttle and Malcolm, 1979, Wardenaar, 1987] often compress the peat during retrieval [Givelet et al., 2004, Farmer et al., 2006]. Additionally, many peat bogs have an extensive root system running through them from larger plants and shrubs, making it even more difficult to obtain an undisturbed core while cutting through these roots. The corers presently available are inadequate for many bogs, especially those with an extensive root system.

We developed a freeze-coring method for difficult-to-core bogs that allows the retrieval of a meter-long core with little compression or disturbance. Additionally, this freeze-coring technique preserves porewater stratigraphy due to the freezing of the peat and porewater *in*

situ. The method works by freezing a cylinder of peat to preserve its structure and provide mechanical strength, at which point it can be cut out of the mat with minimal disturbance. We have applied this method in Thoreau's Bog, a difficult-to-core ombrotrophic bog in Concord, Massachusetts. We retrieved a 90 cm core, three times longer than has previously been accomplished for this bog, while creating little compaction or disturbance. 1-cm slices were readily sectioned from the core, and greater resolution may be possible by using a band saw. Thus this technique allows for a high resolution reconstruction of trace metal stratigraphy.

A suite of metals was measured in Thoreau's bog, with a focus on indium. Indium was measured because of its relatively recent introduction into industrial use, and emerging concerns over its health impacts [White and Hemond, 2012]. Indium is a metal whose use is increasing rapidly due to its use as a conductive coating (indium tin oxide) for LCD displays, flat panel displays, and photovoltaic cells. It also has uses as a substrate in important energy technologies such as LEDs and photovoltaic cells. Despite the rapid increase in use of indium, very little is known about its environmental behavior. Knowing more about indium's atmospheric deposition over the past 100 years is important for understanding how humans may be impacting its cycling.

Here we present the design for this novel freeze coring method for difficult-to-core bogs, along with a detailed dating analysis and indium deposition history for the core obtained.

3.2 Methods

3.2.1 Site Description

Thoreau's Bog, also known as Gowing's Swamp, is an ombrotrophic, floating mat *Sphagnum* bog that is connected to a larger wetland area in Concord, Massachusetts (42°27'43"N, 71°19'42"W). It was studied by Henry David Thoreau in the late 1800s [Thoreau, 1906]. Low shrubs and trees are abundant in and around the floating mat, which provide a root structure in the mat that makes coring difficult. The bog was previously shown to have only atmospheric inputs, and a water table that is 10-20 cm below the moss surface [Hemond, 1980].

3.2.2 Freeze-Corer

The freeze-coring technique used is based on a freeze-coring design previously used for lake sediments [Spliethoff and Hemond, 1996]. The design presented here differs from this previous design by allowing the freezing of significantly more material (~13 cm diameter compared to ~5 cm), a necessity for obtaining enough material for analysis due to the low density of peat compared to lake or ocean sediments. Additionally, the present design employs a smaller tube to allow penetration of the peat with minimal disturbance, and has a mechanism for cutting plant roots in order to remove the core from the bog.

The new corer is made up of two separate tubes, one used to freeze the peat, the other used to extract the core (Fig. 3-1). The inner tube (aluminum alloy 6061) is 1 m long, with a 2.5 cm outer diameter, 2.3 cm inner diameter, and has a pointed aluminum tip welded on to create a water-tight seal. This inner tube can be pushed into the peat with minimal effort and minimal disturbance to the peat.

In order to freeze the peat to the outside of this inner tube, pellets of dry ice are added to fill the tube, which is topped up with 95% ethanol. The ethanol is meant to distribute the cold evenly. An approximately 27 cm polypropylene funnel with a neck just larger than the inner tube is then attached to the top of this tube, with an O-ring to prevent leakage of the freezing mixture. Because dry ice sublimates and ethanol evaporates quickly, both must be fed into the tube constantly until the desired thickness of peat freezes. Because of this evaporation, the bottom of the peat freezes more quickly than the surface peat, which does not get as consistent cooling. In our case, where the bulk of the peat was water-saturated, a 13 cm thickness was obtained in 1 hour.

After the desired peat thickness is frozen, the funnel is removed, and a larger-diameter tube (12.7 cm) with sharp teeth is used to cut roots and unfrozen peat away from the frozen core. This tube is a 91 cm long, 12.7 cm outer diameter steel tube (Acker Drill Company, Inc, Scranton, PA), with teeth cut into it and holes into which a handle can be inserted. The teeth are cut so that there is a rounded side and a vertical side, which is filed for maximal sharpness. The outer tube is rotated so that the rounded sides make the first cut, then the tube can be counter-rotated to cut remaining roots more vigorously. Because the peat is frozen, cutting through the plant roots does not disturb the intact core. When the outer tube has been pushed into the peat as far as possible, or if the frozen core begins to

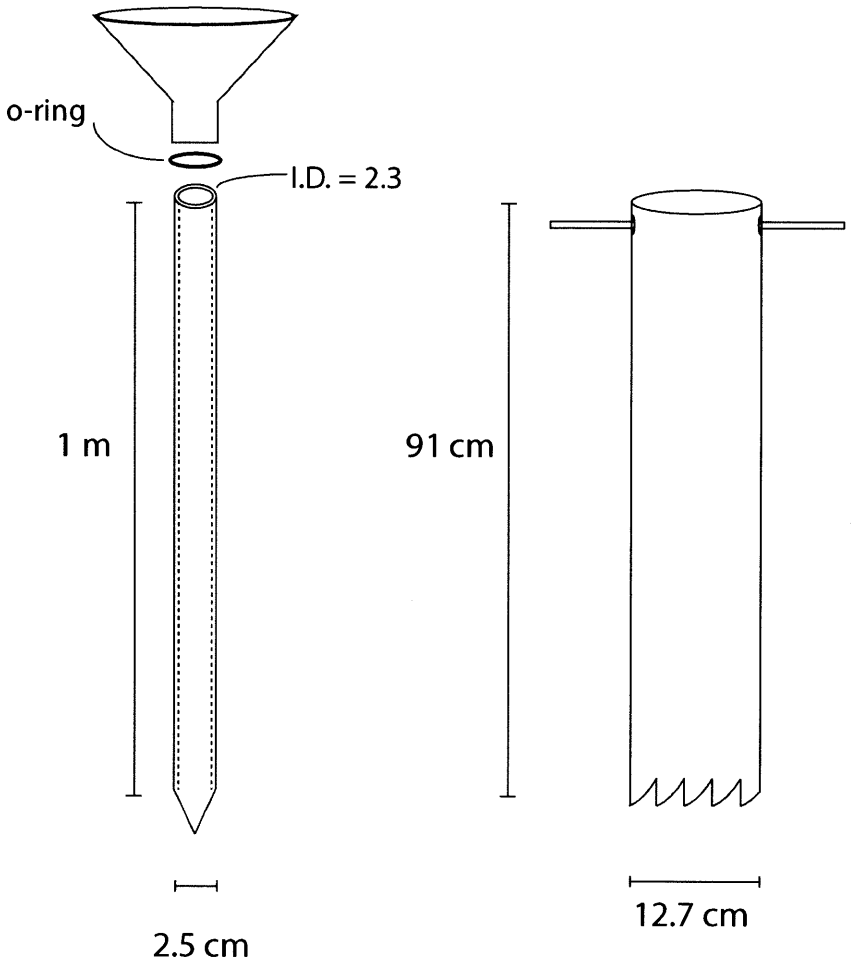

Figure 3-1: A 1 m long, minimally disturbed core can be obtained with a freeze corer developed for hard-to-core peat bogs. An inner tube is pushed into the peat, then filled with ethanol and dry ice to freeze approximately 13 cm diameter of peat around the tube. The undisturbed core can then be cut from the mat with the outer tube, which makes use of sharpened teeth to cut through plant roots.

Figure 3-2: An intact core of 1 m length and 13 cm diameter can be obtained in several hours using the freeze-coring technique

be pushed down by the outer tube, pulling up on the outer tube at a slight angle brings with it the frozen core and the inner tube.

The outer tube can then be removed from the core, and the core photographed, measured, wrapped in plastic, and kept frozen until processing.

3.2.3 Sampling and sample preparation

A 90 cm core was collected from Thoreau's Bog using the above-described corer in May of 2010 (Fig. 3-2). The core remained frozen until processing, at which point it was thawed slightly at room temperature, allowing the center Al tube to be removed. The core was then re-frozen and sliced with a stainless steel butcher saw (Weston Supply 47-1601). The saw blade was cleaned before and between each cut by rinsing with deionized water, wiping with a paper towel, then spraying with deionized water from a spray bottle to rinse thoroughly and remove remaining pieces of peat or paper towel. The saw was then shaken dry. 1-cm slices were easily obtained. Below 15 cm depth, the core was cut into 2-cm slices. The saw blade did not contribute detectable indium to the peat, as discussed below.

Care was taken to remove the surfaces of the core that were in contact with the corer, both outer diameter and inner diameter, using stainless steel scissors that were cleaned with deionized water between samples. The scissors did not contribute indium to the peat samples, confirmed in the same method as for the saw blade, below. The dimensions of the core slices were then measured by hand in order to calculate volume, and the slices were weighed. Each slice was then dried completely in a 60°C oven for 24–48 hours in a glass beaker, covered by a glass watch glass. The dried peat was weighed, then homogenized in polystyrene vials with 8 mm methyl methacrylate balls in a SPEX CertiPrep 8000 Mixer/mill. All containers that contacted the peat were acid-washed with 1M nitric acid (reagent grade, Malinckrodt) at room temperature overnight. Blanks were tested at all steps of the process,

both by exposing the potential contributing surface (saw blade, scissors, vial, ball) to acid as a stringent measure of indium content, and by comparing the indium concentrations in two halves of a peat slice — one that was processed normally, and one that was subjected to repetitive exposure to the saw blade or scissors. In all cases the concentration of indium supplied by these surfaces was undetectable; acid blank signals were below detection limits (and <1% of sample signal), and the peat that was exposed to saw blade and scissors were within 9% of one another, better than the method uncertainty of 20%. While metal inputs to the bog may be heterogeneous over the scale of the bog [Givelet et al., 2004], several tests done on metal concentrations in two halves of one vertical core slice indicate that metal inputs are homogeneous on the scale of the core (13 cm).

3.2.4 Dating

Samples were dated using standard ^{210}Pb and ^{137}Cs chronostratigraphic techniques [Appleby, 2001, Appleby et al., 1988, Appleby and Oldfield, 1978]. 0.75 g (for the upper 15 cm) or 3 g samples were packaged for gamma counting in polypropylene vials (2 oz. and 4 oz., respectively) and left for at least 3 weeks before counting, to allow secular equilibrium to be established between ^{222}Rn production and decay, which translates to secular equilibrium for ^{214}Pb, which is used to determine supported ^{210}Pb activity.

Samples for dating were counted for gamma decays on a γ-counter (Canberra Instruments, GL2020 detector with series 40 multi-channel analyzer). Lead-210 was measured at an energy of 46.5 keV. ^{214}Pb was measured as a proxy for supported ^{210}Pb activity, at 295 and 352 keV. ^{137}Cs was measured at 662 keV. Energies were calibrated initially using pitchblende (U.S. EPA, Environmental Monitoring Systems Laboratory-Las Vegas, Quality Assurance Division, Standard Pitchblend Ore) and individual gamma sources (^{22}Na,^{54}Mn,^{57}Co,^{60}Co,^{109}Cd,^{133}Ba,^{137}Cs, 1 μCi, The Nucleus, Inc, Oak Ridge, TN), and re-checked periodically with pitchblende.

Background ^{210}Pb and ^{214}Pb was measured for an empty plastic vial, and subtracted from the total ^{210}Pb and ^{214}Pb counts. (The ^{210}Pb background was 0.01 counts per minute (cpm), at most 15 % of the sample signal. The ^{214}Pb background was 0.02 cpm, in some cases as much as a 100 % correction due to the low ^{214}Pb signal in the samples.) Counting efficiencies for the samples [(counts per minute)/(decays per minute)] were determined by the addition of two pitchblende spikes. The original sample was counted as described above,

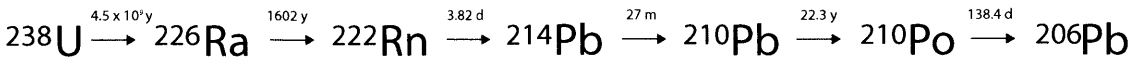

Figure 3-3: U238 Decay Series

then 30–65 mg pitchblende was added, mixed, and counted after 3 weeks equilibration time. A second addition of pitchblende was carried out in the same way. This set of additions was done for two samples of each sample size (0.75 g and 3 g samples), since changes in the geometry of a sample can affect the counting efficiency. In this case, the efficiencies for both sample sizes were the same: 0.5% for ^{210}Pb and 2% for ^{214}Pb. For the 3 g sample, relative error on these efficiencies was as much as 17%, determined by the difference between the efficiency calculated for the two 3 g samples. This error is most likely due to both instrumental error, and in slight density differences in the samples that cause the overall volume of the samples to vary slightly. The 0.75 g samples had one point that was substantially in error, perhaps due to poor mixing of the pitchblende with the sample, which can have a significant effect on efficiency. With this point included, relative error on this sample size was 29% and 38% for ^{210}Pb and ^{214}Pb, respectively. Without this point, relative error was 2-3%.

Model dates were assigned according to the Constant Rate of Supply (CRS) Model [Appleby, 2001, Appleby et al., 1988, Appleby and Oldfield, 1978]. ^{210}Pb is a radioactive decay product in the ^{238}U series (Fig. 3-3).

Because Rn is volatile and has a several-day lifetime in the atmosphere and widespread sources, ^{210}Pb is relatively well-distributed on a hemispheric scale, although concentrations may vary depending on geographic location and rainfall [Baskaran, 2011, Appleby, 2001]. The CRS model assumes a constant rate of input of ^{210}Pb on a year timescale (decays per minute/(cm^2-yr)), but allows for variable sedimentation rates (g sediment/(cm^2-yr)). It therefore allows for any difference in sedimentation rate that may occur each year, based both on changes in *Sphagnum* growth rate from year to year, as well as compaction and decomposition that takes place as the peat ages. After quantification of unsupported ^{210}Pb (by subtraction of the measured ^{214}Pb from the total ^{210}Pb), a total inventory (dpm/cm^2) was calculated following Appleby [2001], and the age of each sediment layer was determined by

$$A_x = A_0 e^{-\lambda t} \tag{3.1}$$

where A_x is the inventory of ^{210}Pb below depth x, A_0 is the inventory of the full core, λ is the decay constant for ^{210}Pb of 0.0311 yr^{-1}, and t is the time before present, in years. Cumulative mass (g/cm^2) can be substituted for depth, and is often a better unit for comparison among cores that may be affected by compression during coring.

Of the 34 core samples analyzed, 25 were dated using this technique. Intervening dates were linearly interpolated for the purposes of plotting indium depth profiles.

Cesium-137 is a non-natural isotope that enters the atmosphere from nuclear activity such as bomb testing and nuclear meltdowns. Peaks in ^{137}Cs can be seen in sediments and peat corresponding to two dates: 1963, the peak year of nuclear bomb testing; and 1987, the nuclear reactor meltdown at Chernobyl [Appleby, 2001]. ^{137}Cs was measured at 662 keV, as discussed previously. The background signal for ^{137}Cs measured for an empty plastic vial was 0.00 cpm/g. Efficiencies were not calculated for ^{137}Cs, since only relative activities are needed for determining the 1963 and 1987 peaks.

3.2.5 Metals analysis

Metals were analyzed in the peat core using Inductively-Coupled Plasma - Mass Spectrometry after digestion with nitric and perchloric acids. Homogenized peat samples (0.5–1 g) were digested with concentrated nitric (Malinckrodt Chemical) and 70% perchloric acid (Alfa Aesar), both reagent grade. The procedure was modeled after EPA Method 3050B with adjustments to use perchloric acid for the oxidation of organic material, and to resuspend in a small volume such that indium is above the detection limits of the instrument. Peat was refluxed on a hotplate with 30 mL concentrated nitric acid for approximately 4 hr before adding 10 mL 70% perchloric acid and refluxing for another 4 h. Another 10 mL nitric acid was added before taking samples to dryness. Perchlorate was driven off finally with the addition of 10 mL nitric acid, which was again taken to dryness. Each sample was resuspended in 10 mL 2% nitric acid. After addition of indium spikes (discussed below), samples were filtered using an acid-washed Whatman or VWR brand polypropylene 0.45 μm syringe filter, and a non-acid-washed Normject 10 ml polypropylene syringe. Reagent blanks and acid blanks were filtered in the same manner and showed no significant indium contamination from this process, and standards showed that indium was not lost significantly in the filtration step.

Acid washed glassware was used for these digests, and reagent blanks were run with

each sample set. Blank corrections were typically less than 5 % of the sample signal, and were attributed to both contaminants in the reagent grade acids and to the non-clean-room facilities used to perform the digests. We have found that background levels of indium in our laboratory are low enough that positive pressure hoods and ultra-pure acids are not necessary. Care is taken to always measure blanks to make sure this is the case.

A Fisons PlasmaQuad 2+ Quadrupole Inductively-Coupled Plasma Mass Spectrometer (ICP-MS) was used for metals analysis, with argon as the carrier gas. A 1 ppb indium solution typically shows about 200,000 counts per second (CPS) at a mass to charge ratio of 115, and the instrument has approximately unit mass resolution. 95.7% of naturally ocurring indium is ^{115}In, and 4.3% is ^{113}In. Sample introduction is via free draw, using a 1000 μL/min nebulizer with attached frit to prevent clogging, and the instrument is run in peak-jumping, pulse-counting mode with 200 sweeps per measurement. In order to account for matrix effects and drift of the instrument signal over time, the method of standard additions was used for quantification of total indium, whereby each sample is split in two, one of those samples is spiked with 0.1 ppb indium, and the samples are run back-to-back on the ICP-MS. Isotope 115 was monitored, and testing of potential polyatomic interferences at 115 has shown that there are none present for these sample matrices. There is, however, an isotopic interferent in ^{115}Sn (0.34% of total Sn). The interference is linear and predictable, therefore ^{117}Sn and ^{118}Sn were monitored in order to subtract this interference out of the 115 signal. The overall calculation then becomes:

$$\begin{aligned} CPS_{In115,smpl} &= CPS_{115,smpl} - CPS_{115,blnk} \\ &\quad -(CPS_{117,smpl} - CPS_{117,blnk}) \times 0.34/7.68 \end{aligned} \tag{3.2}$$

where $CPS_{In115,smpl}$ are the counts that can be attributed to ^{115}In, $CPS_{115,smpl}$ are the total counts at 115 from both indium and tin, $CPS_{115,blnk}$ are the counts at 115 from the reagent blank, $CPS_{117,smpl}$ are the counts at 117 in the sample, $CPS_{117,blnk}$ are the counts at 117 in the reagent blank, 0.34 percent is the relative abundance of ^{115}Sn and 7.68 percent is the relative abundance of ^{117}Sn. The equation can also be used with ^{118}Sn by substituting the 118 signal and the relative abundance of 22.4 percent. Calculations using the two Sn isotope corrections agree to better than 1%, indicating that this is a reasonable correction and that there are no other interferences present.

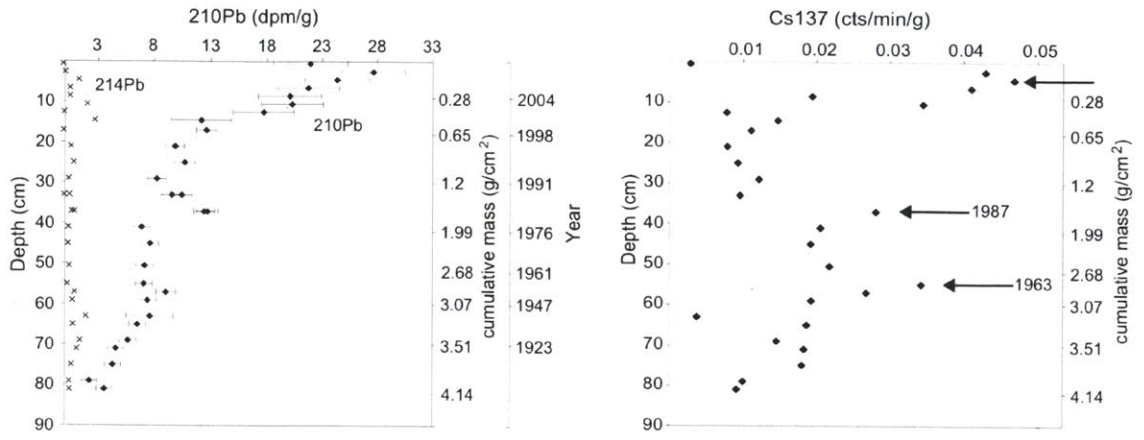

Figure 3-4: (a) Activity of unsupported ^{210}Pb decreases with depth, but does not reach zero. (b) ^{137}Cs has three peaks, one at the surface suspected to result from uptake by *Sphagnum* mosses, one at 37 cm reflecting the 1987 Chernobyl accident, and one at 56 cm reflecting the 1963 peak of nuclear bomb testing.

3.3 Results

3.3.1 Dating

^{210}Pb activity for this core is shown in Figure 3-4a. Cesium 137 shows two peaks, at 55 cm and 37 cm, that correspond well to the ^{210}Pb dating model for 1963, the peak year of nuclear bomb testing, and 1987, the nuclear reactor meltdown at Chernobyl (Figure 3-4b). A third ^{137}Cs peak occurs at the surface, and appears to reflect some mobility of ^{137}Cs, as will be discussed below. The total ^{210}Pb inventory for the core is 38.4 decays per minute/cm^2, and the core is dated to 116 years before present, leading to an average calculated ^{210}Pb flux of 0.33 dpm/(cm^2-yr). This value is somewhat lower than values reported for latitudes 40-50 N of 0.5–1.4 dpm/(cm^2-yr) [Baskaran, 2011], possibly due to the likely overestimate in the deepest age, as discussed below.

Using this ^{210}Pb data, the deepest sample of this core analyzed for ^{210}Pb has been dated to 1894, though uncertainty in the bottom 30 cm is high (Fig. 3-5). The upper 46 cm of the core, however, are dated to within 9 yr, and the upper 60 cm are dated to within 15 yr, and have two independent dating methods ^{210}Pb and ^{137}Cs, that agree well (Fig. 3-5). A third dating means, the depth of a piece of tubing that was placed at the surface of the bog in 1977, buried by peat accumulation for 25 years, and located in 2003, agrees relatively well with the other dating methods (Fig. 3-6).

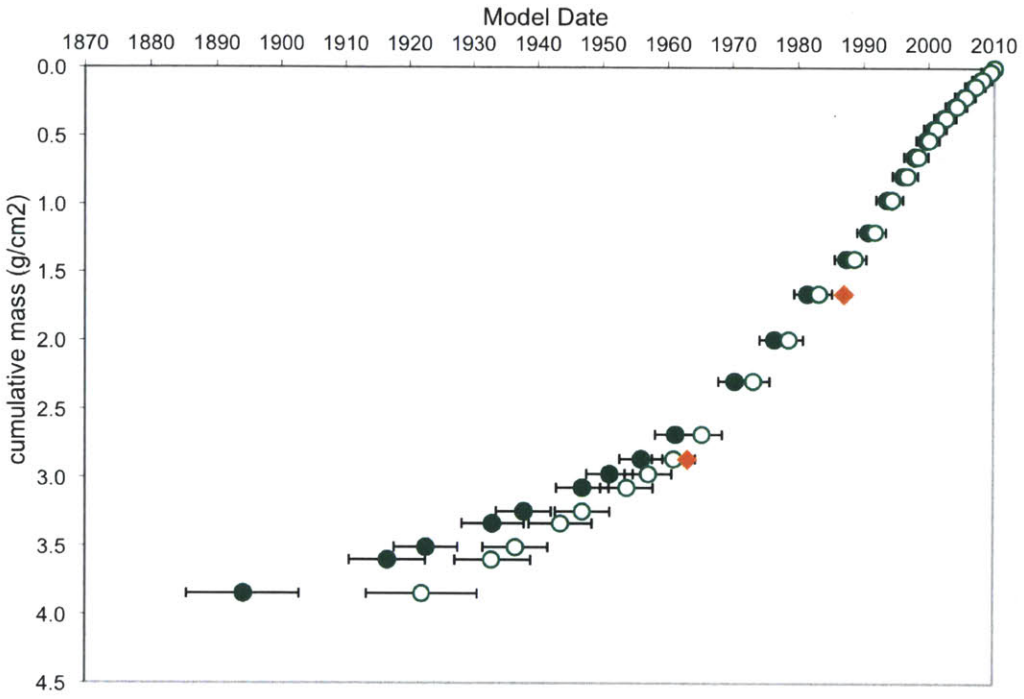

Figure 3-5: Dating for the freeze-core from Thoreau's Bog goes back to 1894. Dark circles are the model dates with the measured inventory. Empty circles are the model dates assuming that the actual inventory is 4% more than was collected. Diamonds are ^{137}Cs dates. Error bars given represent the 1σ statistical uncertainty associated with each point. While uncertainty is high in the bottom of the core, the upper 46 cm is dated to within 9 years, and the upper 60 cm is dated to within 15 years. There is good agreement between the ^{210}Pb dating and the ^{137}Cs dating.

The error for the oldest dates arises from the lower counts associated with peat that is 5 half-lives old, as well as uncertainties in the total inventory of the core. When a core does not go deep enough to capture the horizon at which the unsupported ^{210}Pb is zero, the total inventory of the core is underestimated [MacKenzie et al., 2011]. This is the case with the present core (Fig. 3-4). This can lead to the oldest dates calculated being older than they should be (arising mathematically from $t = -\frac{1}{\lambda}\ln(A_0/A_x)$ (equation 3.1) when the total inventory, A_0, is underestimated, causing the log term to be erroneously large [MacKenzie et al., 2011]). In order to estimate the ^{210}Pb inventory not represented by this core (below 81 cm), one can fit an exponential curve to the bottom 40 cm of the ^{210}Pb activity (Fig. 3-4a) and integrate this function from 81 cm to infinity. This calculation suggests that about 1.4 dpm/cm^2, or 4% of the total inventory is missing. Figure 3-5 shows the date calculations with the inventory given (solid circles), and the date calculations assuming that the total inventory is 4% higher (40 dpm/cm^2 instead of 38.4, open circles). The difference between the two provides an indication of the systematic uncertainty in the model calculations, beyond the statistical error reflected in the 1-σ error bars at each point.

The age profile compares favorably with other published dated peat cores from Thoreau's Bog [Hemond, 1980, Rauch and Hemond, 2003]. The ^{210}Pb activity profiles throughout the cores are very similar, as evidenced by the good match between model dates for the four separate cores using the CRS dating model (Fig. 3-6). This figure adjusts for differences in overall cumulative mass between the cores so that the error discussed previously due to incomplete inventories was not a factor. The Rauch cores were 4x shorter than the present core — 0.88 and 0.93 g/cm^2 cumulative mass compared with 3.9 g/cm^2. In order to increase the ^{210}Pb inventory to reflect what would have been collected with a core as deep as the present study, we determined the percentage of the ^{210}Pb inventory that had been obtained at 0.88 and 0.93 g/cm^2 cumulative mass of the present core, and divided the Rauch inventories by this factor. Similarly, the Hemond core contained 2.41 g/cm^2 cumulative mass, and a similar calculation was carried out to correct for the incomplete inventory relative to the present core. In the end, the Rauch core inventory [Rauch and Hemond, 2003] was increased by 2.5 times and the Hemond core inventory [Hemond, 1980] was increased by 20% (Figure 3-6). Alternatively, the same comparison can be done by truncating the ^{210}Pb inventory of the present core to reflect the inventory that would be present if the total cumulative mass collected was equal to each of the other studies. Dates

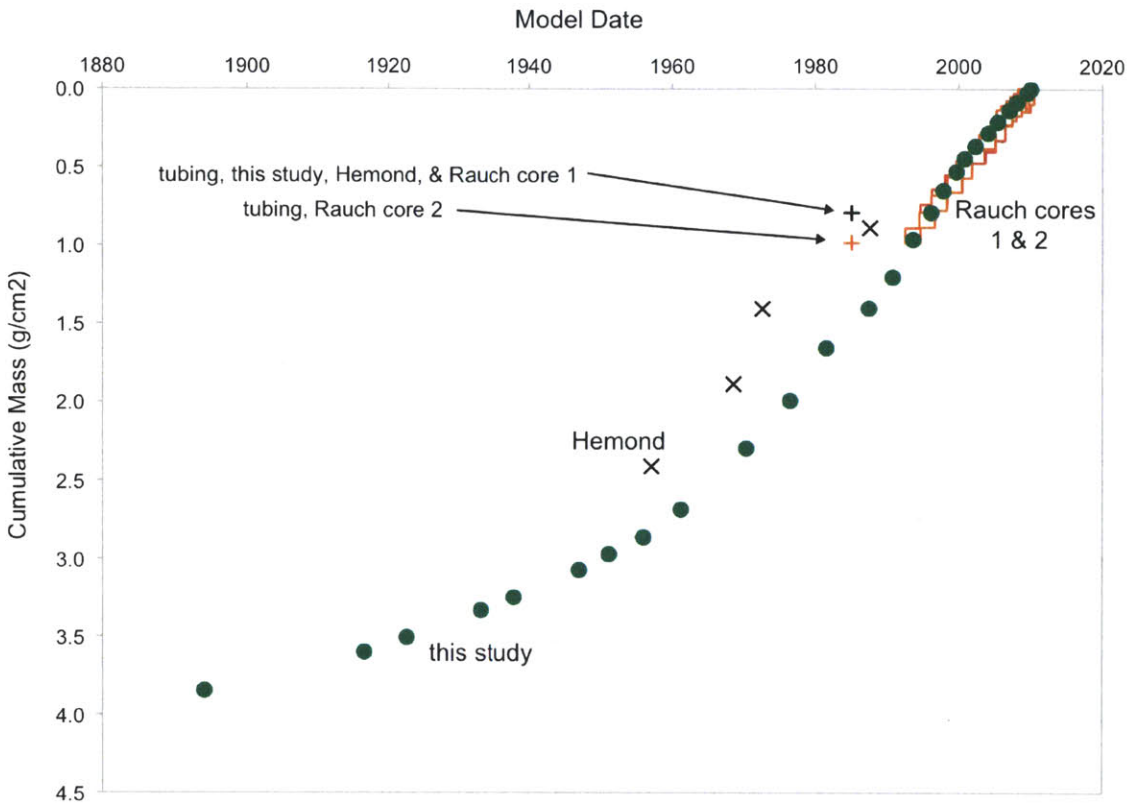

Figure 3-6: ^{210}Pb dating for the present core agrees well with the dating for two previous cores from the same location. Inventories for each of these cores has been adjusted to correct for the differences in overall inventories collected by each researcher, as discussed in the text. The location of buried plastic tubing is also plotted using the densities from each study, and agrees reasonably well with the model dates.

recalculated based on this truncated ^{210}Pb inventory agree well with the dates modeled for the previous core studies (comparison not shown). Note that the model dates presented in Rauch et al. 2004 were calculated using a best fit equation from their CRS-calculated sedimentation rates, and are therefore not the same as those that were calculated for this figure; this figure uses their original data and allows the sedimentation rate at each point to vary, as discussed above, in methods.

A second independent check on the ^{210}Pb dates comes from the location of a length of plastic tubing that was placed on the surface of the bog in 1977 for sampling purposes [Hemond, 1977] and dug up in 2002 in conjunction with the work done by Rauch et al. [Rauch and Hemond, 2003]. This tubing was 25 m in length, and was laid horizontally on the peat surface in 1977. It was buried over the following 25 years as peat grew around

and on top of the tubing. In order to determine the depth of the plastic tube in 2002, a trench was dug perpendicular to the expected tubing location until the tubing was located, and depth to the tubing was measured. Because cumulative mass above the tubing was not measured at the time of retrieval, the amount of compression associated with its retrieval cannot be determined, but the tubing location can be plotted in Fig. 3-6 at four different locations, each calculated with the densities associated with the four individual cores. The placement of this tubing cannot be used as a rigid marker of date due to this limitation, and because of uncertainty as to whether the tubing was buried uniformly. Additionally, the tubing was fragmented during the 25 years that it was buried, which leads to further uncertainty about the exact depth of each piece. Nevertheless, the tubing-based dates agree fairly well with ^{210}Pb and ^{137}Cs modeled dates.

Lastly, ^{206}Pb/^{207}Pb ratios can be used to further constrain the core dates. A peak in the ^{206}Pb/^{207}Pb ratio has been seen to occur near 1850 in both a sediment core from the Pettaquamscutt River in Rhode Island [Lima et al., 2005], and in Atlantic corals [Kelly et al., 2009]. This peak has been attributed to a peak in use of Mississippi Valley lead ore at this time, which has a characteristically high ^{206}Pb/^{207}Pb value. A low resolution study of ^{206}Pb/^{207}Pb ratios in the present core is consistent with the Pettaquamscutt isotope curve, and suggests that the deepest sample from this study does not date back as far as 1850 (Figure 3-10, and further discussion, Supplementary Information).

3.3.2 Application

An intact peat core can have great utility in tracking the history of metal deposition over time. In this case, indium flux to the bog was measured. Indium concentrations peak in Thoreau's Bog near 1940, then decrease to the present (Fig. 3-7(a)). A slight increase in concentrations from 2003 to 2007 can also be seen, with low concentrations again in the top 3 cm. Two different types of error are presented for indium concentrations. The minimum error for each data point was determined to be 20%, based on two samples that were digested and analyzed three separate times, resulting in sediment concentrations as much as 20% different. This error is presented as a central data point flanked by $\pm$ 20% error bars. In addition this error, each sample digest was run at least twice, and sometimes up to 5 times. If the relative error based on this repetition was greater than 20%, the larger error is presented in Figure 3-7a as a central line with a data point on each end.

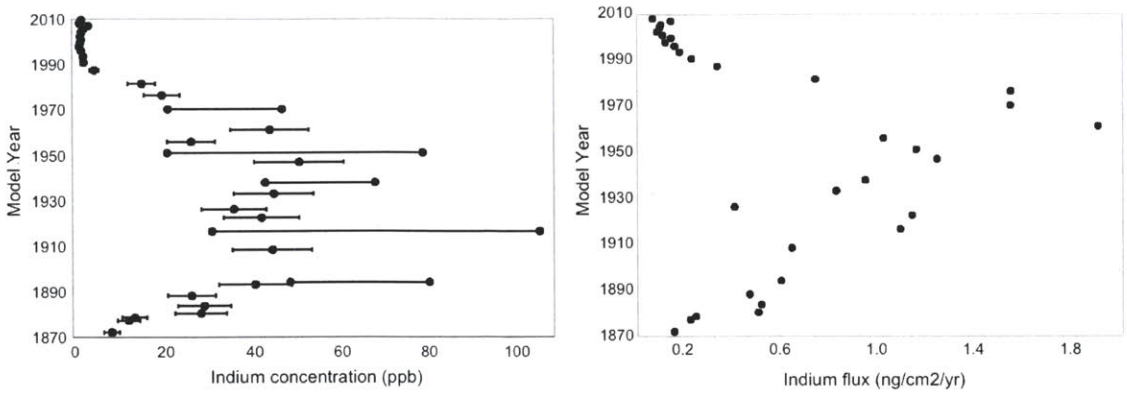

Figure 3-7: Indium concentrations in Thoreau's Bog have been increasing since at least the early 1900s, peak near 1940 and decline to the present. Indium fluxes have been increasing since at least the early 1900s, peak in the 1970s, and decrease to the present. Error bars presented as a central data point flanked by error bars represent the minimum relative procedural error of 20% (1 σ). When duplicate runs produced relative error (1 σ) greater than 20%, error is presented as a central line with a data point on each side. See text for detailed explanation.

Indium flux, [(ng In)/(cm^2-yr)], is a more informative metric, since peat is compressed and degraded as it ages. The indium flux profile (Fig. 3-7b) shows indium flux increasing since the early 1900s, peaking in the late 1970s, then decreasing dramatically to less than 1900 values by 2010. This is similar to the indium deposition pattern seen in Swedish lake sediments by Grahn et al. [2006]. Again a small increase can be seen from 2007-2008. It is unclear whether this reflects a significant change in flux to the bog during this time. Note that one flux point was omitted from this figure at 77 cm depth due to a calculated sedimentation rate 4x higher than the other calculated sedimentation rates, causing the flux to be 10x higher than surrounding fluxes. This outlier is likely due to a lack of precision from the date extrapolation used.

3.4 Discussion

3.4.1 Compression

Density data for each core examined from Thoreau's Bog shows that the cores from Rauch and Hemond [2003] were slightly compressed (as much as 1.75 times more dense) compared with the present core. The core from Hemond [1980] integrates a large depth for each density calculated, which may explain its low density values, particularly at shallow depth,

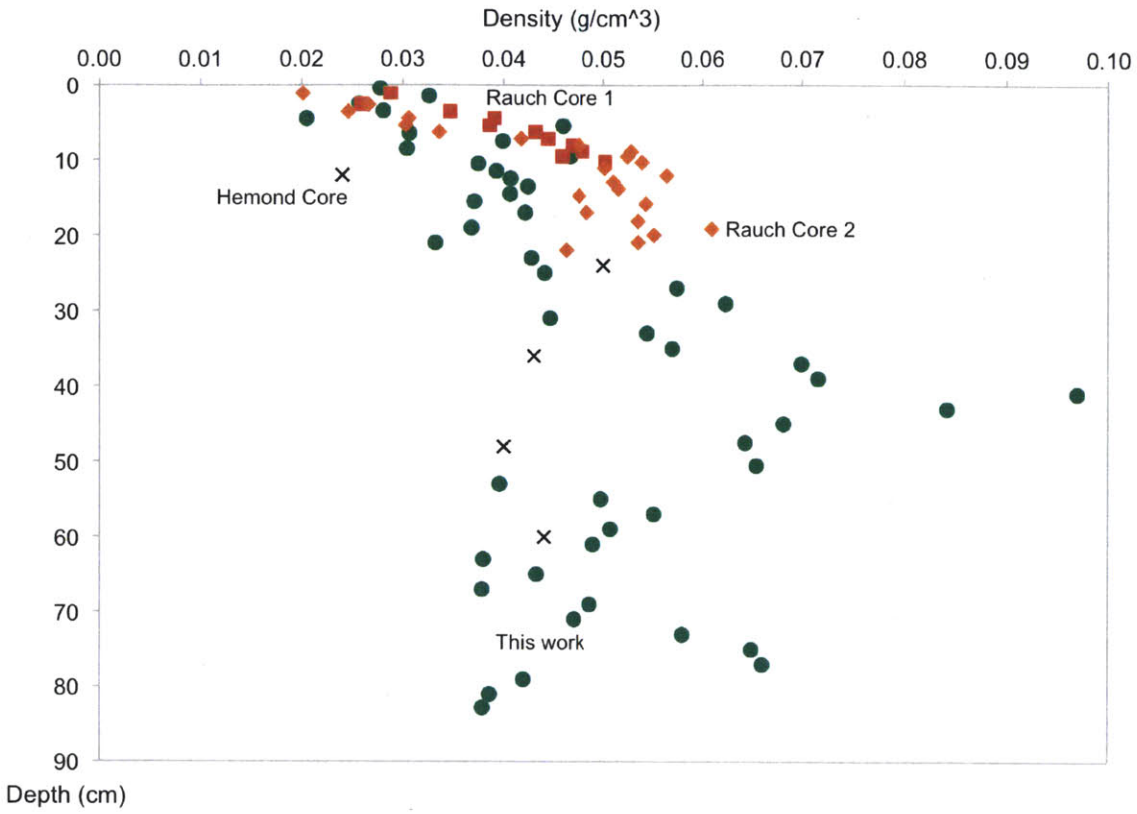

Figure 3-8: Densities for the cores collected for this study, and by Rauch and Hemond [2003] and Hemond [1980].

where density changes rapidly with changes in depth.

3.4.2 Metal Mobility

The measurement and analysis of metal profiles in peat depends on the assumption that those metals are strongly associated with the solid phase, causing them to be immobile and to retain their vertical stratigraphy. Mobility can be estimated if the partitioning of a metal between solid and aqueous phases is known. (The partition coefficient, K_d, is represented by $K_d = C_s/C_{aq}$, where C_{aq} is the concentration in the aqueous phase (g/L) and C_s is the concentration in the solid phase (g/kg)). A retardation factor can then be calculated using R =(mobile fraction + solid fraction)/mobile fraction $= 1 + K_d\rho_{bulk}/\eta$, where ρ_{bulk} is the dry density in g/cm^3, and η is the porosity.

Studies of indium mobility in peat are lacking. K_ds of $10^{4.5}$–10^5 L/kg have been reported for indium in lake sediments [Grahn et al., 2006], although these K_ds are not necessarily

applicable in Thoreau's Bog due to the highly site- and depth-specific nature of these partition coefficients. Our own measurements of indium in porewater samples from several depths are below our analytical detection limits of about 5 ng/L. Taken with the sediment concentrations for those depths, a lower limit K_d for Thoreau's Bog is $10^{4.2}$ L/kg. Using this K_d of $10^{4.2}$ L/kg, In is calculated to travel at least 400 times more slowly than water travels. Hemond [1980] reported an annual precipitation of 1.45 m and evapotranspiration of 1.02 m, for an overall downward water velocity through the bog of 43 cm/yr (assuming that lateral flow and runoff do not change the vertical profile of metals in the bog). This translates to an indium migration of <0.1 cm/yr, or only about 7 cm over the past 70 years.

Extensive study has shown ^{210}Pb to be relatively immobile in multiple types of peat [Shotyk et al., 1998, Novak et al., 2011], and while studies of ^{137}Cs in sediments indicate immobility [Appleby, 2001], studies in peat have indicated some degree of mobility [Olid et al., 2008, Chibowski and Zygmunt, 2002, Appleby et al., 1988]. This is reflected in the present study by a third peak at the surface (Fig. 3-4), which is suspected to result from active uptake of monovalent Cs^+ by *Sphagnum* mosses, as is the case for monovalent K^+ [Hemond, 1980]. A study to determine the K_d of ^{137}Cs in Thoreau's Bog is necessary to determine its mobility. However, the agreement that is seen between the two independent Cs peaks and the ^{210}Pb dating suggests that the Cs peaks have not shifted significantly in this bog over a 50-year time scale.

For all metal data, including ^{210}Pb, ^{137}Cs, and In, the top 1-2 data points exhibit a lower concentration than the points below it. The reason for this drop is unknown, but there is a possibility that when a metal is deposited with rain, it travels downward 1-2 cm before sorbing effectively to the solid fraction and becoming immobile. Further investigation will be necessary to determine the exact cause of this low surface concentration.

3.4.3 Indium Profile

Interestingly, the indium flux profile in Thoreau's Bog is counter to indium's exponential increase in consumption over the past 30 years (Fig. 3-9). Instead, increases in indium flux are seen from 1900-1970, a time of low known industrial indium use, and dramatic decreases in flux are seen since the 1970s, about the time at which indium use began to expand rapidly. This is in fact very similar to the indium deposition pattern seen in Swedish lake sediments by Grahn et al. [2006].

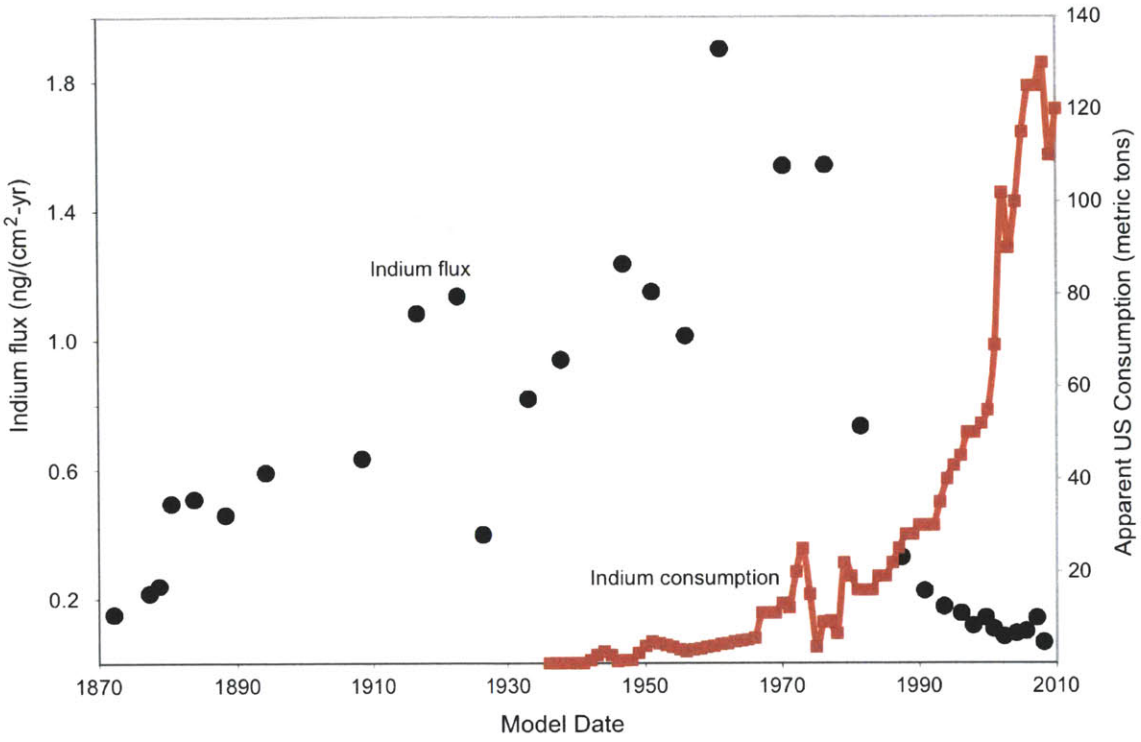

Figure 3-9: Indium flux to Thoreau's Bog is counter to historical consumption of indium in the United States. Consumption data is from [DiFrancesco and George, 2004].

As discussed previously, the indium profile is cannot likely be attributed to mobility. The peak in indium flux in the 1970s falls at about 50 cm depth. Based on the estimate of a maximum of 0.1 cm/year indium migration in this core, the dramatic decline in fluxes since the 1970s is not likely due to indium mobility.

We suggest that the increase since the 1900s is likely due to the increase in both coal consumption and non-ferrous smelting in the United States and Canada. The decrease after 1970 is likely a result of the introduction of particulate matter control technologies in the early 1970s. A more detailed discussion of indium sources to the atmosphere and its subsequent deposition is presented elsewhere (Chapter 4).

3.5 Conclusion

We have developed a freeze coring technique that allows the retrieval of a 1-meter long peat core from difficult-to-core bogs with little compaction or disturbance. This technique can

be deployed in a wide variety of bogs to combat compression inherent in coring peat, which can cause serious problems in the interpretation of historical contaminant deposition. The technique also preserves porewater stratification, and 1-cm resolution is attained using a stainless steel butcher saw for core slicing. Improvements could be made to the technique presented here to obtain even longer cores, and to make the addition of dry ice and ethanol automatic.

^{210}Pb dating for the core obtained for this study agrees well with past cores from the same site, when corrections are made to account for incomplete inventories. While ^{137}Cs may be mobile in peat, dates determined from the ^{137}Cs peaks in Thoreau's Bog agree well with ^{210}Pb dates, suggesting that mobility has not shifted the ^{137}Cs peaks significantly. Additionally, dates estimated by the depth of plastic tubing that was dug up after a known period of burial and by measurements of ^{206}Pb/^{207}Pb ratios with depth are consistent with the dates obtained with ^{210}Pb.

Atmospheric indium fluxes to Thoreau's Bog peak in the 1970s and decline until approximately 2007, at which point deposition may have begun to increase again. The top two samples show the lowest indium concentrations, which may be an artifact of indium that is deposited with rainwater moving downward a few cm before partitioning to the solid phase. We attribute this profile to increases in coal burning and non-ferrous smelting in the United States and Canada since the early 1900s, and the decrease beginning in the late 1970s to enhanced particulate matter controls associated with these two industrial emission sources.

3.6 Acknowledgments

We are grateful to Hanan Karam, Amy Mueller, Charuleka Varadharajan, Jennifer Apell, and Robin Zhao for help with field work. Xanat Flores-Cervantes provided consultation on ^{210}Pb dating. Jessica Fitzsimmons, Jong-Mi Lee, Rick Kayser, and Ed Boyle helped with the measurement of Pb isotopes. Mark Belanger and others in the MIT Edgerton Machine Shop provided assistance with the construction of the corer. Funding was provided by NSF Grant CBET-0853866 and an MIT Earth Systems Initiative Ignition Grant. Additional support was provided by an MIT Earth Systems Initiative Linden Graduate Fellowship and an MIT Energy Initiative Martin Family Graduate Fellowship for Sustainability to

S.J.W., MIT Undergraduate Research Opportunities funding to C.K., and by the William E. Leonhard Professorship to H.F.H.

3.7 Supplementary Information

3.7.1 Lead isotopes – constraint on dating

Lead isotopes were measured to further constrain the dates of the core. Lead 206 and 207 are observationally stable products of ^{238}U and ^{235}U decay, respectively, and the ratio of the two can differ substantially between sources of lead to the atmosphere such as fossil fuels and lead ore [Komarek et al., 2008]. Since sediments and peat reflect both local minerals and atmospheric inputs, historical differences in the lead isotope composition of these materials may be used as a fingerprint of the sources of that lead.

In fact, one such lead isotopic fingerprint can act as a marker with which to independently date a sediment or peat profile. A peak in the $^{206}Pb/^{207}Pb$ ratio has been seen to occur near 1850 in both a sediment core from the Pettaquamscutt River in Rhode Island [Lima et al., 2005], and in Atlantic corals [Kelly et al., 2009]. This peak has been attributed to a peak in use of Mississippi Valley lead ore at this time, which has a characteristically high $^{206}Pb/^{207}Pb$ value. This peak is not seen in low-resolution Pb isotope data from the Thoreau's Bog core from this study, confirming that the core does not date back to 1850. Due to the limited data set for the Thoreau's Bog core, and due to discrepancies between the Pettaquamscutt and coral data, it is hard to say anything more conclusive about the dates of the lowest core depths from $^{206}Pb/^{207}Pb$ isotopes alone. The core from Lima et al. [2005] has been dated most rigorously, with ^{210}Pb, ^{137}Cs, ^{14}C, and varve-counting, and is likely more representative than North Atlantic corals of deposition to Thoreau's Bog, due to its geographical proximity. Corrections for a 'background', pre-anthropogenic Pb isotope ratio have not been applied to the present data due to the failure of the core to extend back 200 years, but the background correction that Lima and colleagues applied was only 0.001-0.002 units for most points (except at the peak, where it was larger); the lack of background correction for the present data is therefore not likely to be significant for this comparison.

A shift of the lowest points of the Thoreau's Bog dating by 30 years would line up the two records nicely. This gives more support for the idea that an incomplete inventory for

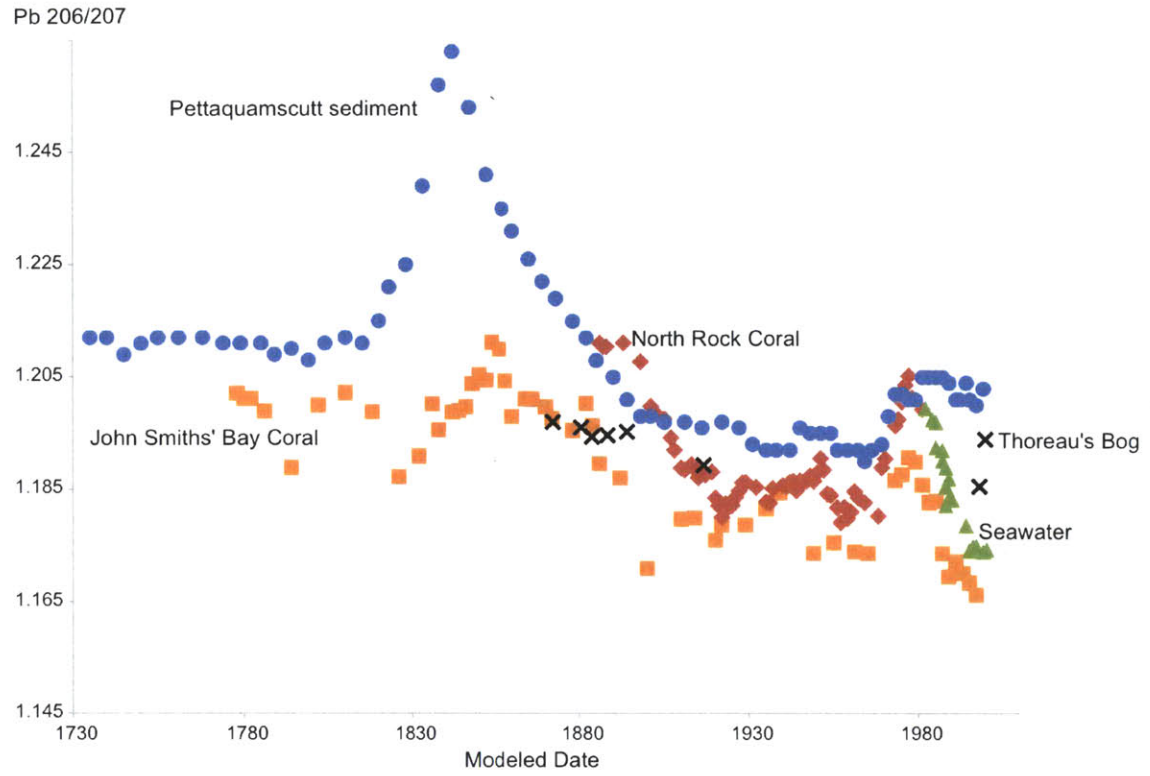

Figure 3-10: $^{206}Pb/^{207}Pb$ ratios confirm that the Thoreau's Bog Core does not extend as far back in time as 1850. Coral and Seawater data is from Kelly et al. [2009]. Pettaquamscutt sediment data is from Lima et al. [2005]

the core collected has overestimated the age of the deepest samples. In fact, the difference between the two model calculations given in Fig. 3-5 for the deepest sample is 28 years. Without a more detailed record of Pb isotopes in the present core, however, and a better understanding of the differences in the Pettaquamscutt sediments and the North Atlantic corals, these Pb isotopes are not able to constrain dates more precisely than to say that the core is younger than 1850.

3.7.2 Methods for Lead Isotope work

All Pb isotope work was performed using trace metal techniques, with double distilled acids, and laminar flow hoods or a class-100 clean room. Blanks were tested for all steps of the process, including combustion.

After combustion of peat samples at 400°C for 12 hours to decrease the presence of organics, 4–50 mg of this combusted material was digested with a mixture of 1 N HNO_3

Table 3.1: Indium $^{206}Pb/^{207}Pb$ data.

Depth interval cm	$^{206}Pb/^{207}Pb$	2 σ
14-15	1.1939	0.0001
16-18	1.1855	0.0038
70-72	1.1893	0.0002
74-76	1.1953	0.0003
78-80	1.1947	0.0001
80-82	1.1944	0.0000
82-83.5	1.1960	0.0003
84.5-87	1.1970	0.0005

and 1.75 N HCl in a sonicator for 90 minutes (following the procedures of Graney et al. [1995]). This leachate was aspirated off twice after centrifugation to remove particles, then evaporated to dryness. HCl was then added and evaporated to drive off residual HNO_3.

Lead was concentrated and other matrix constituents eliminated by chelating lead with Br^-, then binding to an anion exchange resin, Eichrom AG-1x8 (200–400 mesh, chloride form), following the methods of Reuer et al. [2003]. Resin was added to teflon columns, cleaned with 6 N HCl, then conditioned with 1.1 N HBr. Each sample was dissolved in 1.1 N HBr before addition to the column to bind the Pb present in the sample. The sample was then rinsed several times with 1.1 N HBr, followed by 2 N HCl to remove other matrix constituents, then eluted with 6 N HCl. Quantitative lead recoveries for this method of 99.98% have been shown [Reuer et al., 2003]. The sample was reduced to dryness until analysis, at which time it was redissolved in 0.2 M HNO_3 and analyzed using a multi-collector IsoProbe Inductively-Coupled Plasma Mass Spectrometer (MC-ICP-MS).

Conditions for the MC-IC-MS, mass bias corrections, and tailing corrections are described in Reuer et al. [2003]. Mass bias was monitored through the addition of a lead-free thallium spike to each sample, and the periodic analysis of NIST Standard 981, natural lead.

3.7.3 Data Tables

The following tables contain the raw data presented in this chapter for ^{210}Pb dating calculations and for the profile of indium concentrations and fluxes in Thoreau's Bog.

Table 3.2: ^{210}Pb data used for date calculations.

Depth cm	cumulative mass g/cm^2	^{210}Pb dpm/g	±	Inventory dpm/cm^2	±	Age y	±	Model Date
0	0			38.4	6.2	0	0	2010
1	0.03	21.9	3.4	37.8	1.2	1	1	2009
3	0.09	27.6	2.9	36.2	1.2	2	1	2008
5	0.13	24.4	3.0	35.0	1.2	3	1	2007
7	0.21	21.7	2.8	33.4	1.1	5	1	2005
9	0.28	20.1	2.9	32.0	1.1	6	2	2004
11	0.37	20.3	2.8	30.3	1.1	8	2	2002
13	0.45	17.7	2.7	28.9	1.0	9	2	2001
15	0.53	12.2	2.7	27.8	1.0	10	2	2000
18	0.65	12.6	0.9	26.3	1.0	12	2	1998
22	0.79	9.8	0.8	24.9	1.0	14	2	1996
26	0.96	10.7	0.9	23.1	0.9	16	2	1994
30	1.20	8.2	0.8	21.1	0.9	19	2	1991
34	1.40	10.4	0.9	19.0	0.9	23	2	1987
38	1.65	12.7	1.0	15.8	0.9	29	2	1981
42	1.99	6.9	0.8	13.5	0.8	34	2	1976
46	2.30	7.6	0.8	11.2	0.8	40	3	1970
52	2.68	7.1	0.8	8.4	0.8	49	3	1961
56	2.86	7.1	0.8	7.1	0.7	54	3	1956
58	2.97	9.0	0.9	6.1	0.7	59	4	1951
60	3.07	7.4	0.8	5.4	0.7	63	4	1947
64	3.25	7.6	2.1	4.1	0.5	72	4	1938
66	3.33	6.5	0.8	3.5	0.5	77	5	1933
70	3.51	5.7	0.8	2.5	0.4	87	5	1923
72	3.60	4.6	0.7	2.1	0.4	93	6	1917
76	3.85	4.3	0.7	1.0	0.3	116	9	1894
82	4.14	3.6	0.7	0				

Table 3.3: Indium depth profile data.

Depth Interval cm	year	In conc ppb	±	In flux ng/(cm^2-yr)	sedimentation rate cm/yr	density g/cm^3
0-1	2009	2	0.4			0.03
2-3	2008	2	0.4	0.06	1.43	0.03
4-5	2007	4	0.7	0.14	1.88	0.02
6-7	2005	3	0.5	0.10	1.28	0.03
8-9	2004	2	0.4	0.09	1.44	0.03
10-11	2002	2	0.4	0.08	1.14	0.04
12-13	2001	2	0.4	0.11	1.30	0.04
14-15	2000	2	0.4	0.14	1.75	0.04
16-18	1998	2	0.3	0.12	1.65	0.04
20-22	1996	2	0.4	0.15	2.31	0.03
24-26	1994	2	0.5	0.18	1.61	0.04
28-30	1991	3	0.5	0.22	1.39	0.06
32-34	1987	5	1	0.33	1.21	0.05
36-38	1981	16	3	0.73	0.67	0.07
40-42	1976	20	4	1.54	0.79	0.10
44-46	1970	34	13	1.54	0.66	0.07
49-52	1961	44	9	1.90	0.66	0.07
54-56	1956	27	5	1.02	0.76	0.05
56-58	1951	50	29	1.15	0.41	0.06
58-60	1947	51	10	1.24	0.48	0.05
62-64	1938	56	12	0.94	0.44	0.04
64-66	1933	45	9	0.82	0.42	0.04
66-68	1926	36	7	0.40	0.29	0.04
68-70	1923	43	9	1.13	0.55	0.05
70-72	1917	69	38	1.08	0.33	0.05
72-74	1908	45	9	0.64	0.24	0.06
74-76	1894	65	16	0.59	0.14	0.06
76-78	1893	41	8	*5.67	*2.09	0.07
78-80	1888	27	5	0.46	0.41	0.04
80-82	1884	30	6	0.51	0.45	0.04
82-83.5	1880	29	6	0.50	0.45	0.04
83.5-84	1879	14	3	0.24	0.28	0.06
84-84.5	1877	13	3	0.22	0.36	0.05
84.5-87	1872	9	2	0.15	0.48	0.04

*This point was omitted from Figure 3-7 because of a calculated sedimentation rate 4x higher than the other calculated sedimentation rates, causing the flux to be 10x higher than surrounding fluxes. See text for discussion.

Chapter 4

Atmospheric Cycling of Indium in the Northeastern United States

4.1 Introduction

Indium is an increasingly important metal in semiconductors and electronics, and its use is growing rapidly [White and Hemond, 2012]. While there is little known about the natural cycling of indium or its releases from industrial processes, releases of indium to the atmosphere are estimated to be dominated by industrial sources, mostly by coal-fired power plants and non-ferrous smelters (Fig. 4-1; [White and Hemond, 2012]). There is significant uncertainty about these estimates, however, and much of the present knowledge of atmospheric concentrations and cycling of indium comes from studies that are 30 years old [Smith et al., 1978, White and Hemond, 2012].

The atmospheric cycling of metals is important for several reasons, including the fact that human health can be adversely impacted by inhalation of particulate matter, which contains organic matter and metals. Several studies have shown that inhaled indium can have serious health impacts [Homma et al., 2003, 2005, Nakano et al., 2009, Chonan et al., 2007, Hamaguchi et al., 2008], especially in occupational settings where indium concentrations in the air can reach concentrations a million times higher than ambient air [Homma et al., 2003]. Studies are lacking, however, about the health effects of more modest elevations in concentration, or of prolonged exposures to these moderately elevated levels. Additionally, the physical and chemical form of indium in the atmosphere is poorly understood, and

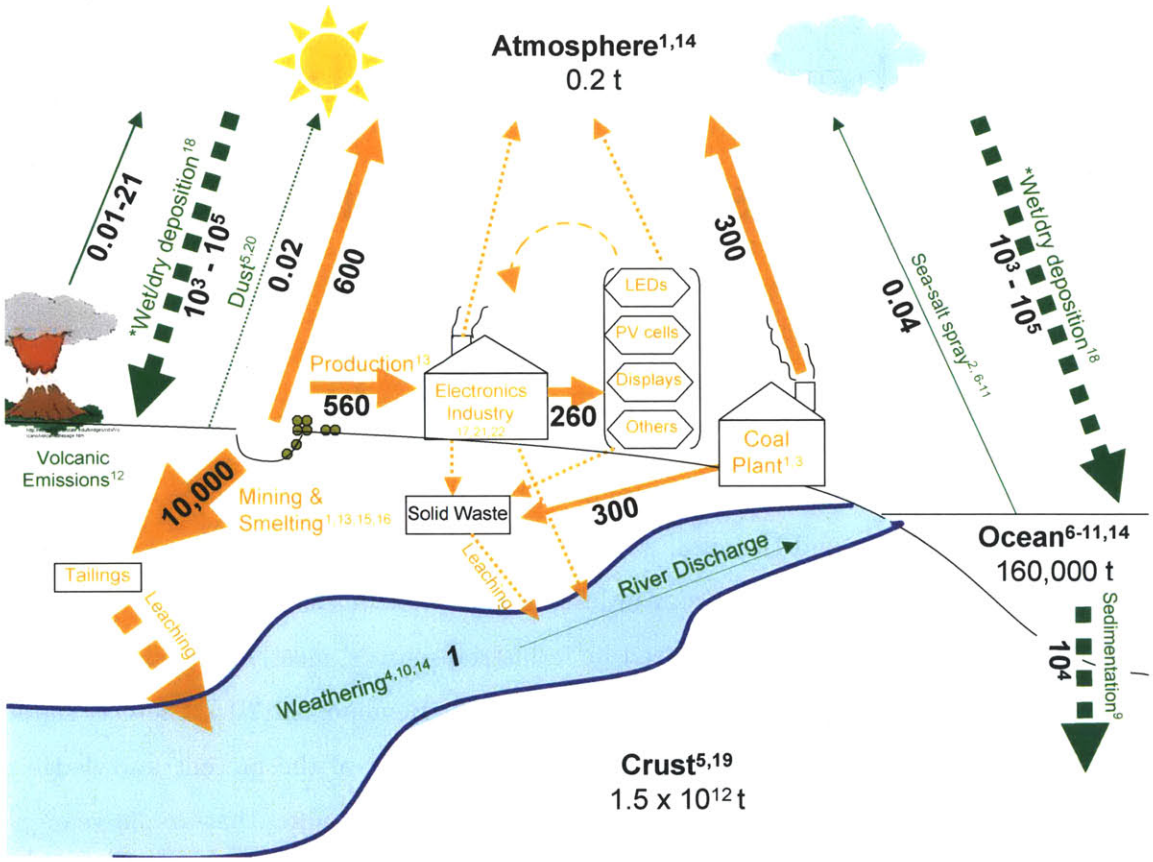

Figure 4-1: Indium's anthrobiogeochemical cycle is dominated by industrial fluxes, with coal-burning and smelting contributing the most indium to the atmosphere. Reprinted from White & Hemond 2012, with permission of the publisher, Taylor & Francis Ltd.

will influence its behavior, transport, and bioavailability; a better understanding of this speciation is important for a thorough understanding of indium's environmental impacts and toxicity.

There are few measurements of indium in the atmosphere, and most were done over 30 years ago. Typical values reported for non-industrial air are on the order of 10 pg/m^3 for all particle size fractions (Total Suspended Particulate, or TSP) [Smith et al., 1978, and references therein]. Indium concentrations in TSP have been measured from 0.053-4.3 pg/m^3 near the South Pole, Canada, and Northern Norway [Maenhaut and Zoller, 1977, Dams and Heindrycx, 1973], to 5-10 ng/m^3 near a lead smelter and a semiconductor industrial area [Ragaini et al., 1977, Chen, 2007]. Note that Total Suspended Particulate includes indium that is bound in the crystal structure of large-diameter silicates, a fraction that is not likely to contribute to human exposure. Respirable particles (those <2.5μm in diameter), and indium that is sorbed to particles rather than bound in the crystal structure are more likely to lead to human or organism exposure.

A more recent measurement of indium in the < 2.5 μm particle fraction (PM2.5) showed an average of 6.7 pg/m^3 from several sites in New York state during 1991 and 1993 [Olmez et al., 1997, Ames et al., 2000]. Ames and colleagues used factor analysis to attribute the mass of indium at each of these sites to the most probable sources during the course of the 2 year study. Depending on the site, they attribute from 35-79% of the PM2.5 indium to smelter sources, 0-25% to a 'Canadian Regional' source that originates from the N/NW, 0-27% to a 'US Regional' source that originates from the W/SW, and 0-12% to a crustal source (i.e. dust). Indium has also been used as a marker of smelter emissions. Sturges and Barrie [1989] show that indium is associated with nonferrous smelting in eastern Canada by correlating peaks up to 20 pg In/m^3 with Pb isotopic signatures of smelters and with wind direction. Non-smelter-influenced air at this site showed concentrations of < 10 pg/m^3 indium. Rahn and Lowenthal [1985] determine that indium contributes 20–100x more to the signature of air particles when air is coming from the nonferrous smelter region of Ontario and Quebec.

A better understanding of the atmospheric cycling of indium can help confirm the most important sources of indium the atmosphere, and to monitor whether those sources are changing local, regional, or global atmospheric concentrations over time. Additionally, atmospheric concentrations influence concentrations in other environmental media such as

the ocean, freshwaters, soils, and sediments through wet and dry deposition. Changes in these reservoir concentrations may cause harmful effects as organisms and humans are exposed to higher concentrations than those with which they have evolved. Determining atmospheric deposition can also help to complete an understanding of the sources and sinks of indium to/from the atmosphere. For example, if we assume a steady-state atmospheric model, wet plus dry deposition must reflect the total input of indium to the atmosphere. Based on Fig 4-1, total inputs to the atmosphere are ~1,000 t/yr, but there is a large uncertainty in the estimate of 1,000–100,000 t/yr from deposition. The estimate of input to the atmosphere is the same order of magnitude as the lower estimate of deposition cited above, but two orders of magnitude less than the upper estimate. If the upper estimate is correct, inputs to the atmosphere have been underestimated.

This paper seeks to gain a better understanding of the atmospheric cycling of indium by analyzing atmospheric particulate matter in the Northeastern United States. Atmospheric particulate samples from five locations in the Northeastern US over the course of a year are analyzed for indium to constrain variations geographically and temporally. In order to constrain the source of indium to the sample locations, atmospheric back trajectories are used to determine the wind directions contributing to peaks in indium concentration. Additionally, in order to understand depositional outputs from the atmosphere and how they have changed over the past century, a peat core from Thoreau's Bog, Massachusetts, is analyzed as an historical archive of indium deposition. The shape of this bog profile can additionally help to constrain the source of indium to this region, as can comparisons with profiles of Zn, Pb, As, Ba, and V in the same core.

4.2 Methods

Archived samples from a network of air monitoring stations in the Northeastern United States were used for this study. These samples were collected as described by Pedersen and colleagues [Pedersen et al., 1999, Salmon et al., 1999]. In short, high volume samplers pulled 300 L/min air, while a dichotomous virtual impactor separated the particles into a 3–10 μm and < 3 μm fraction. (< 2.5 μm is the typical operational cutoff for respirable particles, and we will refer to the < 3 μm fraction as PM2.5, and the 3-10 μm fraction as PM10.) Samples were taken for 24 hours (12am to 12am) every sixth day, and particles

Figure 4-2: Samples were taken in five locations across the northeastern United States. From left to right: Brockport, NY; Rochester, NY; Quabbin Reservoir, MA; Reading, MA; and Boston, MA.

were collected on quartz fiber filters that had been pre-combusted at 550°C. Indium was analyzed in about 30% of the PM2.5 samples and a small number of the PM10 samples.

The locations of the samples were chosen by Pedersen et al. [1999] to reflect urban, rural, and background settings in two separate airsheds (Fig. 4-2). Boston, MA and Rochester, NY are urban areas. Reading is a suburban area 20 km north of Boston, and Brockport is an agricultural community 35 km west of Rochester. The Quabbin site, in a protected watershed in central Massachusetts, was chosen to reflect regional background conditions.

4.2.1 Indium in Air Filters

PM2.5 filters were subsampled using razor blades on a plexiglass template by Pedersen et al. PM10 filters were subsampled with razor blades using a glass template for this study. One third of each filter was digested with concentrated nitric (Malinckrodt Chemical) and 70% perchloric acid (Alfa Aesar), both reagent grade, before measuring metals using an Inductively-Coupled Plasma Mass Spectrometer (ICP-MS). The procedure was modeled after EPA Method 3050B with adjustments to use perchloric acid for the oxidation of organic material, and to redissolve in a small volume such that indium is above the detection limits of the ICP-MS. Air filters were refluxed on a hotplate with 20 mL concentrated nitric acid and 10 mL 70% perchloric acid for approximately 8 hours. After sitting at room temperature overnight, the samples were taken to dryness. Perchlorate was driven off finally with the addition of 5 mL nitric acid, which was again taken to dryness. Each sample was resuspended in 10 mL 2% nitric acid, left for 30 minutes, then the acid decanted into a 15 mL

polypropylene vial. After addition of indium spikes (discussed below), samples were filtered using an acid washed Whatman or VWR brand polypropylene 0.45 μm syringe filter, and a non-acid-washed normject 10 ml polypropylene syringe. Reagent blanks and acid blanks were filtered in the same manner and showed no significant indium contamination from this process, and standards showed that indium was not lost significantly during filtration.

Acid-washed teflon beakers and watchglasses were used for these digests, along with acid-washed glass-ribbed watchglasses for taking the samples to dryness. Reagent blanks were run with each sample set. Field blanks were filters collected as though they were samples, but the pump to the air sampler was not run; these were analyzed by digesting 3 times. These blanks have measurable indium, though in most cases it was less than 10% of the sample indium concentrations, and was subtracted during data analysis. Field blanks and reagent blanks had comparable signals, therefore corrections for each set of digests were made using the Reagent blank signal. Reagent blank signal was attributed to both contaminants in the reagent grade acids and to the non-clean-room facilities used to perform the digests. (We have found that background levels of indium in our laboratory are low enough that positive pressure hoods and ultra-pure acids are not necessary. Care is taken to always measure blanks to make sure this is the case.)

This acid digestion should liberate all of the indium in oxides, sulfides, sulfates, carbonates, and organic fractions [Deis, 2009, Schaider et al., 2007], leaving only what is bound in silicates, and the silicate fraction of indium is thought to be small [Greenberg et al., 1978a,b, Heindryckx and Dams, 1979].

4.2.2 Peat Core Analysis

A 90 cm long peat core was obtained from Thoreau's bog, MA, reflecting deposition over the last century. Thoreau's bog is an ombrotrophic bog that receives only atmospheric inputs, and has been studied extensively [e.g. Thoreau, 1906, Hemond, 1980, 1983, Rauch et al., 2004]. The core was obtained using a freeze coring technique described in detail elsewhere (Chapter 3). Briefly, a thin aluminum tube, closed at one end, is inserted into the peat, and filled with ethanol and dry ice in order to freeze a core around the tube. A larger diameter tube with teeth cut into it can then be used to cut this frozen core from the bog. This technique allows a core to be obtained that is relatively undisturbed and uncompressed, problems that plague other available peat coring techniques.

The processing of this core, and methods for dating and analysis of indium are described in detail elsewhere (Chapter 3). Briefly, the core was subsampled at 1 cm resolution in the top 15 cm and 2 cm resolution in the remaining 75 cm using a stainless steel butcher saw. The peat was dried, homogenized, and subsampled for the measurement of ^{210}Pb by gamma counting, and for measurement of trace metals by digestion followed by analysis with ICP-MS. The Cumulative Rate of Supply (CRS) model was used to calculate model dates for this core using ^{210}Pb data [Appleby, 2001]. Preparation of the peat for trace metal analysis was similar to the preparation of air filter samples for indium analysis. Weighed samples (0.5-1g) of homogenized peat were digested with reagent grade concentrated nitric and 70% perchloric acid in acid-washed glassware, and resuspended in 10 mL 2% nitric acid. Blank corrections were typically less than 5 percent of the sample signal, and were attributed to both contaminants in the reagent grade acids and to the non-clean-room facilities used to perform the digests.

Lead, zinc, arsenic, cadmium, barium, and vanadium were also measured in these peat digests, for profile comparison to help with source tracking. These elements were measured on 1:200 (shallow samples) or 1:2000 (deep samples) dilutions of the same digests used to measure indium. Trace-metal clean techniques were not used during the digestion of the peat, as described above. For the dilutions, however, double distilled nitric acid was used for samples and blanks. Diluted reagent blanks should account for contamination that occurred during digestion, and this signal is subtracted from the sample signal. (This correction was at most 5%, 27%, 42%, 26%, 5%, and 19% of the sample signal for Pb, Zn, As, Cd, Ba, and V, respectively. The correction for As is high due to the low overall concentrations of As in the diluted samples.) However, blanks for these metals were not run in the earliest phases of core preparation, including slicing and homogenizing. Any contamination issues during these steps are assumed to affect all samples equally. Therefore, the shape of these profiles can be used for comparison, but the absolute concentrations of Pb, Zn, As, Cd, Ba, or V are uncertain. Further testing will be necessary to confirm absolute concentrations.

4.2.3 ICP-MS Analysis

A Fisons PlasmaQuad 2+ Quadrupole Inductively-Coupled Plasma Mass Spectrometer (ICP-MS) was used for metals analysis, with argon as the carrier gas. A 1 ppb indium solution typically shows about 200,000 counts per second (CPS) at a mass to charge ratio

of 115, and the instrument has approximately unit mass resolution. 95.7% of naturally ocurring indium is ^{115}In, and 4.3% is ^{113}In. Sample introduction is via free draw, using a 1000 μL/min nebulizer with attached frit to prevent clogging, and the instrument is run in peak-jumping, pulse counting mode with 200 sweeps per measurement. In order to account for matrix effects and drift of the instrument signal over time, the method of standard additions was used for quantification of total indium. In this method, each sample is split in two, one of those samples is spiked with 0.1 ppb indium, and the samples are run back-to-back on the ICP-MS. Isotope 115 was monitored, and testing of potential polyatomic interferences at 115 has shown that there are none present for these sample matrices. There is, however, an isotopic interferent in ^{115}Sn (0.34% of total Sn). The interference is linear and predictable, therefore we monitored ^{117}Sn and ^{118}Sn in order to subtract this interference out of the 115 signal. The overall calculation then becomes:

$$\begin{aligned} CPS_{In115,smpl} &= CPS_{115,smpl} - CPS_{115,blnk} \\ &\quad -(CPS_{117,smpl} - CPS_{117,blnk}) \times 0.34/7.68 \end{aligned} \tag{4.1}$$

where $CPS_{Indium115,smpl}$ are the counts that can be attributed to ^{115}In, $CPS_{115,smpl}$ are the total counts at 115 from both indium and tin, $CPS_{115,blnk}$ are the counts at 115 from the reagent blank, $CPS_{117,smpl}$ are the counts at 117 in the sample, $CPS_{117,blnk}$ are the counts at 117 in the reagent blank, 0.34 percent is the relative abundance of ^{115}Sn and 7.68 percent is the relative abundance of ^{117}Sn. The equation can additionally be used with ^{118}Sn by substituting the 118 signal and the relative abundance of 22.4 percent. Calculations using the two Sn isotope corrections agree to better than 1%, indicating that this is a reasonable correction and that there are no other interferences present. This correction was from 0 to 50% of the total counts at 115 (high correction percentages were caused when tin was high and indium low in the sample), but tests using samples spiked with varying amounts of Sn showed that the contribution of tin at mass 115 was predictable and thus justified use of this correction.

For the quantification of Pb, Zn, As, Cd, Ba, and V, indium was used as an internal standard to account for matrix effects and drift of the instrument signal over time. Because the samples were diluted by at least 200x, natural indium concentrations were much less than the 1 ppb spike of indium added to each sample dilution. Standard curves of metal/indium

signal vs metal/indium concentration were prepared with 1 ppb, 0.1 ppb, and 0.01 ppb multi-element standards (which included all of the elements of interest), with 1 ppb In in each standard. The metal/indium ratios in each sample can then be determined from this standard curve, by plotting the M/In signal (corrected for blanks and instrument background). Multiplication by the indium spike concentration (1 ppb) gives the metal concentration, which can then be converted to a peat concentration with the volume of the digest and the mass of peat digested.

4.2.4 HYSPLIT Analysis

In order to determine the direction of air that was influencing indium concentrations at the Boston and Rochester locations, the HYbrid Single Particle Langrangian Integrated Trajectory model (HYSPLIT4) from the National Oceanographic and Atmospheric Administration (NOAA) was used to generate back trajectories for each day for which indium was measured [Draxler, 1999, Draxler and Rolph, 2012, Rolph, 2012]. A complete description of the model is given in Draxler and Hess [1998, 1997]. The online version was used to generate back trajectories that ran for 48 hours, each starting at 12:00 PM for the indium measurement date and at a height of 500 m. Trajectories were run starting both at a 10m height and a 500m height. The direction of each is the same, although the distance traveled by the 500m height trajectory is much farther. The 500m trajectory height is presented here, with the assumption that stack heights of the most likely emitters are > 150 m, and the Sudbury Super Stack, a possible source of indium to these samples, is 380 m. Archived meteorological data from the Nested Grid Model (NGM) database was used, except for several dates when data was missing from this database, at which time the REANALYSIS database was used. Tests showed that these two databases produced similar results.

Indium removal (e.g. by chemical reaction, gravitational settling, or washout by rain) was not taken into consideration when analyzing back trajectories, although rainfall was qualitatively monitored; therefore, care must be taken in their interpretation. Chemical reaction is not expected to change total indium concentrations, and here the time of the back trajectory is limited to 48 hours to minimize the influence of settling of the PM2.5 fraction.

4.3 Results

The average concentration of indium in PM2.5 particles in the air in the Northeastern United States is 2.1 pg/m^3, with peaks up to 8 pg/m^3 (Fig. 5-1). Normalizing to the total PM2.5 mass in the sample, average particle concentrations are 0.2 μg In/g PM2.5, with deviations in the New York sites up to 0.95 μg/g. Average indium concentrations in the earth's crust are 0.052 μg/g sediment [Wedepohl, 1995].

There are significant differences in indium concentrations both geographically and temporally (Fig. 5-1). One metric of temporal variation at each site is the standard deviation of all data for one location divided by the mean of that data. For air concentrations (pg/m^3) at each location, this relative change in concentrations over the course of a year is at least 56% of the mean (65%, 97%, 73%, 81% and 56% respectively for Boston, Reading, Quabbin, Brockport, and Rochester.) For particle-normalized concentrations (μg/g) at the Massachusetts locations, this relative change is slightly less (46%, 50%, and 74% respectively for Boston, Reading, and Quabbin), while at the New York sites the relative change is slightly higher (93% and 90% for Brockport and Rochester, respectively).

Air concentrations in Boston, Reading, and Quabbin, (urban, suburban, and background locations in Massachusetts) correlate relatively well with one another (Fig. 4-4), suggesting that the source of indium to these locations is not local, but instead comes from long-range transport. (The correlation coefficient used here, r, is the Pearson product-moment correlation coefficient, which is the covariance normalized by the product of the standard deviation of each sample. An r of 1 denotes perfect correlation. This correlation coefficient is symmetric, meaning that it does not change if the x and y variables are interchanged. r = 0.81 for Boston and Quabbin; 0.69 for Boston and Reading; and 0.44 for Reading and Quabbin, low due to one outlier.) Particle-normalized concentrations for these locations correlate less well than the air concentrations (r = 0.54, 0.42, and 0.48, respectively), as is expected due to less significant deviations from the mean for these normalized concentrations. There are several peaks in the air concentration in Massachusetts samples, in February and August, but they reflect only a small change in particle-normalized concentration.

Air concentrations in Rochester and Brockport (urban and rural locations in New York) correlate relatively well with one another (r = 0.62), but show a different pattern from the Massachusetts sites (r = 0.23) (Fig. 4-4). Particle normalized concentrations for the New

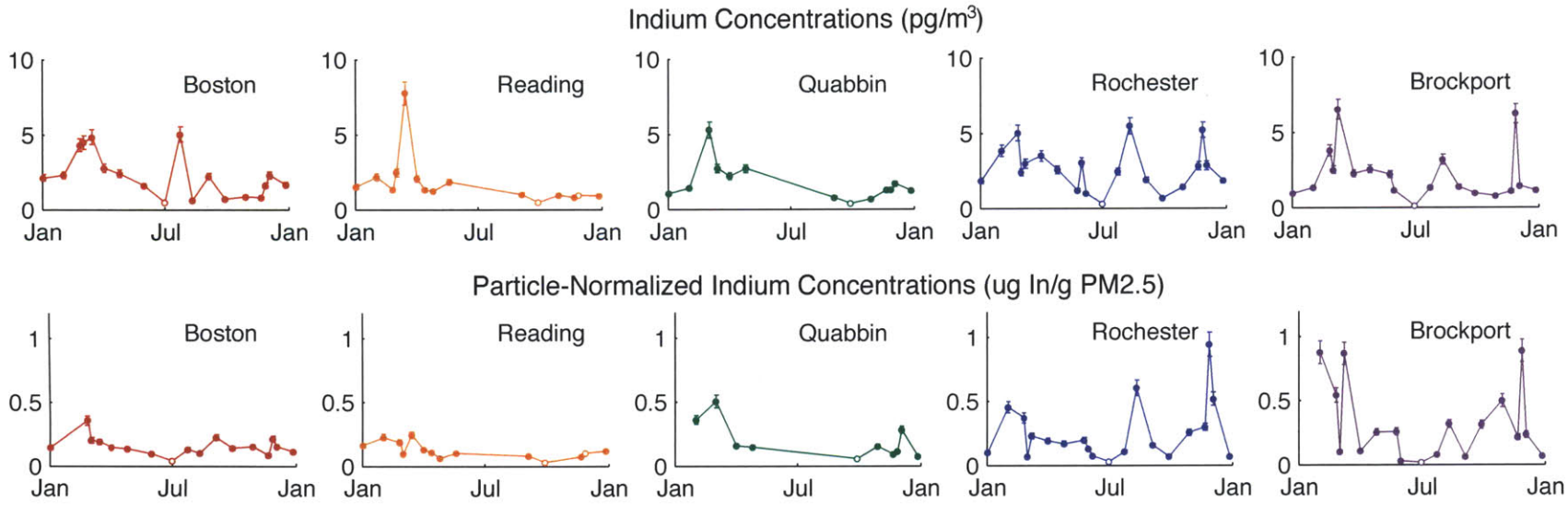

Figure 4-3: Indium air concentrations (a) and fine particle-normalized indium concentrations (b) vary significantly across five locations in the northeastern United States, and over the course of a year. Hollow data points indicate samples that were below the detection limit. Error bars reflect the method uncertainty of 20%, based on multiple digestions of the same sample.

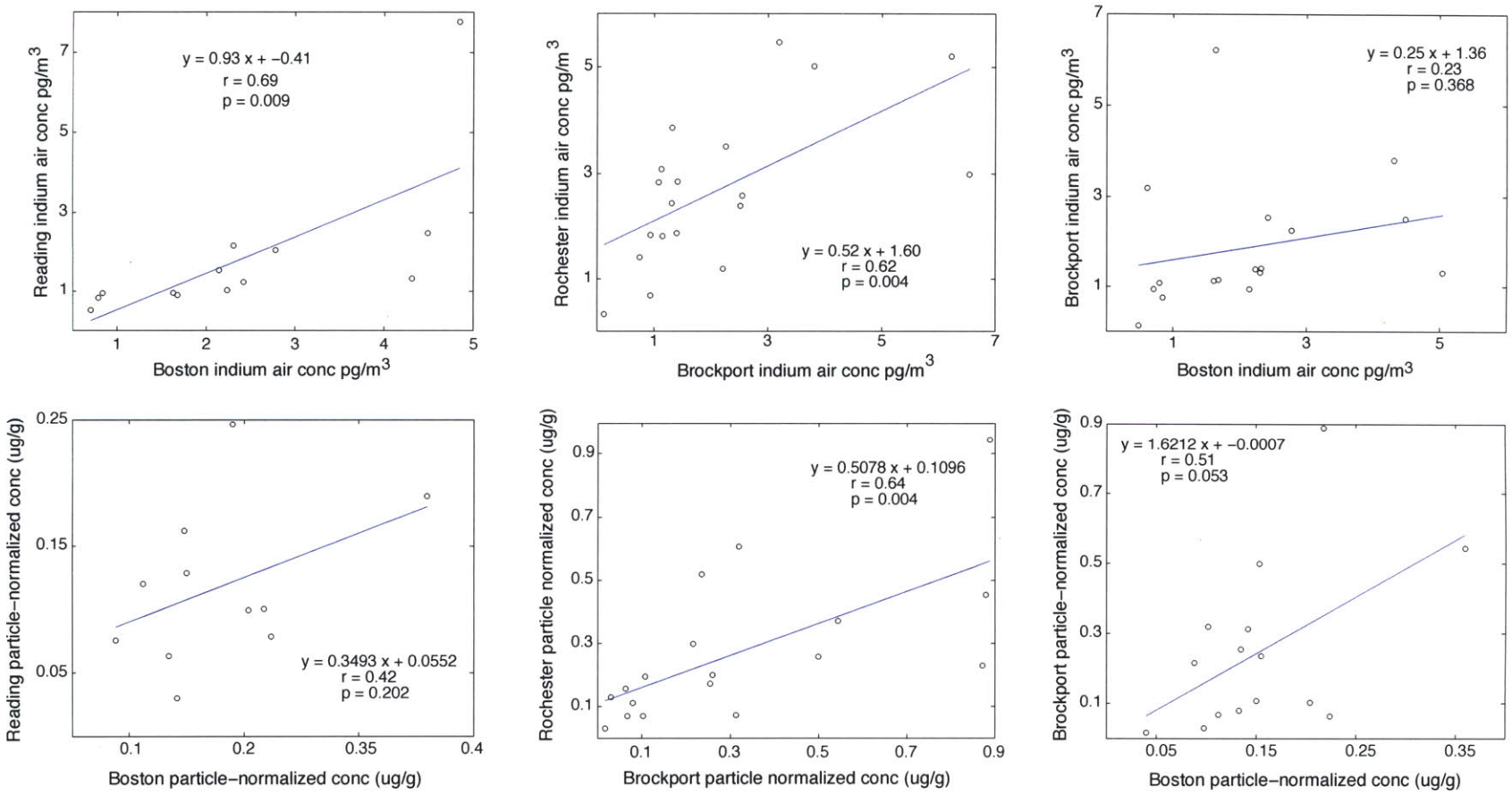

Figure 4-4: Indium concentrations in the Massachusetts sites correlate relatively well with one another, as do the New York sites. The pattern of indium concentrations in the Massachusetts sites are distinct from the New York sites.

York sites also correlate relatively well with one another ($r = 0.64$), and interestingly show some correlation with the eastern Massachusetts sites ($r = 0.51$). The concentration of particulate indium (pg/m^3) in these sites varies significantly throughout the year, and upon normalization to fine particle mass ($\mu g/g$), most of these peaks are retained. Peaks in the particle-normalized indium concentration suggest that there is a different source of indium to this area on the peak days. Alternatively, the low particle-normalized concentrations could reflect a dilution of high particle-normalized source contributions with low particle-normalized source particles.

There is no apparent seasonality to this data, unlike other components of these samples such as organic carbon and mutagenicity ([Pedersen et al., 1999]). Additionally, even at the smallest sampling interval of 6 days, data points are not well autocorrelated (correlations typically <0.25, except for Quabbin air concentrations (0.31) and Reading particle-normalized concentrations (0.39)), indicating that meteorological conditions that affect indium concentrations change more quickly than 6 days.

4.3.1 Atmospheric Back Trajectories

For the Rochester and Brockport data, atmospheric back trajectories show that air is coming from the north or northwest on 6 out of 7 of the days when indium concentrations are >0.35 $\mu g/g$ in at least one of the two locations. (0.35 $\mu g/g$ is a somewhat arbitrary cutoff for a 'peak' value, based on the average concentrations for Rochester and Brockport of 0.25 and 0.3 $\mu g/g$ respectively). The days when particle-normalized concentrations are <0.35 $\mu g/g$ in both locations, back trajectories show that air is coming from the west, southwest, or south on 9 of 11 of the days.

For the Boston site, the story is different. Back trajectories show air coming from the north/northwest and the west/southwest/south on a roughly equal number of days, although there are only three days that have an indium concentration >0.35 $\mu g/g$. (Two of these days show air coming from the northwest, while one shows air coming from the southwest.)

4.3.2 Historical Indium deposition

Analysis of peat cores can have great utility in tracking the history of metal deposition over time. In this case, indium concentrations in Thoreau's bog, MA, were measured, and

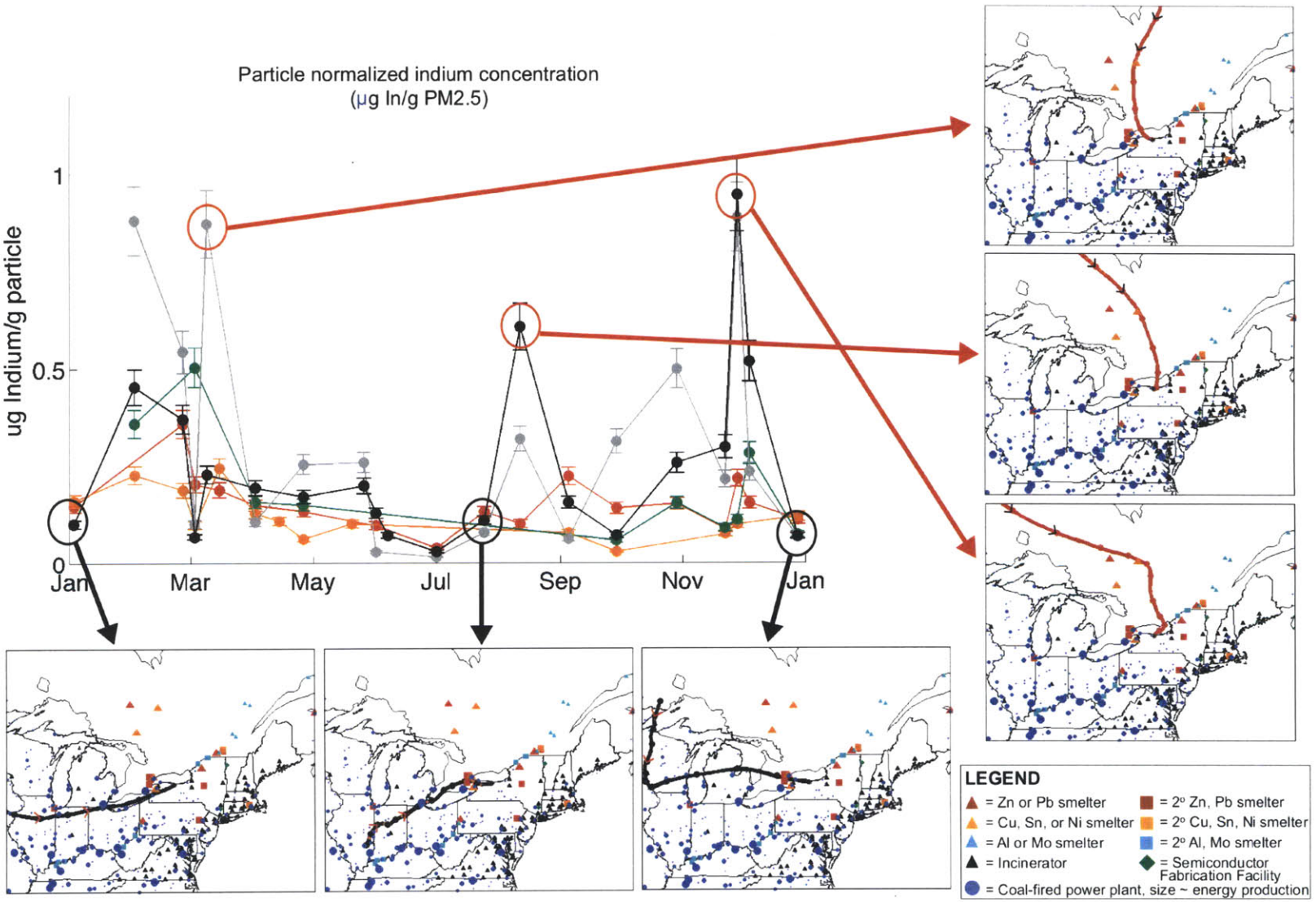

Figure 4-5: Atmospheric back trajectories generated with the HYSPLIT model show that peaks in particle-normalized indium concentration occur on days when air is coming from the north/northwest.

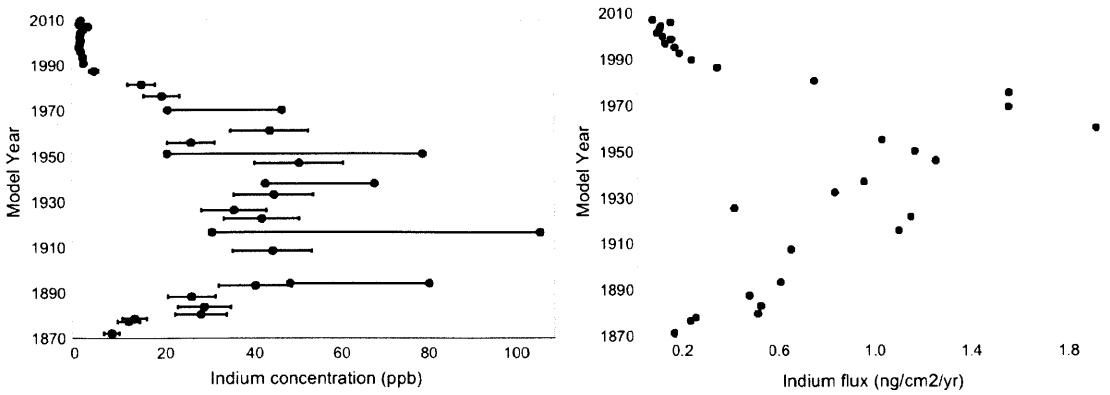

Figure 4-6: Indium concentrations in the bog have been increasing since the early 1900s, peak in about 1940, and decline to the present. Indium fluxes increase from the early 1900s, peak in the early 1970s, then decline rapidly to less than 1900 values.

show indium concentrations peaking in about 1940, then decreasing to the present (Fig. 4-6(a)). A slight increase in concentrations from 2002 to 2007 can also be seen, with low concentrations again in the top 3 cm.

Indium flux to Thoreau's bog increases from the early 1900s, peaks in the 1960s or early 70s, then decreases dramatically to pre-1900 values in 2010 (Fig. 4-6(b)). Again a small increase can again be seen from 2007-2008. It is unclear whether this reflects a significant change in flux to the bog during this time.

Deposition is made up of both wet and dry forms, and is calculated by $J = V_d C_a + V_w C_a = C_a(V_d + V_w)$, where J is the total depositional flux (ng/(cm^2-yr)), V_d is the dry depositional velocity, V_w is the wet depositional velocity, C_a is the air concentration, and the total deposition velocity, $V_t = V_d + V_w$. Indium is expected to deposit in a similar way to ^{210}Pb, and ^{210}Pb total depositional velocities of 0.6-1.9 cm/s have been reported, with a 1 cm/s V_t for the Northeastern United States [Baskaran, 2011, Turekian et al., 1983]. Using this range of deposition velocities and an average air concentration for 1995 (the year air filter samples were collected) of 2.3 pg/m^3, an indium flux of 40–140 pg/(cm^2-yr) can be calculated. The indium deposition observed to Thoreau's Bog in 1995, 150 pg/(cm^2-yr), is just outside of this range. However, PM10 should be included in this calculation, and analysis of a limited number of PM10 samples show that indium concentrations are roughly equal to those in PM2.5 (Figure 4-11, Supplementary Information). If PM10 concentrations are used in this calculation, such that total C_a = PM10 + PM2.5 $\sim$5 pg/m^3, an indium

flux of 90–300 pg/(cm^2-yr) is calculated. The estimated flux to Thoreau's Bog falls within this range.

A similar calculation of ^{210}Pb deposition velocities supports the idea that the fluxes observed in Thoreau's Bog are of the right magnitude: using the range of deposition velocities given above of 0.6-1.9 cm/s, and an estimate of 0.58 mBq/m^3 ^{210}Pb in air from New Haven, CT [Baskaran, 2011] results in a ^{210}Pb flux to the surface of the earth of 11–35 mBq/(cm^2-yr), which agrees well with the ^{210}Pb flux of 20 mBq/(cm^2-yr) measured at the surface of Thoreau's Bog.

The deposition rates suggested from the core can also be used to inform the wide range of depositional estimates (1,000-100,000 t indium/yr) in Fig. 4-1. Assuming that the deposition seen in Thoreau's Bog is applicable globally (although this is likely a poor assumption), multiplying by the surface area of the earth results in a global flux of ~770 t/yr. This is an slightly less than the lowest box model estimate, and may be due to this core not being representative globally—particulate emissions controls in the US and Canada may cause the Northeastern United States to have lower indium concentrations than less-developed countries—or due to an overestimation of atmospheric inputs and depositional fluxes in the box model.

4.4 Discussion

4.4.1 Indium air concentrations

Mean air concentrations reported here of 2.1 pg In/m^3 for all locations agree within a factor of 3 to measurements from 1993 of 6.7 pg/m^3 in PM2.5 in five rural sites across New York [Ames et al., 2000]. Our values are as much as 10x lower than literature values for non-industrial air reported in Smith et al. [1978]. This could be due to several factors, including regional differences, and the fact that total particulate emissions in the United States decreased by 60% between 1970, around the time most of these studies were completed, and 1991 [EPA, 1992, 2000]. Additionally, the literature values report concentrations for all size fractions, not PM2.5. Preliminary evidence from PM10 particles from this study suggest that coarse particles contribute roughly equal concentrations of indium to the atmosphere (Supplementary information, Fig. 4-11), which could explain some of this difference. Differences in sample digestion and analysis techniques between studies are

not likely to contribute to large changes in indium measured. Literature values are given as 'total' indium, measured by neutron activation analysis or x-ray fluorescence, whereas this study reports 'acid-digestible indium. As discussed above, the oxide, sulfide, sulfate, carbonate, and organic fractions of indium should be dissolved in this digest and are thought to contain the majority of indium present in these samples. Further testing of 'total' indium versus that liberated from the digest employed for this study is necessary to confirm the fraction liberated.

4.4.2 Source of indium to atmosphere: Concentration Patterns and Wind Direction

In Rochester and Brockport, there appear to be at least two sources of indium to PM2.5. At least one source, with low particle-normalized indium concentrations, contributes a background of $\sim$2 pg/m^3 indium to the atmosphere. Back trajectories show these samples predominately have air contributed from the west, and the source is hypothesized to be from coal burning in the midwestern United States. Emissions from coal combustion are expected to show a seasonal pattern, with a peak in emissions in the summer, and a less-pronounced peak in the winter [EIA, 2008]; this pattern is not evident in the indium data. Peaks in particle-normalized concentration suggest another source of high-concentration indium that is intermittent. Back trajectories show that these peaks are associated with air that is coming from the north, and the source is hypothesized to be smelters in eastern Canada.

These hypotheses are supported by measurements of indium in coal fly ash and in zinc smelter emissions. Coal fly ash samples from six different types of coal (four bituminous, one sub-bituminous, and one lignite) have shown indium concentrations of 0.14-0.34 μg/g in the < 2.5 μm fraction (Chapter 5). This is similar to the low particle-normalized indium concentrations of 0.2 μg/g seen in all five locations in this study. Alternatively, zinc smelter emissions have been shown to contain 52 μg/g in the < 2.5 μm fraction (Chapter 5). This value is 50x higher than the peak concentrations of indium seen in the New York sites of 1.1 μg/g, suggesting that the peaks in the New York sites are either a different source entirely, or may be a mixture of a smelter source with other lower particle-normalized concentration sources.

In the Massachusetts sites, there are no high particle-normalized indium concentrations.

If smelters are indeed the high concentration source, this may be due to the further distance of these sites from Canadian smelters, allowing particles emitted from these sources to disperse sufficiently to blend in with the background signal. The presence of peaks in air concentration at the Massachusetts sites despite the relatively constant particle-normalized concentrations suggest that significant variations in these source(s) can occur. Again, coal is hypothesized to be the main source contributing indium to the Massachusetts sites.

4.4.3 Source tracking: Enrichment Factors

In order to determine if these average concentrations are due to crustal material or whether they come from, e.g. volcanic activity or industry such as coal-burning or smelting, one can examine indium's enrichment relative to aluminum. Enrichment factors (EF) for indium in our samples ($EF = (In/Al)_{sample}/(In/Al)_{crust}$) are for the most part much greater than 1, indicating that the observed background indium concentration is not due to dust (Supplementary data, Fig. 4-12). Only one of the points (Brockport, on July 2) was near 1. In all other cases the EF is greater than 15, and in some cases it is >1000, indicating a predominately high-temperature source of indium to the atmosphere in this region.

A study of indium in 6 different cities in Europe and 1 in the United States found enrichment factors of 4–140 relative to soil values [Heindryckx and Dams, 1979], supporting the idea that a non-dust input of indium dominates its atmospheric concentration in these areas, even when the coarse size fraction is included. Studies of indium in incinerator emissions found enrichment factors of 120–2300 [Greenberg, 1976], supporting the idea that high temperature processes contribute to the high enrichment factors that we see in our northeastern US samples.

Indium has been shown to be enriched in volcanic emissions [Hinkley et al., 1994, 1999, Hinkley and Matsumoto, 2001, Matsumoto and Hinkley, 2001]. Our own work has shown enrichment factors of indium in PM2.5 fly ash from coal combustion of 3–5 (Chapter 5), and data from EPA's SPECIATE database [Reff et al., 2009, EPA, 2011] suggest that lead smelting results in enrichment factors of 10^5. This may be further evidence that the highest concentrations of indium seen in these samples, which have the highest enrichment factors, may be associated with a smelter source, while the bulk of the samples with moderate concentrations and moderate enrichment factors, may be associated with a source such as coal emissions. However, without a more detailed source-tracking model, we cannot determine

which combination of these sources contributes to the background indium concentrations that we see in this region.

4.4.4 Source tracking: Historical Indium Deposition Patterns

Historical indium flux from the atmosphere, as reflected in Thoreau's Bog, may help in the identification of the source of indium to this region.

The indium flux to Thoreau's bog increases from the late 1800s to the early 1970s, at which point it drops dramatically. The same type of profile has been seen previously for indium in a Swedish lake sediment, though 2002 concentrations remained 3x higher than 1900 values [Grahn et al., 2006]. It is possible that watershed inputs of indium to the Swedish lake account for this difference. A low resolution ombrotrophic bog core in Norway also shows a similar profile [Steinnes et al., 2003]. This type of profile is also typical of lead, albeit with the peak offset to the late 1970s, due to its use as a gasoline additive and subsequent phasing out in the late 1970s (e.g. [Lima et al., 2005]). Lake cores from remote areas in Massachusetts show similar trends for Cd [Norton et al., 2007], and ombrotrophic bog profiles from Europe show similar trends for V, As, and Sb [Cloy et al., 2009, 2005, 2011], suggesting that metals that are released from stationary sources show similar trends due to increases in consumption and production over the 20th century, and decreases in particulate emissions post 1970s. In Thoreau's Bog specifically, this type of trend has been seen with lead [Hemond, 1980], while the story is quite different for platinum, which increases in concentration in the top 5 cm of the core, presumably due to its extensive use in catalytic converters [Rauch et al., 2004].

The dramatic decrease in indium flux to the bog appears to coincide with increased particulate control technologies for stationary sources (Fig. 4-7), regulated in the United States beginning in 1971 with the establishment of the National Ambient Air Quality Standards for Total Suspended Particles (a program of the Clean Air Act of 1970) [EPA, 2012a,b]. Canada did not federally regulate particulate matter until 2000, when the Canada-wide Standards for Particulate Matter (PM) and Ozone was signed by all provinces except Quebec. However, Canada has had recommended PM levels since the National Ambient Air Quality Objectives were established in the early 1970s, and there have been regulations at the provincial level that control particulate matter emissions since the early 1980s: Ontario's General Air Pollution Regulation was established in 1990 and Quebec's 'Regulation

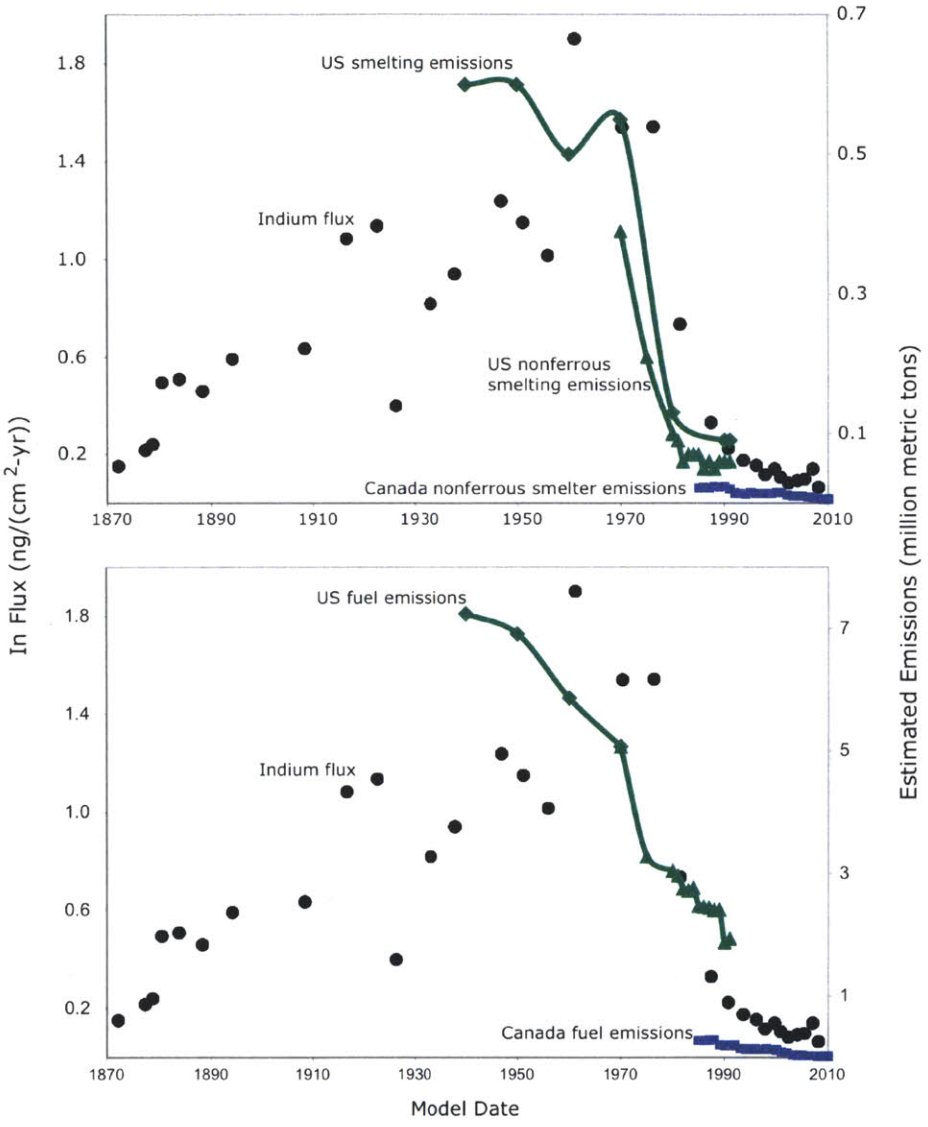

Figure 4-7: The drop in indium flux to Thoreau's Bog since the early 1970s coincides well with estimated particulate emissions from non-ferrous smelting (a) and fuel combustion (b). Data comes from [EPA, 2000] for the United States and [Environment Canada, 2012] for Canada.

Respecting the Quality of the Atmosphere' was established in 1981 [Minerals and Metals Division, 2002]. Thus the trend toward PM control appears to be similar in Canada and the United States.

Indium appears to correlate better with smelting emissions estimates than with fuel emissions predictions, although there is uncertainty associated with these emissions estimates that does not allow a definitive assignment of the best correlation. First, emissions in each case are estimated by the EPA based on historical data on emissions rates, fuel consumption, and the assumption that 0% of these stationary sources employed PM control technologies prior to 1974, and 100% of them employed PM control technologies after 1974 [EPA, 2000]. It is unclear how valid this assumption is due to lack of data on the historical adoption of PM control technologies. Additionally, Canadian emissions estimates are only available since 1985 [Environment Canada, 2012]. From 1985 onward, Canadian fuel emissions are only 10% of US fuel emissions, suggesting that the emissions profile for fuel would not be changed much with the addition of Canadian estimates. Canadian smelting emissions estimates since 1985 are as much as 40% of US smelter emissions estimates, meaning that the overall emissions profile may be altered with the addition of Canadian emissions estimates prior to 1985. However, because of the similarities in PM control regulations in the United States and Canada, this profile is not likely to shift substantially with the addition of Canadian emissions estimates prior to 1985.

Note that total fuel emissions are plotted rather than specific emissions from coal combustion. This is due to the fact that a breakdown by individual fossil fuel is not available prior to 1970. In 1970, coal was 70% of the total emissions from stationary source fuel combustion. The fraction of coal dropped to 56% in 1975, and then to about 30% in the remaining years; wood combustion emissions have not declined over the past 35 years, and therefore are becoming a larger fraction of total fuel emissions as the other fuel source emissions decline. The assumption is that prior to 1975, coal emissions accounted for the majority of the total fuel emissions. Note also that categories for US smelter emissions are slightly different for the 1940–1991 dataset (smelters) and the 1991–2009 data set (nonferrous smelters). And although fuel emissions are an order of magnitude higher than smelter emissions, average concentrations in ore are 500x larger than in coal, suggesting that the smelter emissions could still account for the indium deposition seen.

4.4.5 Source tracking: other metal profiles

Clues as to the source of indium to Thoreau's Bog may be gleaned from similarities to other metal profiles in the bog. Here a comparison is made with Zn, As, and Cd as markers of smelter emissions, V as a marker of residual oil combustion, Ba as a marker of coal emissions, and Pb as a marker of leaded gasoline use. There are similarities between the depth profiles of each of these metals and indium (Figures 4-8, 4-9).

In order to get a quantitative measure of how well these profiles match, indium can be plotted versus each of these other metals, and a correlation coefficient can be determined (again the Pearson product-moment correlation coefficient, described above) (Figure 4-10). Squaring this r value gives a measure of the fraction of variance in Y that is explained by X in a simple linear regression. For these metals, arsenic has the closest profile match to indium, with an r value of 0.88 and an r^2 of 0.77. Arsenic has been shown to be associated with smelting emissions [Sturges and Barrie, 1989, Rahn and Lowenthal, 1985], and is in fact a byproduct of the same sulfide ores of which indium is a byproduct [Loebenstein, 1994]. The other two metals that are associated with smelting, Zn, and Cd, have lower correlation ($r = 0.46$ and $r^2 = 0.21$ for Zn; $r = 0.65$ and $r^2 = 0.42$ for Cd). Cadmium is a byproduct of sulfide ores and zinc is a primary smelted ore. Zinc is enriched in the top of the core, possibly suggesting some mobility and plant uptake [Weiss et al., 2007]. Vanadium, often used as a marker of residual oil combustion [Pacyna, 1986], correlates relatively well with indium concentrations ($r = 0.74$ and $r^2 = 0.55$), suggesting that oil combustion may contribute to indium concentrations in Thoreau's Bog. Lead has some correlation with indium ($r = 0.66$ and $r^2 = 0.44$), but correlates less-well than As and V. Lead peaks in 1981, according to this dating scheme, 10–20 years after indium peaks. In other cores, lead has been shown to peak in the late 1970s, coincident with the phase-out of leaded gasoline [Lima et al., 2005], and in agreement with the timeline for lead deposition seen in Thoreau's Bog. Ba does not correlate well ($r = 0.34$ and $r^2 = 0.12$).

Note that metal mobility in this core could be an issue for these metals. Indium mobility is likely to be low (< 7 cm in 70 years; Chapter 3), there is some evidence that As is immobile in peat [Cloy et al., 2009], and Pb is typically considered immobile [Shotyk et al., 1998, Novak et al., 2011], but the other metals have unknown mobility. Additionally, because trace-metal-clean techniques were not used except for indium, the absolute fluxes for these

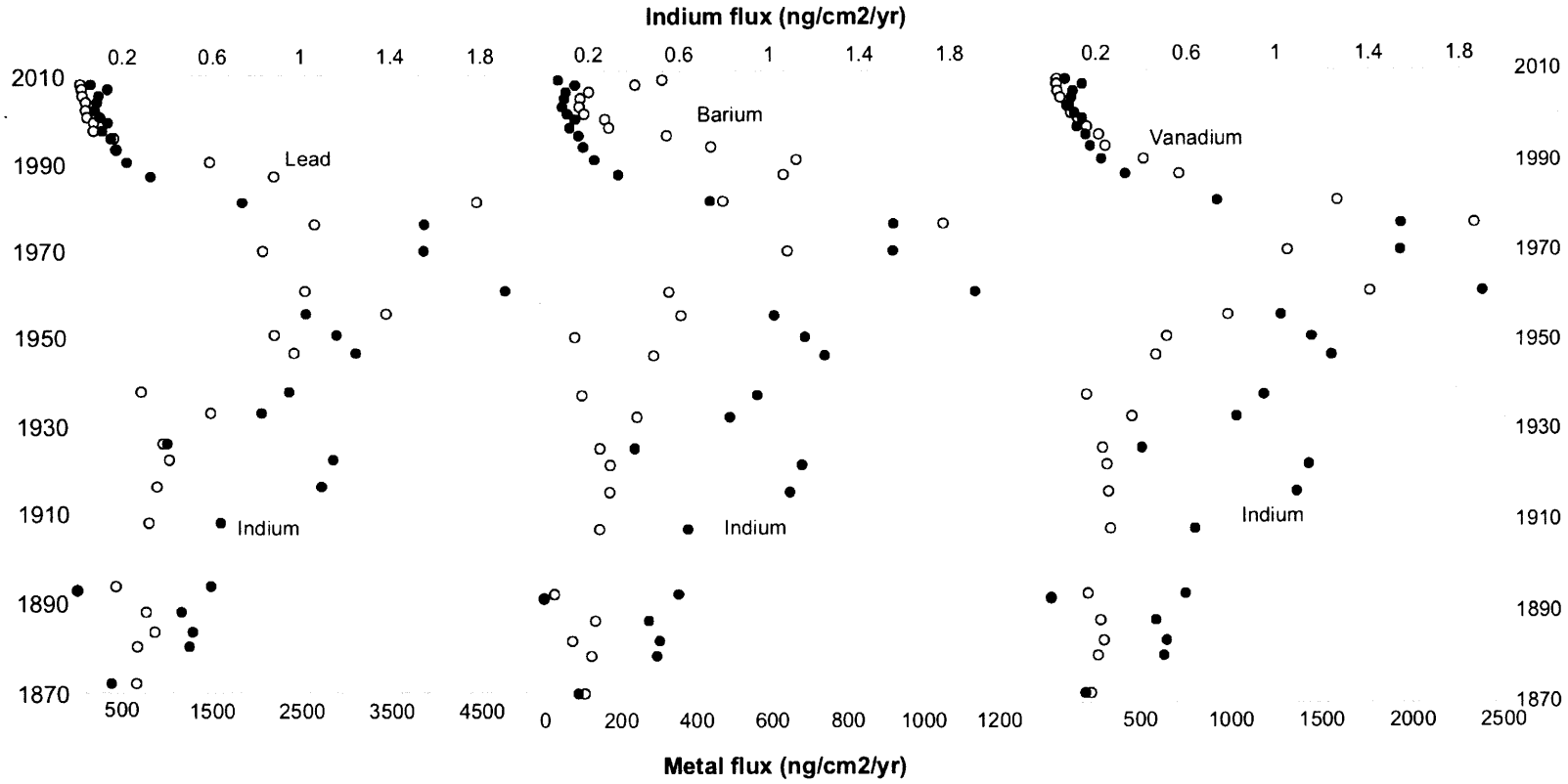

Figure 4-8: Indium's historical flux to Thoreau's Bog shows similarities with Pb, Ba, and V fluxes.

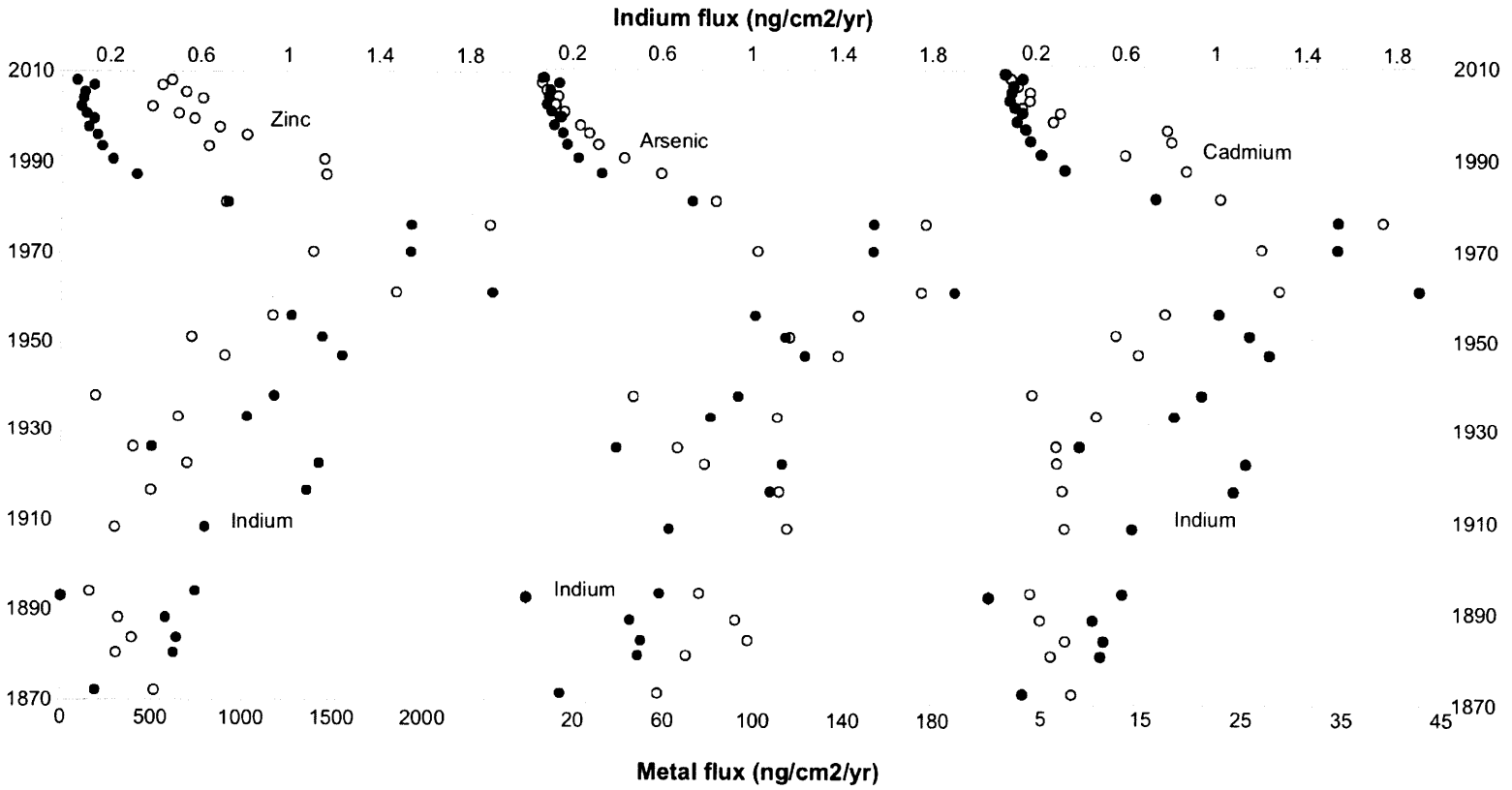

Figure 4-9: Indium's historical flux to Thoreau's Bog shows similarities with Zn, As, and Cd fluxes.

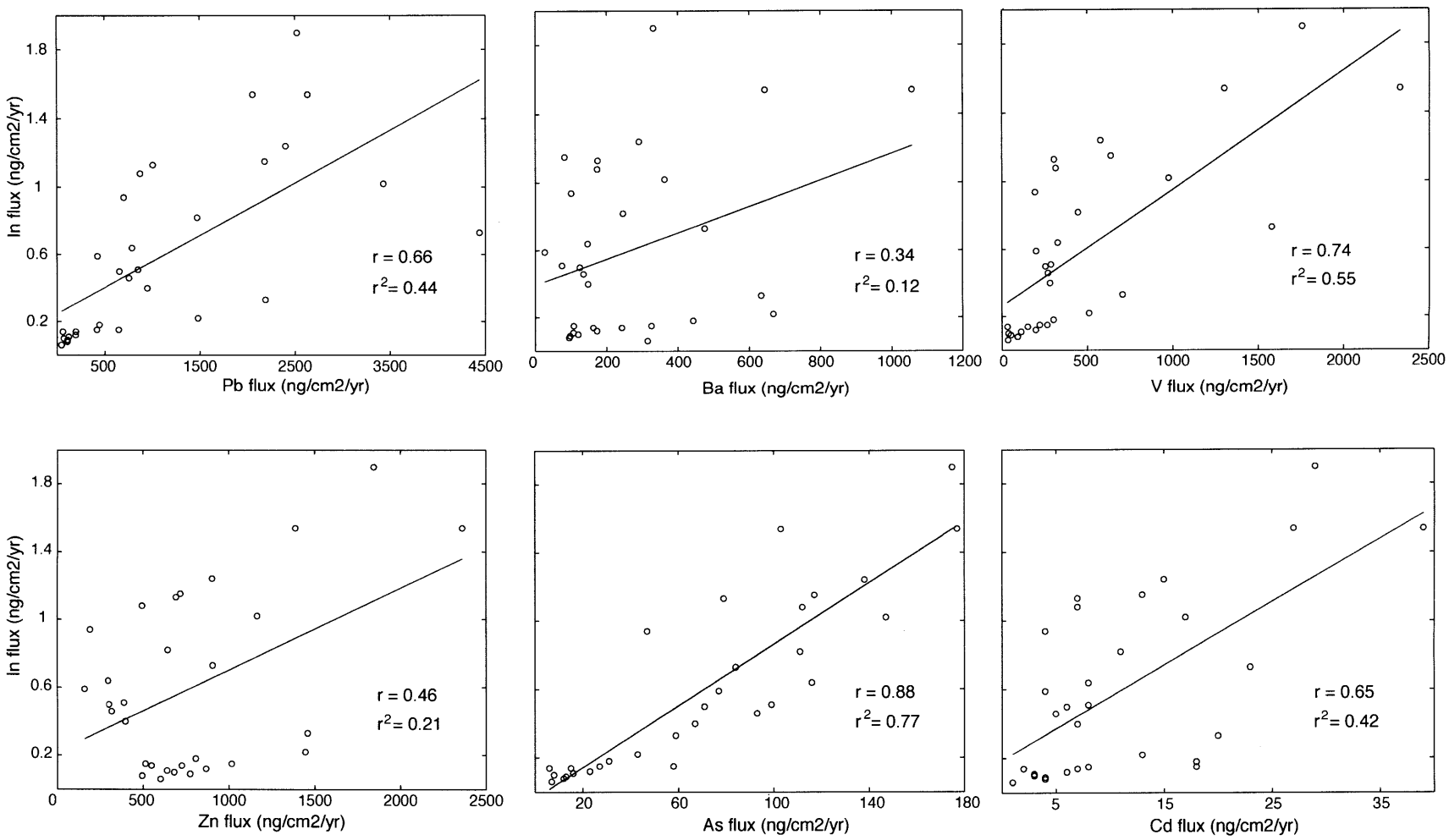

Figure 4-10: Indium's historical flux to Thoreau's Bog shows similarities with other metal fluxes, specifically arsenic.

metals may have large uncertainty, but their profiles should be valid, as discussed above.

4.5 Conclusions

This study of indium concentrations in the atmosphere in the Northeastern United States has shown mean PM2.5 concentrations of 2.1 pg/m^3, with deviations up to 8 pg/m^3, and particle-normalized concentrations of 0.2 μg In/g PM2.5, with deviations up to 0.95 $\mu g/g$. Peaks in particle-normalized concentrations in the New York sites suggest that there is a distinct source supplying indium to the atmosphere on those days, and back trajectory analysis has shown those peaks to be associated with air traveling from N/NW of the New York sites.

The hypothesis that smelters in Eastern Canada are a large source of indium to this region is supported by the literature, and by historical indium deposition patterns observed in a peat core from Concord, Massachusetts. The flux of indium to this bog increased since the early 1900s, peaked in the early 1970s, and then declined dramatically to pre-1900 values by 2010. This profile coincides well with the estimated particulate emissions from smelting and fuel combustion in the United States and Canada. Arsenic fluxes to the bog show a similar pattern, and may be further evidence of the large contribution of smelting emissions of indium to the atmosphere in this region.

There is still much to be learned about industrial sources of indium to the atmosphere, and its subsequent cycling and deposition. A more rigorous atmospheric model, along with an investigation of the other metals present in these atmospheric samples, may help constrain the sources of indium to these sites. More detailed studies of specific industrial emitters will also improve our understanding of the impact of human activity on the natural cycling of indium. Finally, research into the influence of indium deposition on aquatic indium concentrations will be necessary to fully assess the impact of human activities on the environment.

4.6 Acknowledgments

We gratefully acknowledge Daniel Pedersen, John Durant, and Lynn Salmon for providing the atmospheric particulate samples for this study, data for metals besides indium in these samples, and consultation. Rick Kayser and Ed Boyle provided help with metals analysis,

laboratory space, and trace-metal clean acids. Carrie Keach helped to develop the corer used in this study. Hanan Karam, Amy Mueller, Charuleka Varadharajan, Jennifer Apell, and Robin Zhao helped with the retrieval of peat cores. Funding was provided by NSF Grant CBET-0853866 and an MIT Earth Systems Initiative Ignition Grant. Additional support was provided by an MIT Earth Systems Initiative Linden Graduate Fellowship and an MIT Energy Initiative Martin Family Graduate Fellowship for Sustainability to S.J.W., and by the William E. Leonhard Professorship to H.F.H.

4.7 Supplementary Information

4.7.1 Figures and Data Tables

The following figures show indium concentrations in the coarse air particulate fraction, and indium's enrichment factor in the atmospheric samples. The raw data presented in this chapter for indium concentrations in PM2.5 in five locations in the Northeastern United States are included in Table 4.1.

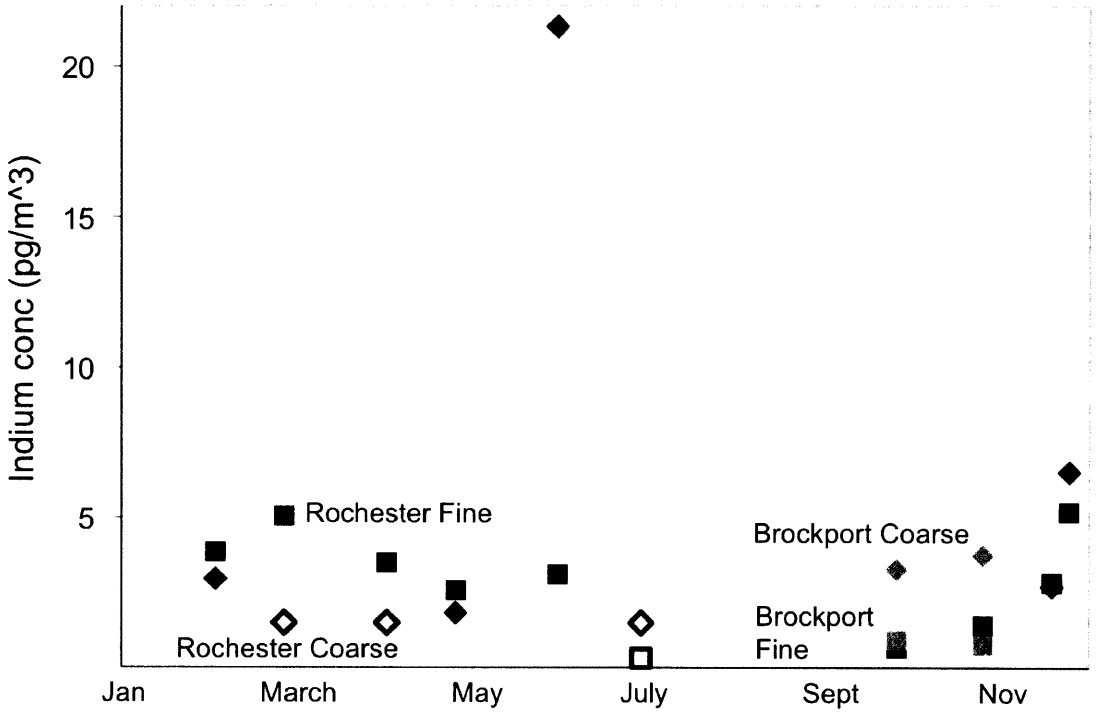

Figure 4-11: Indium concentrations contributed by coarse particles (PM10) are similar to concentrations contributed by fine particles (PM2.5). Hollow data points were below detection limit.

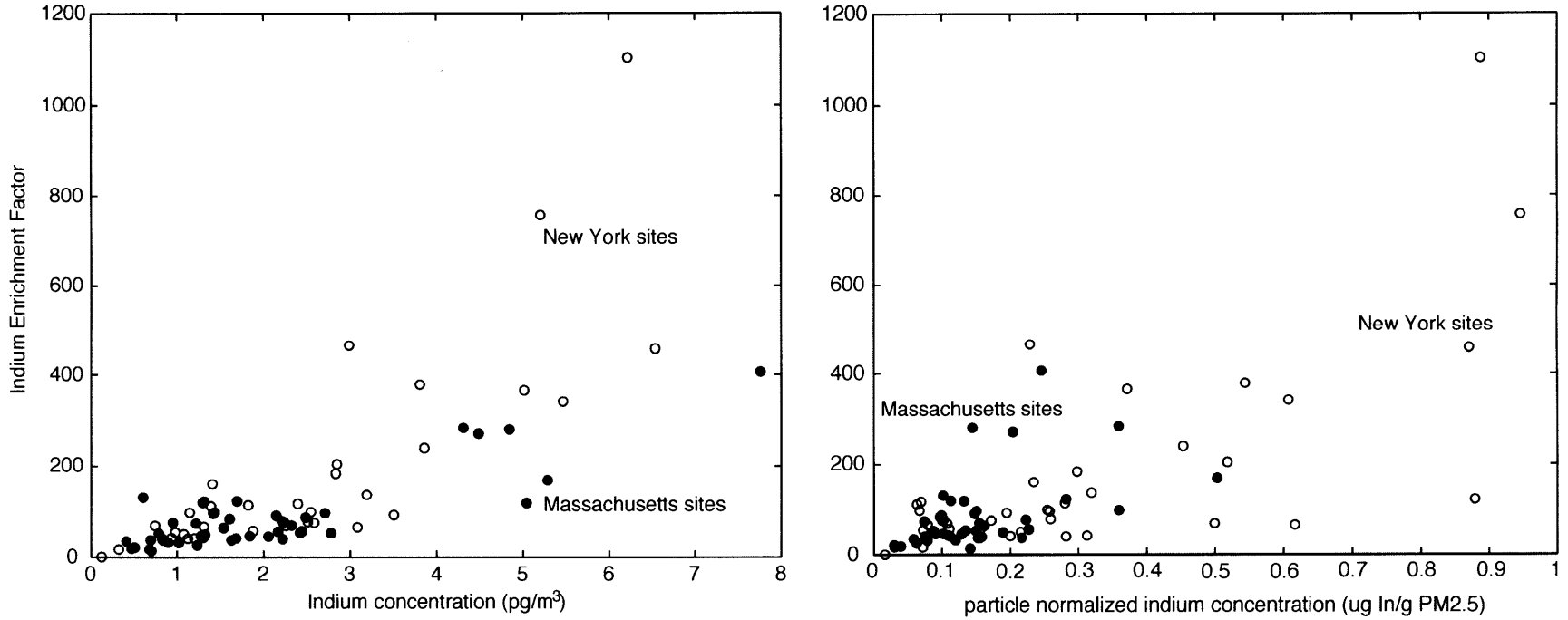

Figure 4-12: Enrichment factors for indium ranging from 15-1100 suggest that the source of indium to this region is likely not dust. Air concentration of indium versus Enrichment Factor (a) is relatively linear, with higher air concentrations generally reflecting larger enrichment factors. Particle-normalized indium concentrations correlate less well with the Enrichment Factor (b) but higher particle normalized concentrations still tend to reflect higher Enrichment Factors.

Table 4.1: Indium atmospheric concentration data for PM2.5 in five locations in the north-eastern United States.

	Boston		Quabbin		Reading		Brockport		Rochester	
Date	pg/m^3	$\mu g/g$	pg/m^3	$\mu g/g$	pg/m^3	$\mu g/g$	pg/m^3	$\mu g/g$	pg/m^3	$\mu g/g$
1/3/95	2.15	0.15	1.06	-	1.54	0.16	-	-	0.94	-
2/2/95	2.31	-	1.44	0.36	2.17	0.23	1.32	0.94	3.86	0.40
2/26/95	4.39	0.37	-	-	1.34	0.19	3.83	0.50	5.06	0.38
3/4/95	4.49	0.20	5.29	0.50	2.49	0.10	2.52	0.10	2.40	0.07
3/10/95	-	-	-	-	-	-	6.54	0.87	2.99	0.23
3/16/95	4.85	0.19	2.74	0.08	7.76	0.25	-	-	-	-
4/3/95	2.78	0.15	2.22	0.16	2.06	0.13	2.26	0.11	3.51	0.19
4/15/95	-	-	-	-	1.31	0.11	-	-	-	-
4/27/95	2.42	0.13	2.71	0.15	1.24	0.06	2.55	0.25	2.59	0.17
5/21/95	-	-	-	-	1.84	0.10	-	-	-	-
5/27/95	-	-	-	-	-	-	2.21	0.26	1.20	0.20
6/2/95	1.69	0.10	-	-	-	-	1.13	0.03	3.12	0.13
6/8/95	-	-	-	-	-	-	-	-	0.98	0.07
7/2/95	0.48	0.04	-	-	-	-	0.13	0.02	0.32	0.03
7/26/95	5.04	0.13	-	-	-	-	1.31	0.08	2.45	0.11
8/13/95	0.61	0.10	-	-	-	-	3.19	0.32	5.45	0.61
9/6/95	2.24	0.22	0.79	-	1.02	0.08	1.40	0.06	1.88	0.16
9/30/95	0.71	0.14	0.41	0.06	0.51	0.03	0.94	0.31	0.69	0.07
10/30/95	0.84	0.15	0.70	0.16	0.95	-	0.75	0.58	1.42	0.31
11/23/95	0.80	0.09	1.28	0.09	0.83	0.08	1.08	0.19	2.84	0.30
11/29/95	1.63	0.22	1.30	0.11	0.96	0.10	6.22	1.07	5.21	0.72
12/5/95	2.32	0.15	1.70	0.28	-	-	1.41	0.19	2.85	0.39
12/29/12	1.68	0.11	1.23	0.07	0.90	0.12	1.15	0.07	1.83	0.07

Chapter 5

Tracking the Source of Indium to the Atmosphere in the Northeastern United States

5.1 Introduction

Mean indium concentrations in PM2.5 at 5 sites from Boston, MA to Rochester, NY, are 2.1 pg/m^3, and vary over the course of a year, with deviations up to 8 pg/m^3 (Chapter 4). Concentrations normalized to PM2.5 mass show that Massachusetts sites average 0.2 μg In/g PM2.5 over the course of a year, with deviations up to 0.5 μg/g. The New York sites have an average of about 0.2 μg/g, but show peaks up to 1.1 μg/g. As confirmed by back trajectory analysis, these peaks in the New York sites tend to occur on days when air to the site is traveling from the north, whereas non-peak days tend to occur when air is traveling from the west.

Because of the locations of nonferrous smelters and coal plants in the United States and Canada (Fig. 5-2), and indium's elevated concentrations in sulfide ores, we hypothesize that nonferrous smelters in Canada supply high concentrations of indium to the atmosphere in the New York sites. Previous studies support this hypothesis. For example, Sturges and Barrie [1989] measured In, Pb, Zn, and several other metals in total particulate matter at a rural site in southern Ontario over a 5-day period. During this time, air changed direction from the west, to the north, and back to the west. On days when wind came from

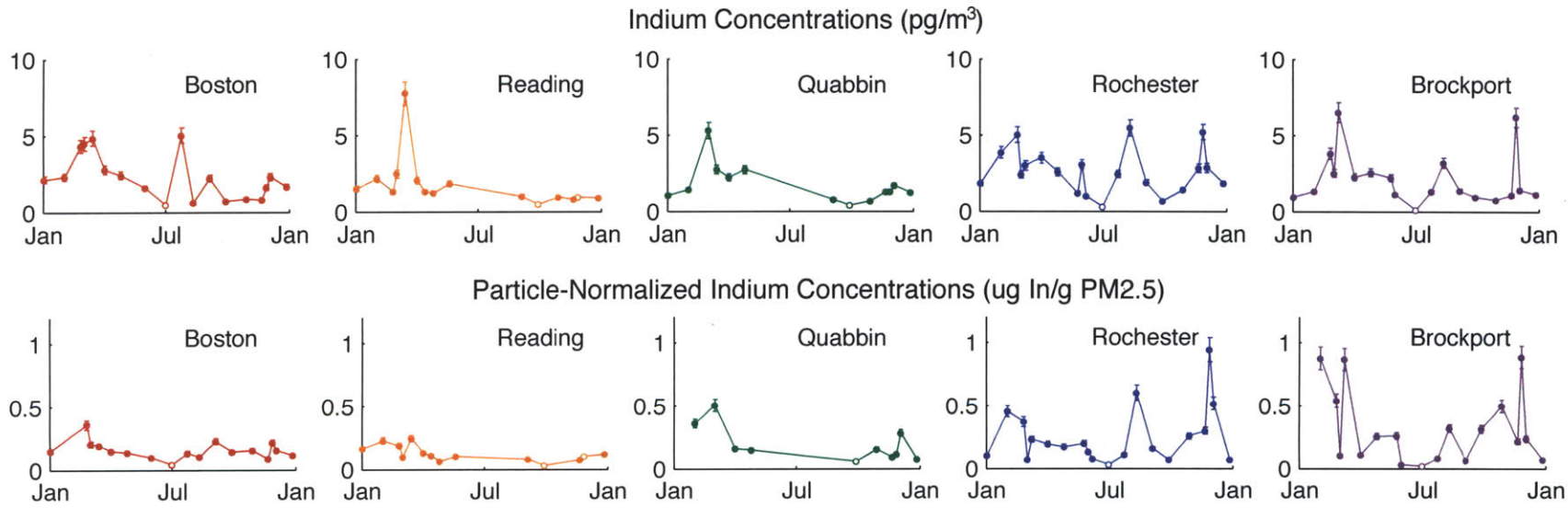

Figure 5-1: Indium air concentrations (a) and fine particle-normalized indium concentrations (b) vary significantly across five locations in the northeastern United States, and over the course of a year. Hollow data points indicate samples that were below the detection limit. Error bars reflect the method uncertainty of 20%, based on multiple digestions of the same sample.

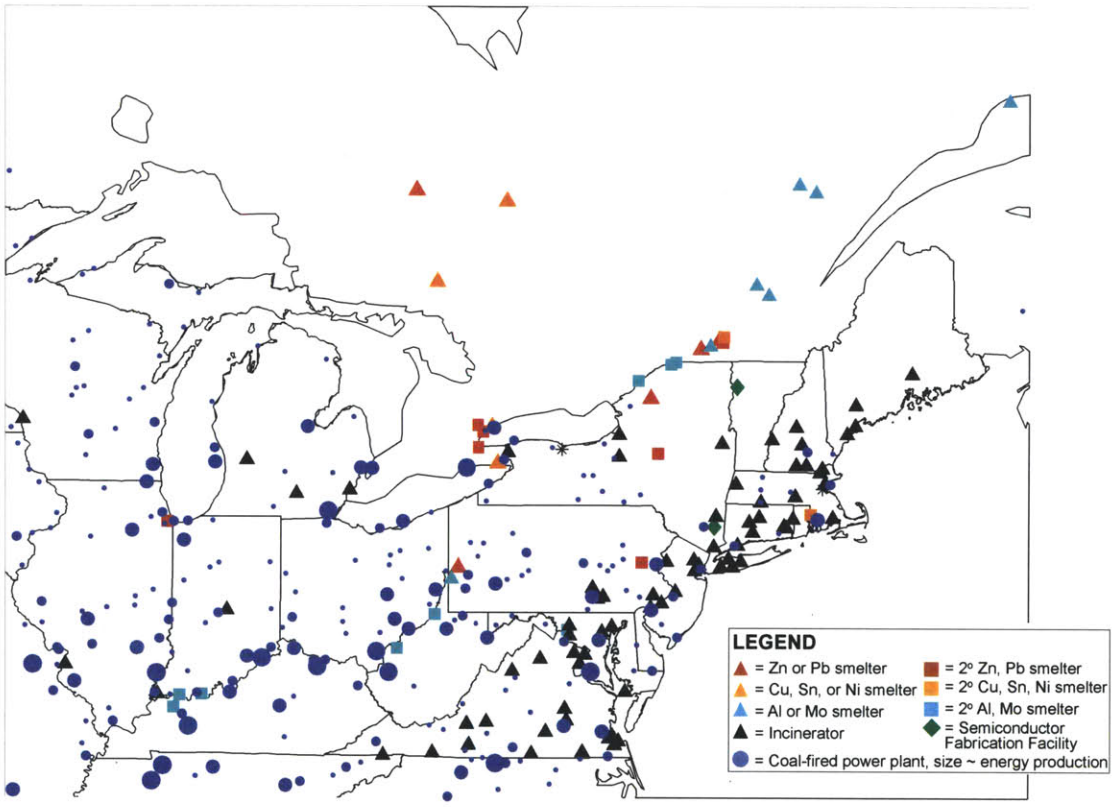

Figure 5-2: Location of potential indium sources in the Northeastern United States and Eastern Canada, including smelters and coal-fired power plants.

the north, Pb 207/206 ratios reflected a smelting source, and correlated well with indium concentrations, which were as high as 20 pg In/m^3. Rahn and Lowenthal [1985] determined that indium was 20–100x higher in total particulate matter when air is coming from the nonferrous smelter region of Ontario and Quebec.

Indium has also been linked to smelting sources by several researchers who used factor analyses or receptor modeling to attribute source contributions. For example, Ames and colleagues used factor analysis to attribute the mass of indium at each of five rural New York sites to the most probable sources during the course of the two-year study [Olmez et al., 1997, Ames et al., 2000]. Depending on the site, they attribute from 35-79% of the PM2.5 indium to smelter sources, 0-25% to a 'Canadian Regional' source that originates from the N/NW, 0-27% to a 'US Regional' source that originates from the W/SW, and 0-12% to a crustal source. Biegalski et al. [1998] measured indium in three different sites in southern Ontario, and used Positive Matrix Factorization (PMF) to show that indium is most closely associated with Sn, As, or as its own factor (unassociated with other metals) at these sites. Based on the overall chemical makeup of the source profiles determined by PMF, they attribute each of the indium-containing source signals to smelting.

In order to further test the hypothesis that smelters are contributing high concentrations of indium to the atmosphere at our study sites, here we present further analysis of the chemistry of air filter samples from the northeastern United States. Indium concentrations are compared to other metal concentrations that have been measured in these samples to show that the chemical signature of air from the north is different than the chemical signature of air from the west. We additionally present measurements of indium concentrations in coal and zinc smelter emissions. Combined with PM2.5 emissions data, these measurements allow a calculation of indium emissions from these processes in the United States and Canada, and provide a reference for the concentrations and ratios of metals contributing to the values in New York and Massachusetts. Lastly, the results of two forms of receptor modeling, Positive Matrix Factorization and Chemical Mass Balance, are presented.

5.2 Methods

5.2.1 Air filter samples

Air filters were collected by Pedersen and colleagues from five locations across the Northeastern United States as discussed previously ([Pedersen et al., 1999, Salmon et al., 1999], Chapter 4). The indium data presented here was analyzed by our group, and is discussed in more detail elsewhere (Chapter 4).

For the other metal analysis, Salmon et al. [1999] used a cyclone separator to collect particles with diameters less than 2.2 μm on 47 mm polytetrafluoroethylene (PTFE) membrane filters. This sampling took place on the same days as the sampling of the quartz fiber filters used for indium analyses, for 24 hours, at a flow rate of 25 L/min. 38 elements were then measured by X-ray fluorescence [Salmon et al., 1999]. Roughly 20 of these elements were below the detection limits of the instrument; those that were above detection limit were used for our subsequent correlation analysis and receptor modeling. Sulfate was measured by Salmon et al. 1999 by the extraction of a second set of PTFE filters with deionized water and subsequent analysis by ion chromatography. Nitrate was not used for the present modeling due to >50% of the samples being below detection limit, and due to documentation by Salmon et al. [1999] that their measurement technique is known to underestimate the true nitrate concentrations present.

5.2.2 Back Trajectory Analyses

As described in Chapter 4, the National Oceanic and Atmospheric Administration's HYbrid Single Particle Langrangian Integrated Trajectory model (HYSPLIT4) [Draxler, 1999, Draxler and Rolph, 2012, Rolph, 2012] was used to generate back trajectories for each day for which indium was measured. A complete description of the model is given in Draxler and Hess [1998, 1997]. The online version was used to generate back trajectories that ran for 48 hours, each starting at 12:00 PM for the indium measurement date and at a height of 500 m. Archived meteorological data from the Nested Grid Model (NGM) database was used, except for several dates when data was missing from this database, at which time the REANALYSIS database was used. Tests showed that these two databases produced similar results.

5.2.3 Correlation of indium with other metals

Correlations were determined between indium concentrations and other metals, using particle-normalized concentrations. Data was separated by location and by wind direction. The angle from which air was traveling was calculated at -24 hours in the back trajectory. The trajectory was considered to be coming from the north (e.g. from the smelter region of eastern Canada) if it was between 292.5°and 22.5°(with due N defined as 0°). It was considered to be coming from the west from 180°to 292.5°. Regression lines and their standard deviations were generated by a Monte Carlo technique, whereby random subsets of the data were selected and linear regressions were calculated for each subset. The mean and standard deviation of these subsets were plotted as the mean regression line for the complete data set and its $\pm 1\sigma$ uncertainty.

The Kolmogorov-Smirnov test was used to obtain a statistical measure of how much the two wind directions differ with respect to their In:metal ratios. The Kolmogorov-Smirnov test is a nonparametric test to determine the probability that two data sets of unknown distribution are drawn from the same distribution [Press et al., 1992]. Both data sets are plotted as a cumulative distribution function, $S_{N_1}(x)$ and $S_{N_2}(x)$, and the maximum value of the absolute difference between the two distribution functions, D, is determined: $D = \max |S_{N_1}(x) - S_{N_2}(x)|$.

The significance of D (i.e. the probability that the two data sets are the same) can be calculated as

$$Q_{KS}(\lambda) = 2\sum_{j=1}^{\infty}(-1)^{j-1}e^{-2j^2\lambda^2} \tag{5.1}$$

with the limits of $Q_{KS}(0) = 1$ and $Q_{KS}(\text{inf}) = 0$. The significance level of a calculated D can be approximated by:

$$Probability(D > observed) = Q_{KS}([\sqrt{N_e} + 0.12 + 0.11/\sqrt{N_e}]D) \tag{5.2}$$

and

$$N_e = \frac{N_1 N_2}{N_1 + N_2} \tag{5.3}$$

where N_1 and N_2 are the number of data points in the first and second distribution, respectively. This approximation tends to be good for $N_e \geq 4$, and is asymptotically accurate as

N_e gets large [Press et al., 1992].

5.2.4 Source Emissions Characterization

Zinc smelter emissions

Particulate emissions from a hydrometallurgical zinc smelter in Canada were sampled by Environment Canada and supplied to the authors for the measurement of indium. The samples were collected with a sampling train as described in the EPA Method for Sampling Particulate Matter from a Stationary Source (201A). A single cyclone was used to separate >2.5 μm particles from <2.5 μm particles. The >2.5 μm particles were collected from a catch cup and the interior surfaces of the cyclone walls. The <2.5 μm particles were collected from the probe and filter of the sampling train, downstream of the cyclone, by rinsing these surfaces with deionized water and acetone into glass jars. Samples were then dried.

The sample masses were reported by Environment Canada, and the entire mass of PM2.5 supplied was transferred to teflon beakers by rinsing with deionized water. These samples were then dried on a hotplate while covered with acid-washed glass ribbed watchglasses. The samples were digested with double distilled concentrated nitric acid and 70% trace-metal grade perchloric acid (Fisher Chemical TraceMetal Grade), before measuring metals using an Inductively-Coupled Plasma Mass Spectrometer (ICP-MS). The procedure was modeled after EPA Method 3050B with adjustments to use perchloric acid for the oxidation of organic material, and to resuspend in a small volume such that indium is above the detection limits of the ICP-MS. Samples were refluxed on a hotplate with 20 mL concentrated nitric acid and 10 mL 70% perchloric acid for approximately 8 hours. After sitting at room temperature overnight, the samples were taken to dryness. Perchlorate was driven off finally with the addition of 5 mL nitric acid, which was again taken to dryness. Each sample was resuspended in 10 mL 2% nitric acid, left for 30 minutes, then decanted into a 15 mL polypropylene vial. After addition of indium spikes (discussed below), samples were filtered using an acid washed Whatman or VWR brand polypropylene 0.45 μm syringe filter, and a non-acid-washed Normject 10 ml polypropylene syringe. Reagent Blanks and acid blanks were filtered in the same manner and showed no significant indium contamination from this process, and standards showed that indium was not lost significantly during filtration.

Acid-washed teflon beakers and watchglasses were used for these digests, along with acid-washed glass-ribbed watchglasses for taking the samples to dryness. The indium concentration in a reagent blank was less than 7% of the sample indium concentration, and was subtracted during data analysis. The smelter stack sample was run at 200,000x dilution in order to keep the concentrations of lead and zinc low enough to prevent contamination of the ICP-MS instrument.

This acid digestion should liberate all of the indium in oxides, sulfides, sulfates, and carbonates [Deis, 2009, Schaider et al., 2007], leaving only what is bound in silicates, and the silicate fraction of indium is thought to be small [Greenberg et al., 1978a,b, Heindryckx and Dams, 1979].

A Fisons PlasmaQuad 2+ Quadrupole Inductively-Coupled Plasma Mass Spectrometer (ICP-MS) was used for metals analysis, with argon as the carrier gas. A 1 ppb indium solution typically shows about 200,000 counts per second (CPS) at a mass to charge ratio of 115, and the instrument has approximately unit mass resolution. 95.7% of naturally ocurring indium is ^{115}In, and 4.3% is ^{113}In. Sample introduction is via free draw, using a 1000 ul/min nebulizer with attached frit to prevent clogging, and the instrument is run in peak-jumping, pulse counting mode with 200 sweeps per measurement. In order to account for matrix effects and drift of the instrument signal over time, the method of standard additions was used for quantification of total indium. In this method, each sample is split in two, one of those samples is spiked with 0.1 ppb indium, and the samples are run back-to-back on the ICP-MS. Isotope 115 was monitored, and ^{117}Sn and ^{118}Sn were monitored to account for an isotopic interferent in ^{115}Sn (0.34% of total Sn). In this case, the correction was less than a 1% correction, and so was neglected.

For the quantification of Pb, Zn, As, Cd, Ba, and V, indium was used as an internal standard to account for matrix effects and drift of the instrument signal over time. A separate aliquot was also diluted 200,000x; natural indium concentrations were $\sim$0.01 ppb in this dilution, only 1% of the 1 ppb spike of indium added to each sample dilution. Standard curves of metal/indium signal vs metal/indium concentration were prepared with 1 ppb, 0.1 ppb, and 0.01 ppb multi-element standards (which included all of the elements of interest), with 1 ppb In in each standard. The metal/indium ratios in each sample can then be determined from this standard curve, by plotting the M/In signal (corrected for blanks and instrument background). Multiplication by the indium spike concentration (1 ppb)

gives the metal concentration, which can then be converted to a particle concentration with the volume of the digest and the mass of PM2.5 digested.

Coal combustion emissions

Coal fly ash samples from six types of coal were obtained from E. Sholkovitz (Wood's Hole Oceanographic Institution) and W. Linak (U.S. Environmental Protection Agency). These coal fly ash samples were generated by combustion in controlled experiments using a down-fired, refractory-lined furnace rated at 50 kW. The combustion process and sample collection are explained in detail in Linak and Miller [2000], and were designed to create conditions similar to those in full-scale utility furnaces. Size segregated particulate matter was collected by passing flue gas through a cyclone for size segregation, followed by dilution with clean filtered ambient air to reduce temperature, then collection on teflon-coated glass fiber filters (see Linak et al. 2000 for complete details). These samples have previously been characterized for a variety of metals, but have not been analyzed for indium [Linak and Miller, 2000].

These coal fly ash samples were analyzed by Standard Laboratories, Inc., for indium, lead, zinc, and copper using Inductively-Coupled Plasma Mass Spectrometry after digestion with nitric and hydrofluoric acids. ASTM Method D6357 was used for the digestion. In order to account for matrix effects and instrument drift, indium was used as an internal standard during the measurement of lead, zinc, and copper, and rhodium was used as an internal standard for the measurement of indium. Laboratory error of 20% was reported, and measurements of lead and copper in NIST Standard 1633b (coal fly ash) were within 5% and 11% of the certified values, respectively, and zinc was within 14% of the reported, but non-certified value. Indium concentrations in this NIST standard are not reported. Concentrations for lead, copper, and zinc in three of these samples were previously measured by Linak et al. [Linak and Miller, 2000]. Copper concentrations reported here differ from the Linak et al. values by 11-82%; lead concentrations differ by 3-66%, and zinc concentrations differ by 13-51%. These values are not consistently biased higher or lower than the Linak values.

5.2.5 Receptor Modeling

Two types of receptor modeling were used to test the hypothesis that smelters are contributing high concentrations of indium to the atmosphere in the Northeastern United States. Receptor models are source attribution models that use ambient data collected at a receptor to infer sources, as opposed to using data of source emissions to infer ambient concentrations [Watson et al., 2008].

The equation solved in most receptor models is:

$$x_{ij} = \sum_{k=1}^{p} g_{ik} f_{kj} + e_{ij} \tag{5.4}$$

where x is the sample data, f is the species profile of each source factor, and g is the mass contribution of each factor to a particular sample. i indexes the number of samples, j indexes the number of chemical species measured, and k indexes the number of source factors.

Positive Matrix Factorization (PMF) solves this equation for both the species profiles of each source factor, f, and the mass contributions of each factor, g. The Chemical Mass Balance (CMB) model used here solves the same equation with user-inputted source profiles, f. The two models have different strengths and weaknesses. The PMF Model does not require the source profiles to be known, and can weight each data point individually, allowing for data with high uncertainties or that are close to a detection limit to be used [Norris et al., 2008]. A drawback of the PMF model is that a large number of data points are necessary for the model to be successful [Watson et al., 2008]. On the other hand, using a large data set can act to average out temporal changes in source profiles. The CMB model fits one sample at a time, and if the main sources are not known, or if their specific chemical profiles are not known, non-convergence can be an issue [Coulter, 2004, Watson, 2004]. Thus a thorough understanding of the sources to a region is necessary for a successful CMB apportionment, and region-specific source profiles, which often are not available in the literature, should be used [Coulter, 2004, Watson, 2004]. For a particulate matter apportionment, the CMB model also requires the main species contributing to particle mass to be used, including organic carbon, elemental carbon, sulfate, nitrate, and ammonia [Coulter, 2004, Watson, 2004]. Both models have some degree of subjectivity; the user must determine the appropriate number of factors to use, determine which fitting species

to assign as weak or to discard, and interpret the source profiles that result from the PMF model; measured source profiles are used as inputs for the CMB model, but the user must determine which sources are important to use, and how to combine similar sources to avoid collinearity between profiles.

Receptor modeling can be useful, but care must be taken in the interpretation of results. There are many subjective inputs to these models, and different models can often result in different results [Watson et al., 2008]. PMF modeling is optimized with larger numbers of samples and species, and CMB modeling is optimized with larger number of species measured, by measuring 'tracer' species that prevent collinearity between source profiles, and by having source profiles that match the profiles in the study region.

Positive Matrix Factorization

Positive Matrix Factorization is a type of factor analysis by which the concentrations of a suite of chemical species in a large number of receptor samples are used, along with the measurement uncertainties, to determine chemical profiles of sources that contribute to those samples and the contributions of each source to each sample [Norris et al., 2008]. The model used in this study was PMF3.0, provided by the US Environmental Protection Agency [Norris et al., 2008].

Positive Matrix Factorization allows each point to be individually weighted, by defining uncertainties for each chemical species measured, and constrains the results so that negative source contribution are not permitted. The model determines the g_{ik} and f_{kj} that minimize the function:

$$Q = \sum_{i=1}^{n} \sum_{j=1}^{m} \left(\frac{e_{ij}}{u_{ij}} \right)^2 \tag{5.5}$$

where u_{ij} is the measurement error.

The user defines how many source factors to solve for, and which chemical species will be used in the fitting process. Huang et al. [1999] suggest that a plot of Q versus the number of factors can inform the optimal number of factors, along with observation of how the source profiles change with a change in factor number. Solutions can be checked for stability by running the model a number of times (typically 20) to assure stability in Q and in the profiles. Additionally, a final solution can be run in the 'bootstrapping' mode, whereby random subsets of the sample set are chosen and used to rerun the model and remap the

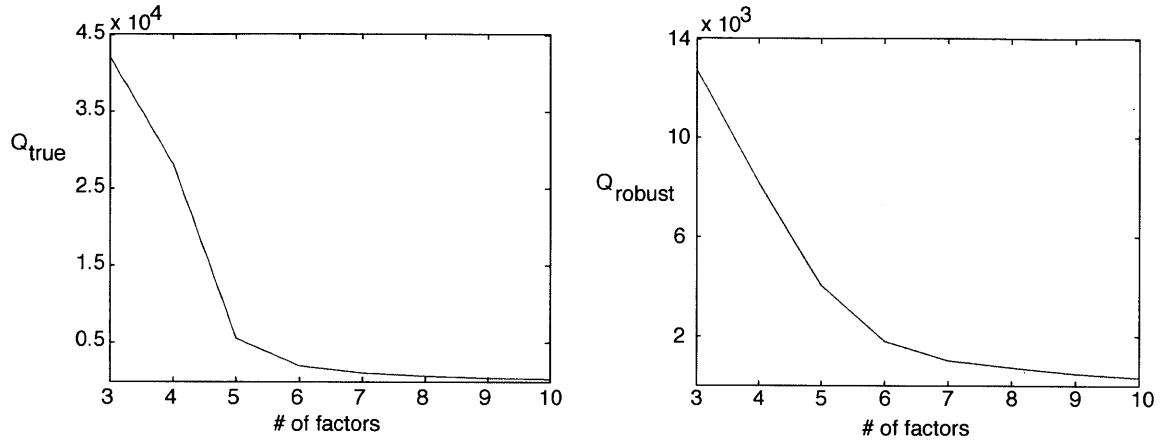

Figure 5-3: The optimal number of factors for fitting can be determined in part by finding the point at which Q is no longer decreasing rapidly. Q_{true} is calculated using all of the data points, while Q_{robust} excludes outliers. These plots are for the fitting of the New York sites.

source profiles. Despite these tests for stability, PMF modeling remains subjective, and the user is seeking results that are 'interpretable' [Huang et al., 1999].

Due to the probability of different sources influencing the New York sites and the Massachusetts sites, they were modeled separately from one another.

For PMF modeling, five factors were chosen as the optimum number for each set of sites, based on a plot of Q vs. number of factors (Fig. 5-3). The model reports both a Q_{true}, which includes all of the data points, and Q_{robust}, which excludes outliers. Four factors were also examined, but were discarded due to the instability of the four factor solution.

Species can be designated as 'weak' in this model, which designates its uncertainty to be 3x higher than reported. Paatero and Hopke [2003] show that the solution is not affected much by the assignment of weak species, and can be hurt by keeping poorly fit species designated as strong. The chemical species used for the fitting of each set of sites in this study were: Si, S, Cr, Fe, Ni, Cu, and Zn as 'strong'; Al, K, Ca, Mn, Mo, Ag, Pb, organic carbon (OC), and elemental carbon (EC) as 'weak'. The assignment of weak species was based on poor fitting of that species during initial runs with all factors designated as strong.

Indium was measured in 30% of the samples; this was too few data points in either New York or Massachusetts to perform a PMF analysis using indium as a fitting species. (One of the drawbacks of this type of model is the large number of data sets required, over 100 according to Watson et al. [2008].) Therefore this model cannot give a direct assignment

of the relation of indium to the overall profile, but by determining which source factors contribute the most on days that have peak indium concentrations, one can probe which source factors are contributing indium to the samples, and whether they fit the hypothesis that most indium comes from nonferrous smelting sources.

Chemical Mass Balance

A chemical mass balance model solves the same equation presented above for PMF modeling (Eq. 5.4), but uses user-inputted source profiles (f_{kj}) to apportion the contributions of each source for a particular sample [Coulter, 2004]. The model used here is CMB8.2, made available by the EPA [Coulter, 2004].

For a rigorous source attribution using a Chemical Mass Balance Model, a full analysis should include the measurement of trace metals, sulfate, nitrate, ammonium, organic carbon and elemental carbon [Watson, 2004] in the receptor samples and the source profiles, and source profiles should be used that are specific to the receptor location. For example, the composition of dust can vary geographically, and it is important to use a dust profile that is representative of the study location. In the present case, nitrate measurements are typically below the detection limit of the method used to obtain them [Salmon et al., 1999] and thus are not usable. Ammonium values are not available. Additionally, source-specific profiles are not readily available for this region, and were not measured for this study. Coal fly ash samples were analyzed for this study, and an average value of this data was used as the coal source profile (Table 5.4). The zinc smelter emissions analyzed in this study can inform the smelting source profile, but the entire suite of species analyzed in the receptor samples has not been analyzed for these emissions. Source profiles are thus mainly taken from EPA's SPECIATE database [EPA, 2011]. Specifically, composite profiles were used for PM2.5 emissions from bituminous coal, subbituminous coal, lead production (smelting), copper production, crustal material, solid waste combustion, residual oil combustion, wildfires, and gasoline exhaust [Reff et al., 2009]. These profiles were further averaged in some cases in order to obtain average profiles that are not collinear with one another. Though not reported, uncertainty of these profiles is likely high due to natural variation. For the purposes of the CMB modeling, uncertainties of 20% were used; higher uncertainties employed cause collinearity between profiles and subsequent nonconvergence of the model.

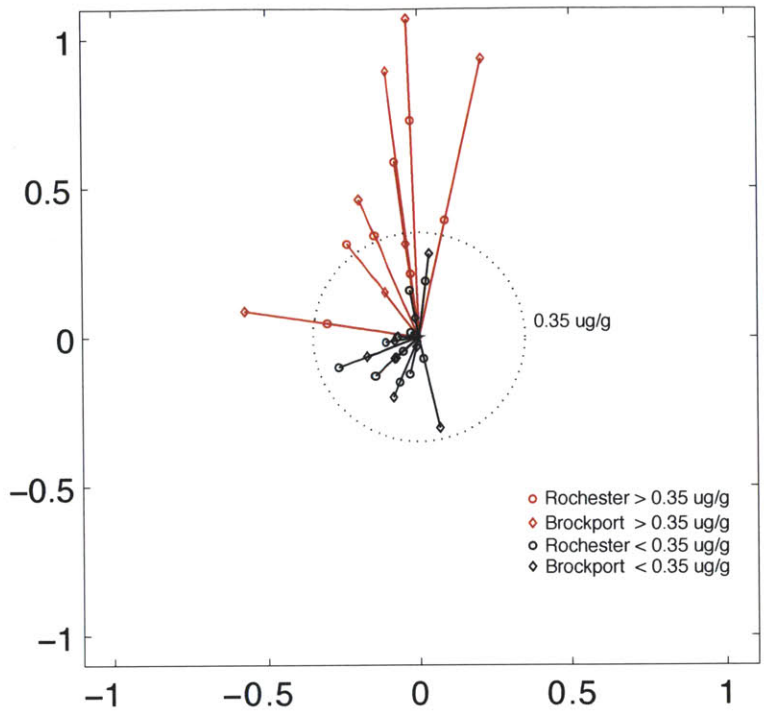

Figure 5-4: Atmospheric back trajectories generated with the HYSPLIT model for the New York sites show that peaks in particle-normalized indium concentration occur on days when air is coming from the north/northwest. The length of each ray is equal to the magnitude of the particle-normalized indium concentration; red denotes concentrations > 0.35 μg/g. The direction of the ray is the angle from which the wind is traveling at a time of -24 hours. North is at 12 o'clock.

5.3 Results & Discussion

5.3.1 Back Trajectory Analyses

As was discussed in Chapter 4, back trajectories for the New York sites show that air is coming from the north or northwest on 6 out of 7 of the days when indium concentrations are > 0.35 μg/g in at least one of the two locations (Fig. 5-4). (0.35 μg/g is a somewhat arbtrary cutoff for a 'peak' value, based on the average concentrations for Rochester and Brockport of 0.25 and 0.3 μg/g respectively.) The days when particle-normalized concentrations are <0.35 μg/g in both locations, back trajectories show that air is coming from the west, southwest, or south on 9 of 11 of the days.

For the Boston site, back trajectories show air coming from the north/northwest and the west/southwest/south on a roughly equal number of days, although there are only three days that have an indium concentration >0.35 μg/g (Fig. 5-5). Two of these days show air

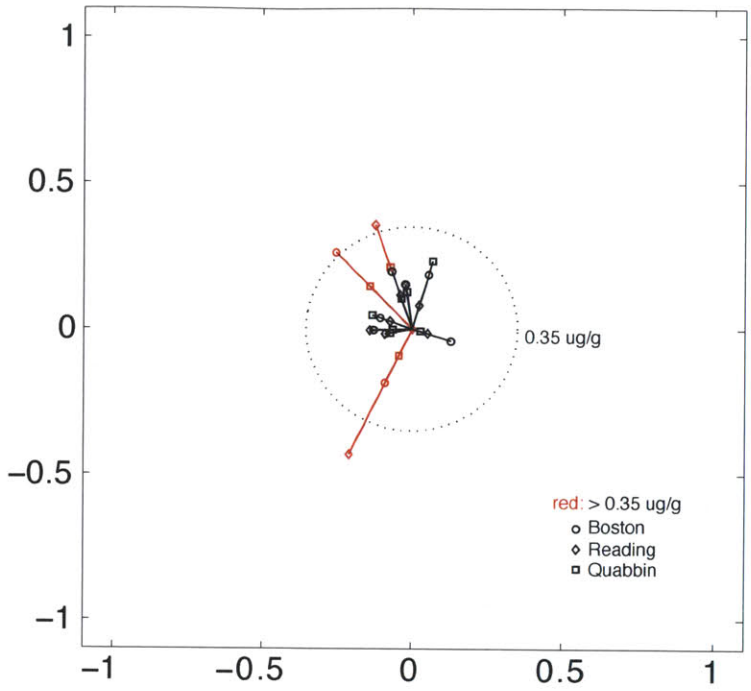

Figure 5-5: Atmospheric back trajectories generated with the HYSPLIT model for the Massachusetts sites show that few peaks occur in particle-normalized indium concentration in these sites, and there is no strong correlation between indium concentration and wind direction. The length of each ray is equal to the magnitude of the particle-normalized indium concentration; red denotes concentrations > 0.35 μg/g. The direction of the ray is the angle from which the wind is traveling at a time of -24 hours. Compass north is at 12 o'clock.

coming from the northwest, while one shows air coming from the southwest. It is interesting to note the presence of a secondary smelter and a coal-fired power plant directly southwest of Boston, on the border of Massachusetts and Rhode Island, as well as multiple incinerators along the east coast (Figure 5-2).

If the hypothesis proposed is correct, that high indium concentrations are associated with air that is passing by smelters, then air from the same direction in the New York sites should be high in other smelter-associated metals such as Zn, Cu, and Pb. In fact, the trend is similar, but less pronounced than with indium (Figure 5-6).

5.3.2 Correlation of Indium with other metals

Using the New York sites, and distinguishing between when air is coming from the north (defined as the angle made from a trajectory at -24 hours being between 292.5°and 22.5°, if

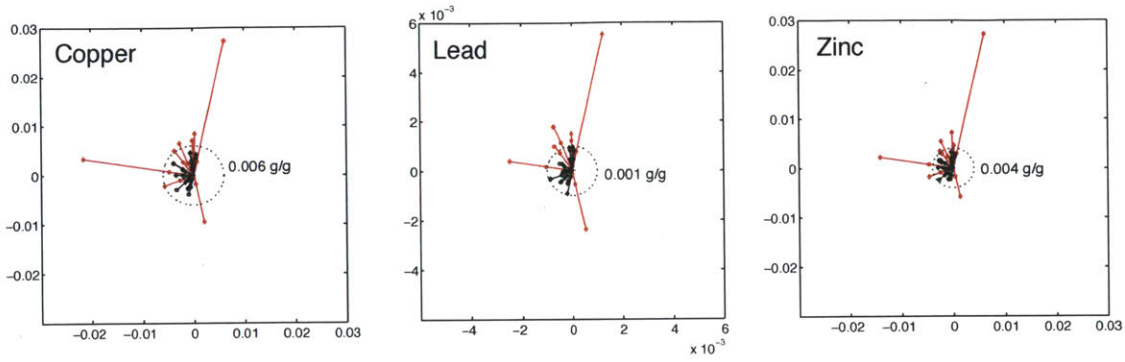

Figure 5-6: Atmospheric back trajectories generated with the HYSPLIT model for the New York sites show that high Cu, Pb, and Zn concentrations tend to come from the north, but do not have as pronounced a trend as indium does. The length of each ray is equal to the magnitude of the particle-normalized indium concentration; red denotes concentrations above a threshold, denoted by the dotted circle, and chosen just above the mean concentration. The direction of the ray is the angle from which the wind is traveling at a time of -24 hours. Compass north is at 12 o'clock.

Table 5.1: Probability that air from the north is chemically different than air from the west (Kolmogorov-Smirnov test results for In:metal ratios).

	P
In:Zn	0.997
In:Cu	0.87
In:Pb	0.85
In:S	0.9999
In:Fe	0.98
In:Ag	0.98

due north is 0/textdegree) and from the west (all other angles, since winds from the south or east are extremely rare), shows that these two air directions carry PM2.5 of distinctly different chemical makeup (Fig. 5-7). Plotted are the mean regression for each set of data, forcing the intercept to be zero, and the 1σ standard deviation of this slope.

Cumulative distribution functions for the In:metal concentrations for each of the two air types highlight the difference in distribution between air from the north and air from the west. Using these cumulative distribution functions, the Kolmogorov-Smirnov test shows that the two populations are different from one another with more than 85% probability for In:Zn, In:Cu, In:Pb, In:S, In:Fe, and In:Ag ratios (Table 5.1).

The correlation of indium with other metals is mainly useful in determining whether the

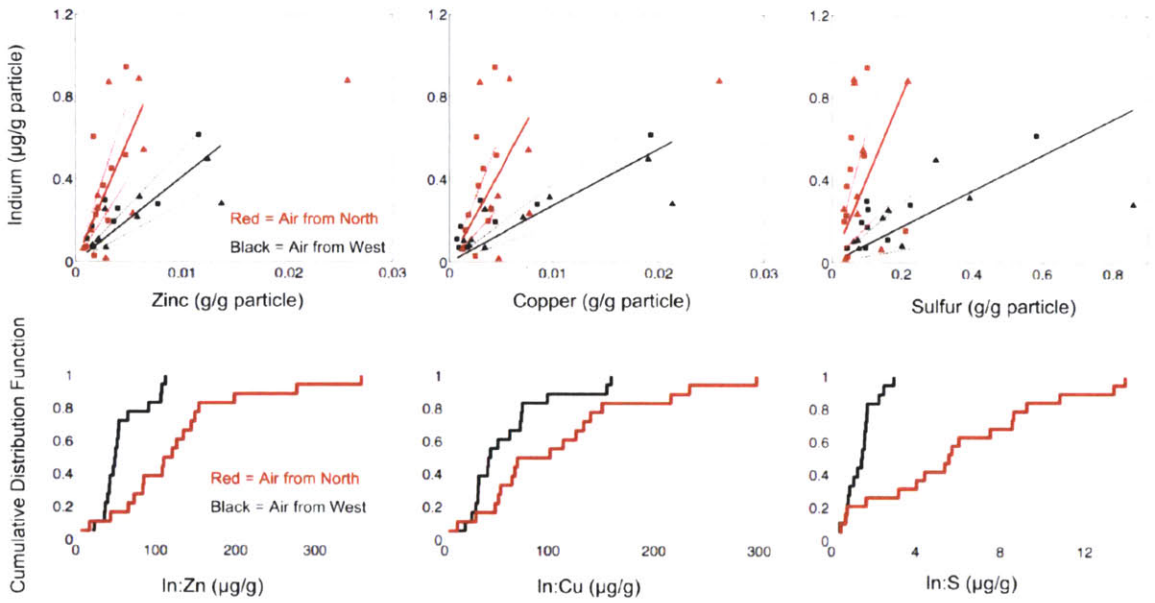

Figure 5-7: Air from the north has a distinctly different chemical makeup than air from the west. This can be seen in a correlation plot, in cumulative distribution functions, and by computing a Kolmogorov-Smirnov statistic.

chemical makeup of the air from the north is different from the chemical makeup of air from the west. The specific ratios of In:metal can be determined from Fig. 5-7, then compared to metal ratios seen from coal fly ash and zinc smelter emissions. Care must be taken, however, in comparing these numbers, because the metals for the various samples were measured using slightly different methods. The coal fly ash samples were measured using a 'total' digest with nitric and hydrofluoric acids. The zinc smelter emissions sample was measured using a partial digest with nitric and perchloric acids. This partial digest, as discussed above, is expected to account for the majority of the indium present, but will not liberate the metals in the silicate fraction, which may be significant for the other metals measured. For the air samples, indium was measured with the same nitric/perchloric digestion, while the other metals measured were analyzed using X-Ray Fluorescence (XRF), which reflects a 'total' concentration. Nonetheless, the comparison of these ratios is useful, and error induced by the differences in analysis method are likely no higher than uncertainties in these ratios caused by natural variation in source composition, which is significant.

The differences between the metal ratios from northern air versus western air, while statistically significant, are small (Table 5.2). The only three metals measured in all of the

Table 5.2: A comparison of the In:metal ratios seen in air samples, source PM2.5, and another atmospheric study [Sturges and Barrie, 1989].

			Zn smelter emissions	Coal fly ash	Ratios in Sturges & Barrie	
	North	West	PM2.5	PM2.5	N	W
In:Cu	0.00006	0.00003	> 0.02	0.002	-	-
In:Pb	0.0003	0.0002	> 0.8	0.003	0.002	0.006
In:Zn	0.00007	0.00005	0.001	0.001	0.003	0.006

samples are Cu, Pb, and Zn. In these three cases, the In:metal ratio in the northern air is higher than in western air. As can also be seen, the In:metal ratio of these metals is significantly higher in zinc smelter emissions than in coal fly ash, but these emissions ratios are significantly higher than the air concentrations seen in this study. This suggests dilution of these emissions with other low In:metal particles.

Also presented is a comparison of ratios from a detailed study of indium and other metals in atmospheric particulate matter in Dorset, Ontario [Sturges and Barrie, 1989]. This study found high indium concentrations associated with air traveling from the Canadian smelter region north of the study site. The Sturges and Barrie ratios are 1–2 orders of magnitude higher than the ratios in the present samples. This could be due to Dorset's closer proximity to the smelter sources, differences in the ore smelted at the time of each study, and changes in emissions controls that could alter the size distribution of emitted particles (which may in turn have different metal ratios associated with them).

5.3.3 Source emissions characterization

Zinc smelter emissions

Zinc smelter emissions of PM2.5 from a hydrometallurgical smelter operation have an indium concentration of 52 μg/g (Table 5.3). This is similar to average indium concentrations in sphalerite ((Zn,Fe)S) of 1-100 μg/g [Smith et al., 1978]. This is significantly higher than even the peak concentrations of indium seen in New York of 1.1 μg/g.

Coal fly ash

Coal fly ash has concentrations of indium of 0.14-0.34 μg/g in the <2.5μm fraction and 0.03-0.09 μg/g in the >2.5μm fraction (Table 5.4). Lignite, sub-bituminous, and bituminous coal

Table 5.3: Metal composition of zinc smelter PM2.5 emissions (concentrations in μg/g).

	Process A <2.5 um
V	<39
Mn	4000
Cu	<2600
Zn	96400
As	209
Cd	255
Ba	<19
Pb	<66

only differ in their indium content by a factor of 3. The indium concentration in these coals is comparable to mean concentrations of indium seen in New York and Massachusetts of 0.2 μg/g.

The indium concentrations measured in coal fly ash and in zinc smelter emissions can be used to estimate total indium emissions from coal combustion and zinc smelting, and to constrain previous estimates of global emissions [White and Hemond, 2012].

Estimates for Canada and the United States can be calculated. PM2.5 emissions for coal combustion in the United States were estimated to be 85,000 t/yr in 2005 [Drukenbrod, 2012a,b]. In the same year, Canadian PM2.5 emissions from all electric utilities were estimated at 8,100 t/yr [Canada, 2012]. Multiplying this by the average indium concentration measured in PM2.5 coal fly ash, 0.22 μg In/g PM2.5, and doing the same for PM10 estimates (Canada + US emissions = 186,000 in 2005 x 0.07 ug In/g PM10) results in an estimate of 33 kg/yr of indium released to the atmosphere from coal combustion in the US and Canada. Global PM2.5 and PM10 emissions estimates are needed in order to compare this number to the global estimate of indium emissions from coal combustion of 300 t/yr [White and Hemond, 2012], but this 300 t/yr number appears to be an overestimate.

For non-ferrous smelting, PM2.5 emissions in the United States were estimated to be 51,700 t/yr in 2011 for metals processing [Drukenbrod, 2012a]. In 2010, Canadian emissions from non-ferrous smelting and refining were estimated at 1749 t/yr [Canada, 2012]. Assuming that the indium concentration of 52 μg/g measured in PM2.5 emissions from a zinc smelter is representative of all non-ferrous smelting, then 2.8 tons of indium is released per year with the PM2.5 fraction. Concentrations of indium in PM10 released from zinc

Table 5.4: Metal composition of coal fly ash (concentrations in μg/g)

	W. KY - Bituminous		OH - Bituminous		MT - Sub-Bituminous		ND - Lignite		PA - Bituminous		UT - Bituminous		NIST 1633b Coal Fly Ash	NIS 164 Ur- ban Dus
;	<2.5 um	>2.5 um	<2.5 um	>2.5 um	<2.5 um	>2.5 um	<2.5 um	>2.5 um	<2.5 um	>2.5 um	<2.5 um	>2.5 um		
	86	61	82	65	208	118	107	46	73	134	75	193	97	370
	0.17	0.08	0.28	0.08	0.34	0.09	0.14	0.06	0.26	0.06	0.15	0.03	0.17	0.35
	76.6	44.2	153	50.7	62.5	21.5	60.9	18.4	71	32.1	41.9	12.2	63.4	116
	655	336	269	107	218	57	166	66	139	249	68	20	173	139
n Linak et al. 2000:														
	132	68.4			62.7	45.3					89	59.6		
	8.7	3.3			<1.0	<1.0					<1.0	<1.0		
	132	108			17.5	19.6					110	78.7		
	73.5	51.9			96.7	55.6					95.8	51.5		
	76500	88300			4000	3810					16000	14400		
	34.5	16.1			93.2	48.4					40.2	<12.3		
	110	86.2			41.5	29.3					109	39.4		
t %)	1.12	0.46			0.74	0.01					0.68	0.27		
	356	330			111	84.9					186	123		
	548	265			141	31.9					144	40.3		

smelting are not yet available, but adding the release associated with PM10 will likely not change this estimate by more than 2-3x. Global PM2.5 and PM10 emissions estimates are needed in order to compare this number to the global estimate of indium emissions from smelting processes of 600 t/yr [White and Hemond, 2012].

Caution must be used when estimating emissions from coal combustion using coal fly ash. The coal fly ash samples measured for this study may not be representative of actual emitted particles. These samples were collected upstream of emissions controls. Emissions controls tend to control particles with diameters above 1 μm better than 99%, while smaller diameter particles (< 1 μm) are more likely to escape (control efficiencies of 80-90% have been reported) [Linak, 2008]. This smaller size fraction is typically formed by volatilization and subsequent nucleation of coal constituents, which may enrich some metals in this fraction, compared to the bulk PM2.5, which can have a makeup more typical of the uncombusted coal [Linak, 2008]. Therefore some care should be taken when extrapolating the concentrations measured for PM2.5 fly ash to actual emissions estimates. The smelter stack sample was collected downstream of particulate matter controls, and so should be representative of the chemical makeup of actual emissions.

5.3.4 Receptor Modeling

Using Positive Matrix Factorization, the five factors found for the New York sites are a high Al/K/Ca factor that appears to be crustal in origin, a high sulfur factor, a high Zn/Pb factor, a factor that contains multiple anthropogenic metals, and a high Cu factor (Fig. 5-8). The last three factors tend to peak on days when wind direction is from the north—and when particle-normalized indium concentrations peak—and support the idea that air from the north carries with it metals that are associated with nonferrous smelting (Fig. 5-9). This is not universally true, however, and the fact that the high-metal-factors sometimes peak when wind is coming from the west or south, may denote another significant source of indium besides northern smelters. The sulfur and crustal factors have a more well-distributed factor contributions over the course of the year, with the sulfur factor being stronger in the summer. This supports the assignment of this factor as a secondary sulfate factor, mostly attributed to coal combustion. The Zn/Pb and Cu factors have profiles similar to Pb and Cu smelting, but it is possible that they are due to another source or a combination of sources. Bootstrapping indicates a stable solution, as at least 97 of the 100

boot strap runs map to the correct factor. (The model reports factor contributions relative to the average contribution of that factor over all time; the average factor contribution is one. Thus peaks represent days when the factor is contributing more to PM2.5 in the New York or Massachusetts sites than it normally does, but does not indicate what fraction of the total PM2.5 mass is provided by the factor.)

The source profiles resolved for the Massachusetts sites are similar to those resolved for the New York sites. There is a high Al/K/Ca factor that appears to be crustal in origin, a high sulfur factor, a high Zn/Pb factor, and two multi-metal factors—one high in Ni and Ag, and one containing Cr, Mn, Fe, Ni, Cu, and Mo (Fig. 5-10). The metal factors peak on some of the same days as the metal factors did in the New York sites, but do not have as strong a correlation with wind direction. Bootstrapping shows that 98 of the 100 boot strap runs map to the correct factor for factors 1-4, while only 88 map correctly to factor 5. This indicates some uncertainty in the factor 5 profile.

The Chemical Mass Balance Model fails to produce acceptable results. Model goodness parameters are unacceptable (χ^2 values of close to 100), % mass accounted for is either low or extremely high, and the model cannot estimate more than 2 sources, a coal source and a smelter source, in each case. If all New York sites are averaged and fitted with the coal and smelting sources, the model does not converge. Further results are not reported here due to the poor outcome of the model. This poor outcome is likely due to the small number of species used for the fitting, and lack of tracer species, as well as a lack of region-specific source profiles.

Successful CMB source attributions seem to be attainable when the number of chemical species used for the fitting is large and tracer species for individual sources are measured [Watson, 2004]. For example, the use of both PM2.5 and VOCs in the same analysis appear to attain results that are viable [Watson, 2004]. Additionally, source profiles that are specific to the region of study are needed for a successful application of this model. The poor performance of the CMB model for the data set presented here is likely due to the few number of chemical species measured, the lack of nitrate and ammonium data (which could be significant contributors to overall PM2.5), and the lack of region-specific source profiles.

The PMF model overcomes some of the drawbacks of the CMB model because it does not depend on the region-specific source profiles having been measured, and because it uses a large dataset to estimate the source profiles that are contributing to the region.

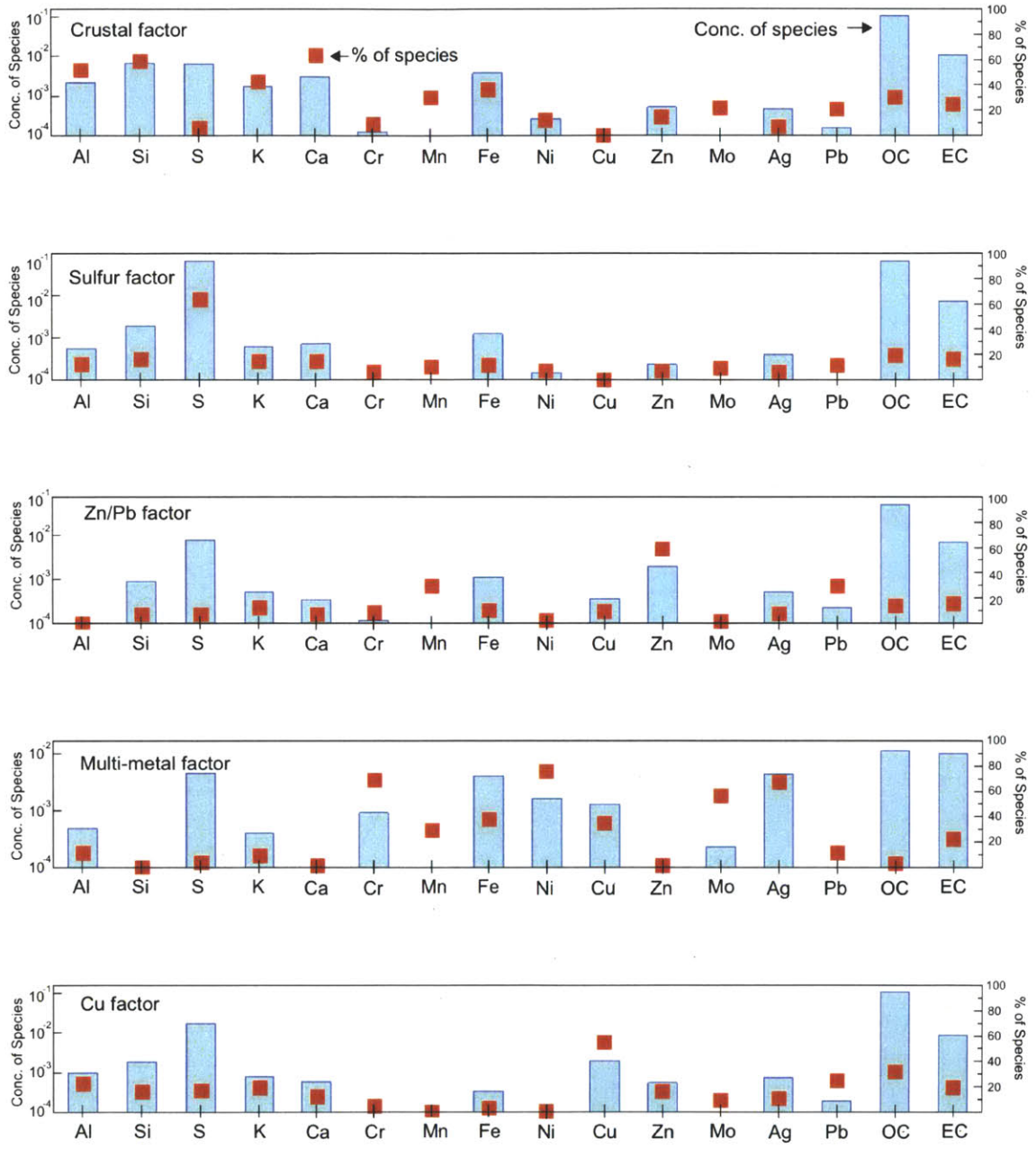

Figure 5-8: PMF profile outputs for New York sites, indicating a high Al/K/Ca factor that appears to be crustal in origin, a high sulfur factor, a high Zn/Pb factor, a factor that contains multiple anthropogenic metals, and a high Cu factor.

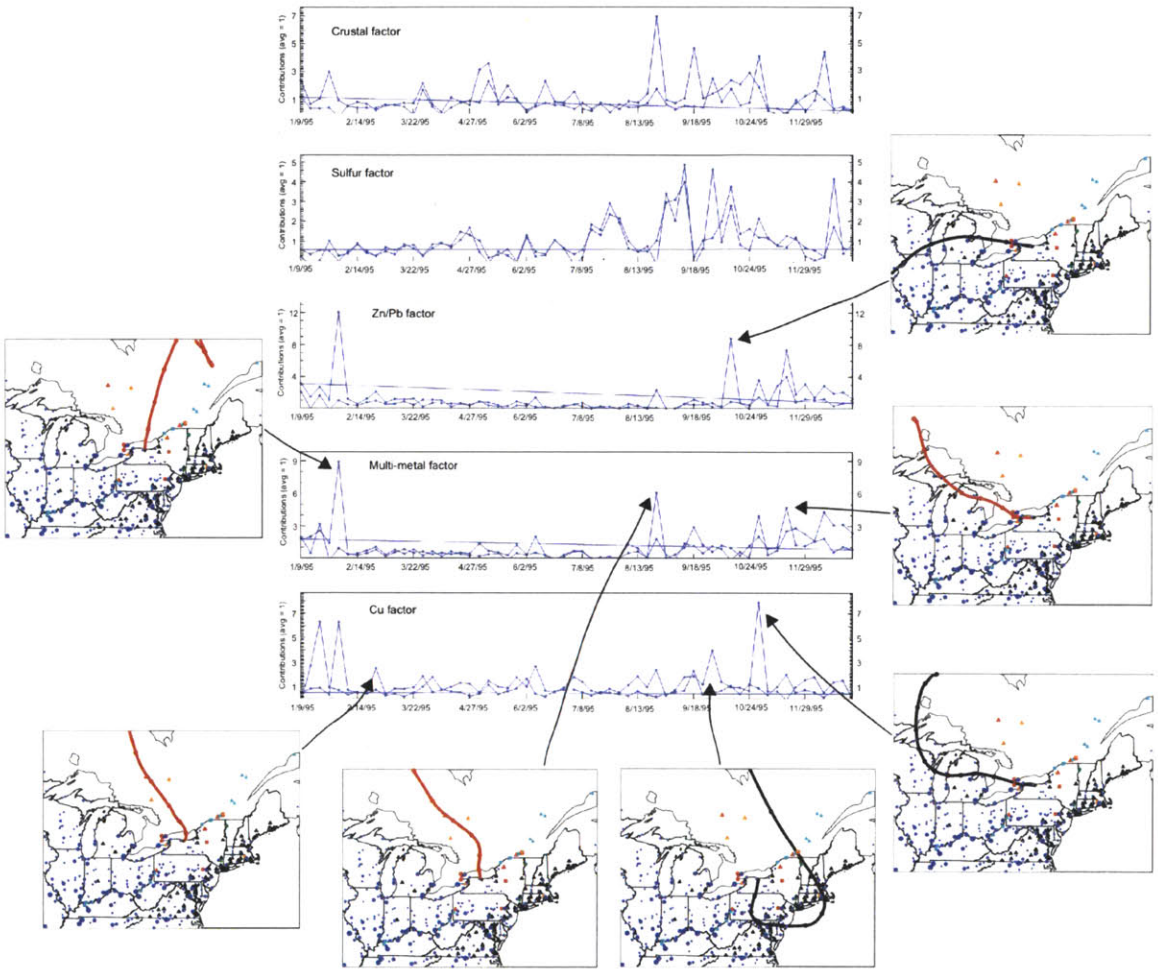

Figure 5-9: PMF factor contributions for New York sites show that the metal factors that may denote smelting tend to peak on days when wind comes from the north, although some of the peaks are associated with wind from the west or south. The model reports factor contributions relative to the average contribution of that factor over all time; the average factor contribution is one. Thus peaks represent days when the factor is contributing more to PM2.5 in the New York sites than it normally does.

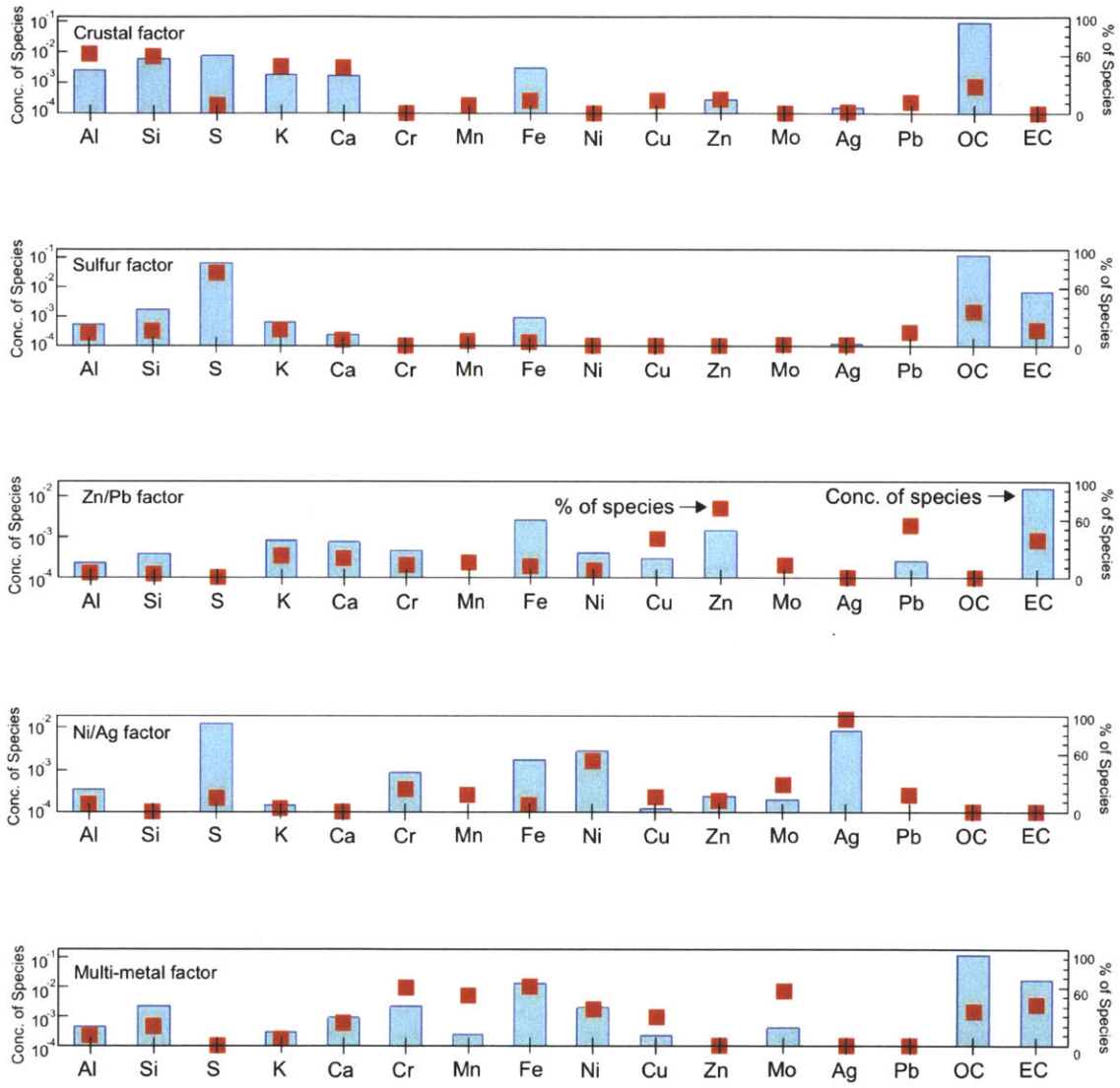

Figure 5-10: PMF profile outputs for Massachusetts sites, indicating a high Al/K/Ca factor that appears to be crustal in origin, a high sulfur factor, a high Zn/Pb factor, and two multi-metal factors—one high in Ni and Ag, and one containing Cr, Mn, Fe, Ni, Cu, and Mo.

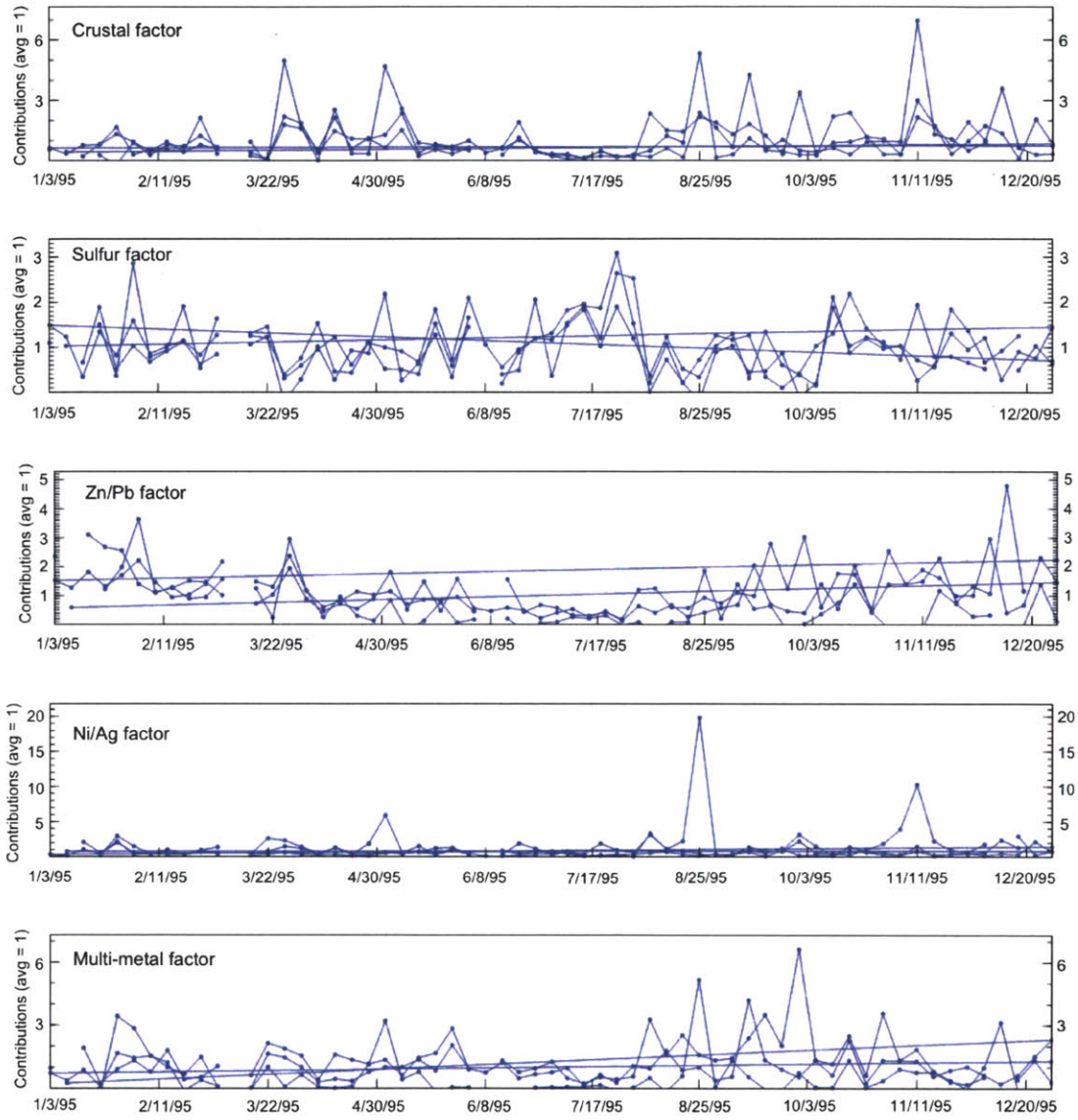

Figure 5-11: PMF factor contributions for Massachusetts sites. The model reports factor contributions relative to the average contribution of that factor over all time; the average factor contribution is one. Thus peaks represent days when the factor is contributing more to PM2.5 in the Massachusetts sites than it normally does.

While receptor modeling can be useful for estimating the source of particulate matter to a particular location, there are still large uncertainties associated with using this type of analysis. For example, several studies of source estimates to the Northeastern United States and Southeastern Canada have been conducted using a variety of receptor models, and they do not always agree. For example, Polissar et al. [2001] find 11 sources of PM2.5 to Underhill, VT, using PMF. These include coal burning (split into a winter and a summer component), oil combustion, soil, woodsmoke, Canadian smelting, Cu smelting, and a Zn-Pb component. Using a Potential Source Contribution Function (PSCF) model, which combines PMF data with back trajectory data, the Cu smelting factor is shown to come from the south, while the Canadian smelter factor comes from the North. In another paper by the same group [Song et al., 2001], 11 different factors were resolved using the same dataset, including secondary sulfate, coal combustion, oil combustion, soil, woodsmoke, Canadian smelting, Canadian Cu smelting, and incineration. The Cu smelter signature in this case was attributed to sources from the north, by a back trajectory analysis. These papers highlight the fact that this model is subjective, and can result in different answers depending on the user inputs. Caution must be employed when interpreting its results.

Further studies that are designed to overcome the difficulties in model input constraints would be necessary to employ receptor modeling effectively to this site, but care must always be taken to account for the inherent problems with these types of models.

5.4 Conclusion

This paper has presented further evidence that indium in the atmosphere in the northeastern United States may be supplied at low levels by coal burning in the US Midwest, and that peaks in indium concentration in two sites in New York may be supplied by smelting operations in eastern Canada. Correlations with other metals suggest that the direction that air is traveling from influences its chemical makeup, with air from the north having higher In:metal ratios than air from the west. An analysis of coal fly ash and Zn smelter emissions suggests that Zn smelter emissions are enriched with indium by 100x compared to coal emissions. Again, this supports the hypothesis that smelter emissions are contributing high amounts of indium to the New York sites. Using these values to calculate emissions in the US and Canada shows 30 kg/yr emitted by coal emissions and 3 t/yr emitted by

nonferrous smelting.

While indium could not be included in the receptor modeling because of too few indium data points, Positive Matrix Factorization shows that a high Zn/Pb factor and a high Cu factor, which may be attributed to smelting, peak on days when air is coming from the north, and coincide with peaks in particle-normalized indium concentration.

There is still much unknown about the sources of indium to the atmosphere. A more detailed receptor modeling study may be useful, but would require a larger number of data samples, chemical species measured, and source profiles from the region characterized. An important contribution to the knowledge of indium sources to the atmosphere would be a more detailed study of indium emissions from nonferrous smelting and a mass balance of how much indium partitions during smelting to purified metal, bottom ash, fly ash, and different particle size fractions.

Lastly, a global emissions estimate for indium from coal burning and smelting could be achieved if global estimates of PM2.5 and PM10 emissions from these sources were available. Considering that much of the production of nonferrous metals take place in other countries, and that environmental regulations in other countries are often not as stringent as in the United States, these estimates will be important for understanding the global cycling of indium and for predicting its impacts.

5.5 Acknowledgments

We gratefully acknowledge Daniel Pedersen, John Durant, and Lynn Salmon for providing air filter samples for the measurement of indium, data for other metals in these samples, and consultation. Dominic Cianciarelli at Environment Canada provided zinc smelter emissions samples. Ed Sholkovitz (WHOI) and Bill Linak (EPA) provided coal fly ash samples. Funding was provided by NSF Grant CBET-0853866 and an MIT Earth Systems Initiative Ignition Grant. Additional support was provided by an MIT Earth Systems Initiative Linden Graduate Fellowship and an MIT Energy Initiative Martin Family Graduate Fellowship for Sustainability to S.J.W., and by the William E. Leonhard Professorship to H.F.H.

Chapter 6

Indium Behavior in Mineral Creek, Colorado, before and during an experimental pH modification

Authors: Sarah Jane O. White, Fatima A. Hussain, Harold F. Hemond, Robert L. Runkel, Katherine Walton-Day, Briant A. Kimball

6.1 Introduction

Indium is an increasingly important metal in semiconductors and electronics, and its use is growing rapidly as a semiconductive coating (in indium tin oxide) for LCD displays, flat panel displays, and photovoltaic cells [Jorgenson and George, 2005]. It also has uses in important energy technologies such as LEDs and photovoltaic cells. Despite its rapid increase in use, very little is known about its environmental behavior, and concerns are emerging over its health impacts [Homma et al., 2003, 2005, Chonan et al., 2007, Hamaguchi et al., 2008, Nakano et al., 2009, White and Hemond, 2012].

One significant flux of indium to the environment is from nonferrous mining and smelting [White and Hemond, 2012]. Indium is mined economically as a byproduct of zinc and lead sulfides, and is also found at elevated concentrations in copper, nickel, and tin sulfides [Smith et al., 1978]. The local release of metals from mining and smelting has been shown to occur for many elements (e.g. [Douay et al., 2008, Mighall et al., 2002, Sterckeman et al.,

2002]). Boughriet et al. [2007] showed high indium concentrations (up to 75 mg/kg) in river sediments near smelters. This can be influenced by short-range atmospheric transport, the leaching of tailings by natural waters, the production and leaching of slags and residues by metallurgy, and the specific chemistry of the waste stream and the degree of influence of acid mine drainage [Lottermoser, 2007]. Previous estimates show that ~10,000 tons of indium per year end up in solid tailings, based on calculations showing that only 5% of indium extracted from the earth with sulfide ores is produced as pure indium metal for industrial use [White and Hemond, 2012]. It is unknown how much of the indium in solid mining wastes leaches into freshwaters.

There are numerous abandoned mining sites in the world that continue to impact the water quality of nearby surface waters [Johnson and Hallberg, 2005a]. Acid mine drainage affects stream water quality by lowering the pH, thus maintaining high amounts of metal ions in solution. Both the low pH and high metal content have adverse effects on freshwater ecosystems (e.g. [Griffith et al., 2012]).

Mineral Creek is a fresh water river in south western Colorado, severely affected by heavy metal contamination as a result of acid mine drainage. The US Geological Survey (USGS) has done detailed experiments using tracer injection to quantify streamflow, and chemical analysis of stream samples and inflows, allowing the identification of the main sources of metal contamination to the stream [Runkel and Kimball, 2002, Runkel et al., 2009a]). There have been a variety of remediation efforts in this watershed, including the installation of bulkheads to reduce water flow from mining tunnels, and removal of tailings piles [Runkel et al., 2009a]. These remediation efforts appear to have reduced metal loadings in the system, though they remain above chronic aquatic standards, and definitive measurements of remediation effectiveness are confounded by short term changes in source chemistry that cause error in mass balance calculations [Runkel et al., 2009a].

More recently, a pH modification experiment was conducted in August 2005 to investigate the effects of an active remediation proposal to increase the pH of the creek [Runkel et al., 2009b, Runkel and Kimball, 2002, Runkel et al., 2012]. Active remediation to increase the pH of a system has been shown to reduce metal concentrations due to the precipitation mainly of Fe-oxides, accompanied by coprecipitation and/or sorption of the other metals to these precipitates [Johnson and Hallberg, 2005a].

Indium has not been measured in this system, and few measurements of indium exist

for acid-mine drainage systems. Rainwater runoff from an abandoned silver mine showed 0.53 μg/L of indium, and river drainage from a tungsten mine showed 6.7 μg/L indium [Florence et al., 1974, Smith et al., 1978, and references therein]. There are presently no water regulations or criterion for indium. Natural rivers contain picomolar ($\sim$0.1 ng/L) concentrations of indium [White and Hemond, 2012].

This paper presents data for indium concentrations and metal loadings before and during the Mineral Creek pH modification experiment. Concentrations 10,000x those found in natural rivers were found, existing completely in the dissolved phase at pH near 3. Upon raising the pH of the system to > 8, all of the indium became associated with the suspended solid phase. This information is important for determining the behavior of indium in acid-mine drainage systems, for estimating how much indium could be being released from past and present mining sites, and for highlighting basic aqueous parameters of indium that must be empirically determined in order to better understand indium's aqueous behavior in a variety of systems.

6.2 Methods

6.2.1 Study Site

Mineral Creek is part of an acid mine drainage system in southwestern Colorado, and is devoid of typical montane aquatic life due to low pH and high metal loadings. It is a headwater system starting at the top of Red Mountain Pass north of Silverton, CO, and gaining flow from slow seeps and large tributaries as it runs 15km through a steep canyon before entering the Animas River. The region encompasses the Red Mountain mining district, where silver, lead, and copper were mined extensively, resulting in acidic drainage to this unnamed reach that causes pHs from 2.9-3.1, and Cu, Fe, Pb, Zn, Al, Cd, Mn, and As concentrations well above Colorado chronic aquatic-life standards. The entire system has been well-characterized by the US Geological Survey [Runkel and Kimball, 2002, Runkel et al., 2009a,b, 2012]. This study focuses on an upstream unnamed reach that is most heavily influenced by acid-mine drainage. Downstream of site 850 m, this unnamed reach joins Mineral Creek, a large circumneutral-pH inflow that dilutes the creek waters, causing pH to rise by about one pH unit, and dissolved metal concentrations to drop by 4-10x [Runkel and Kimball, 2002, Runkel et al., 2009a,b, 2012].

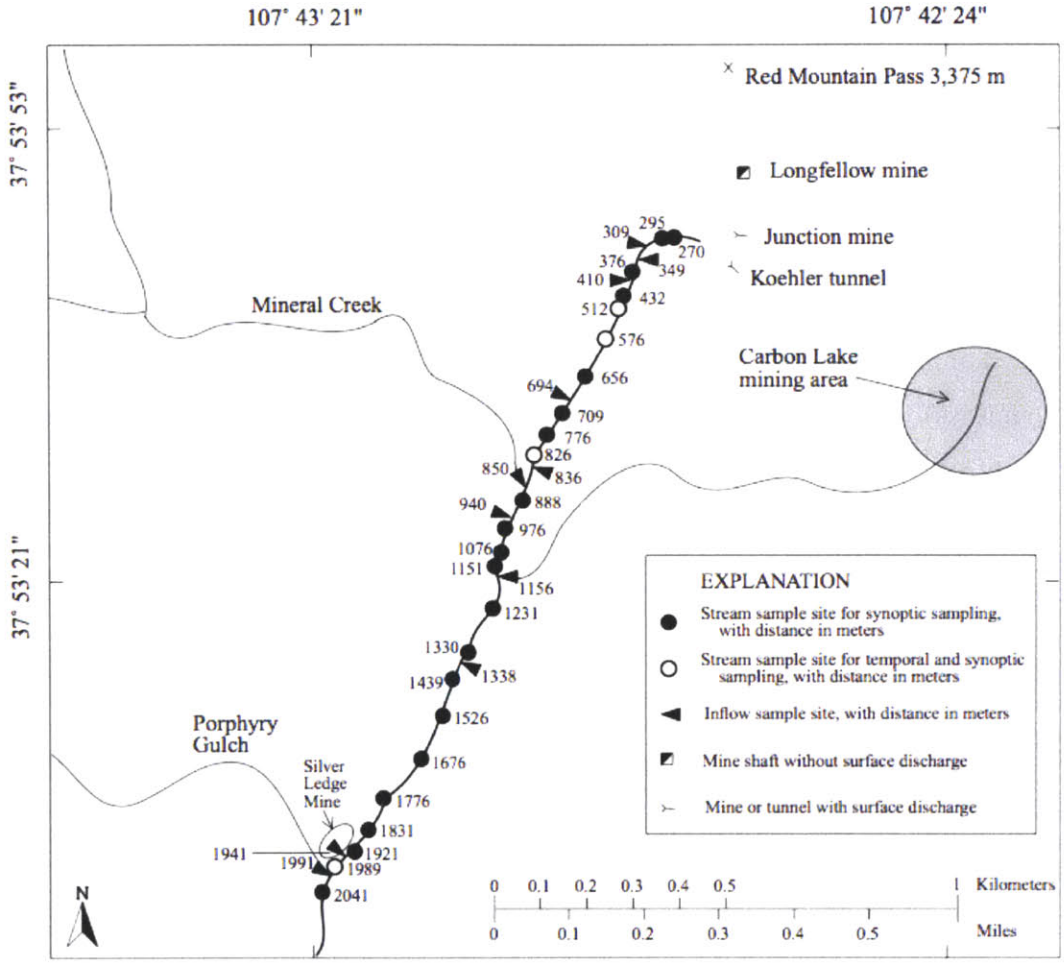

Figure 6-1: The Mineral Creek system has been the subject of several thorough investigations to determine the greatest sources of metal loading to the creek. This study will focus on the unnamed reach from 270m-850m, at which point circumneutral Mineral Creek joins the unnamed reach, raising pH by one unit and diluting metal concentrations substantially. Map from Runkel et al. [2009b].

Previous studies of this site were conducted to characterize inflows and the largest sources of metal loading to the system. The Junction mine and Koehler tunnel make up over half of the flow that enters the upstream reach being studied here. A bulkhead was installed in Koehler tunnel in 2003 to reduce this flow, and appears to have reduced metal loadings, though they remain above Colorado chronic aquatic life standards [Runkel et al., 2009a].

6.2.2 pH Modification experiment and sampling

In August of 2005, the USGS conducted a pH modification experiment, during which they raised the pH of the river by pumping in strong base, NaOH. The goal was to determine if active addition of a base could successfully reduce acidity and metal concentrations to below Colorado chronic aquatic-life standards. This is a longstanding remediation strategy and is based on the oxidation and precipitation of iron, which can co-precipitate and sorb metals [Johnson and Hallberg, 2005a, Dzombak and Morel, 1990]. The pH for the reach under consideration for this study was raised from 2.9-3.1 to 8.4-11.5.

Before and during this pH modification experiment, LiBr was injected as a tracer in order to gauge stream flow and account for dilution from identified and unidentified inflows. Full details of the sample collection and pH modification are described in Runkel et al. [2009b]. In brief, on August 21st, 2005, beginning at 1407 hours, LiBr was added to the stream 1 m downstream of sampling location 270m at a rate of approximately 123 mL/min of 1.7 M LiBr. (By comparison, streamflow for this reach during the study averaged 0.12 ft^3/s, or 2 x 10^5 mL/min [Runkel et al., 2009b]; the injection was <0.1% of the total streamflow.) After the establishment of steady state of the tracer concentration, stream and inflow samples were collected along the entire study reach over the course of approximately 5 hours on August 22nd, 2005. For the pH modification, LiBr and NaOH were injected simultaneously beginning at 1430 hours on August 23, and sampling took place over about 3.5 hours on August 24th. For this campaign, LiBr was injected at approximately 104 mL/min, and 25% NaOH solution was injected at a rate of 340 mL/min. The LiBr was prepared by mixing anhydrous lithium bromide with stream water collected at the injection site. The NaOH was prepared by mixing 50% sodium hydroxide solution with water from a circumneutral-pH tributary.

Samples were collected sequentially from downstream to upstream in order to prevent

resuspension by sampling from influencing downstream samples. Sampling was done as quickly as possible to allow a 'snapshot' of stream conditions [Kimball et al., 2002, 2007]. At each site, samples were collected in 1.8 L HDPE bottles after triple rinsing with the sample water, by submerging the neck of the bottle into the stream. The samples were then taken to a central processing location where they were aliquoted for individual analyses. Two of these aliquots were used for the present study; the first was filtered with 0.45 μm disposable AquaPrep filters (polyester reinforced polysulfone membrane with polypropylene housing, Pall Corporation), and the second remained unfiltered. Both were then acidified to pH<2.0 with ultrapure nitric acid. Complete details of the sampling campaign and analyses are given in [Runkel et al., 2009b].

Samples from this study were provided by USGS researchers, and were stored for six years before the measurement of indium concentrations. Indium concentrations are not expected to have changed, except due to evaporation of the sample, which was minimized by relatively large sample volumes (200-300 mL) and small-necked, tightly sealed polypropylene sample vials. Thus error on indium concentrations due to evaporation are expected to be <10%.

The streambed of Mineral Creek is coated with hydrous iron oxides. These coatings were non-quantitatively sampled prior to the pH modification experiment by taking streambed rocks and native water, shaking in a polypropylene container to dislodge the iron oxide coatings, then decanting the water and coatings from the rocks.

Iron oxide precipitates during the pH modification experiment were sampled to compare their chemical makeup to Fe-oxides formed at ambient conditions. During the pH modification experiment, gelatinous iron floc would collect in low-energy side pools. This floc was sampled using a syringe. Floc data was compared to data from iron precipitates that settled out of water samples taken during the pH modification experiment.

6.2.3 Indium analysis

Indium analyses were performed on samples provided by the USGS using a PerkinElmer 4100-ZL Graphite Furnace Atomic Absorption Spectrophotometer (GFAA). An indium source lamp was used, and absorption at 325.6 nm with a slit width of 0.7 nm was measured. This instrument employs a Zeeman correction to correct for non-specific absorption by atoms other than the analyte of interest. A matrix modifier (0.005 mg Pd and 0.003 mg

$Mg(NO_3)_2$ was used to assure uniform volatilization of indium at the atomization temperature of 2100°C. Standard curves with indium in 2% HNO_3 provided a benchmark detection limit of ~3 μg/L. Because the matrix of these samples is expected to be complex due to the high metal loadings, a method of standard additions was used to quantify suppression or enhancement of the indium signal due to matrix effects, and to account for instrumental drift over the course of the analysis. Each sample was split in two, one of those samples was spiked with 10 μg/L indium, and the samples run back-to-back on the GFAA. The original sample concentration of indium was then determined by integrated peak areas (PA):

$$[In]_{smpl} = ([In]_{spike}/(PA_{spikedsmpl} - PA_{smpl})) \times PA_{smpl} \tag{6.1}$$

where $[In]_{spike}$ is the concentration of the indium spike, $PA_{spikedsmpl}$ is the peak area of the spiked sample, and PA_{sample} is the peak area of the unspiked sample.

Matrix effects calculated by comparing the indium concentrations obtained using a non-matrix-matched standard curve and the method of standard additions could change the final calculated concentrations by up to 50%. Therefore, approximately half of the samples were cross-checked using Inductively-Coupled Plasma Mass Spectrometry (ICP-MS). (Details of ICP-MS methods are described in Chapter 3 of this thesis.) A comparison of concentrations obtained by GFAA versus ICP-MS showed good agreement—within 10% in most cases, and within 26% in all cases.

Field blanks that were collected during the sampling campaign were measured for indium and typically resulted in a 30% correction on the total peak area of the sample. Most of this correction is due to background signal from the GFAA, and not from indium contamination of the field blank itself. This is confirmed by the field blank for samples run on the ICP-MS being typically less than 5%. Relative corrections were larger for the filtered samples during conditions of raised pH due to their extremely low values.

Metal mass loading (flux, in μg/s) was calculated by multiplying metal concentrations by the flow rates reported for each sampling location in [Runkel et al., 2009b].

USGS researchers performed the analysis of indium in the Fe-oxide precipitate samples. Iron-oxide precipitates (0.1–0.2 g) were digested using a mixed-acid procedure consisting of HCl, HNO3, HClO4, and HF acids at low temperature, with a final dilution factor of 1:100, and then analyzed by ICP-AES [Briggs, 2002] for major elements and some trace elements,

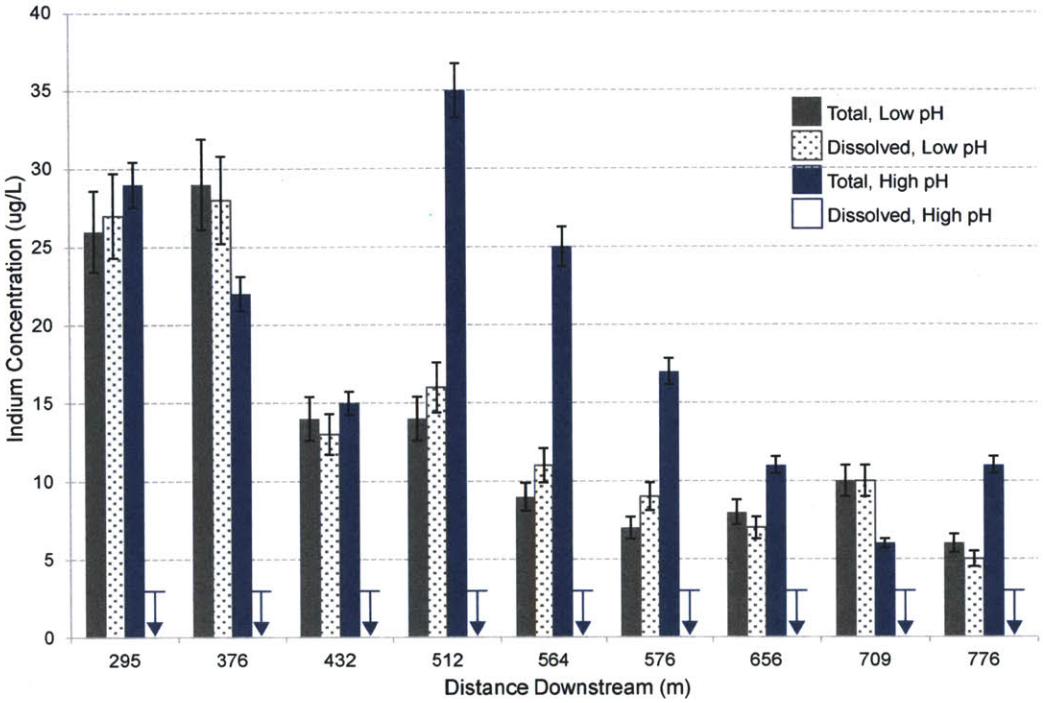

Figure 6-2: Indium concentrations in existing low-pH conditions in Mineral Creek range from 6 to 29 μg/L, and are all dissolved. Upon raising the pH to greater than 8, indium associates completely with the suspended particulate phase, within the limits of analytical capability.

and by ICP-MS [Briggs and Meier, 2002] for additional trace elements.

6.3 Results

Indium concentrations in existing conditions of low pH in Mineral Creek range from 6 to 29 μg/L, with all of it existing as dissolved indium (i.e. indium that passes through a 0.45 μm filter) (Fig. 6-2).

Upon raising the pH to above 8, the indium associates with the suspended particulate phase, within the limits of analytical capability, such that dissolved concentrations are below the detection limits of the analysis.

Indium mass loading to the stream (mass/time) follows the same pattern, with indium loading of 24-46 μg/s at existing conditions, all in the dissolved phase, and indium loading of 21-113 μg/s at raised pH, all in the particulate phase.

Total indium concentrations and mass loadings unexpectedly increase during the pH

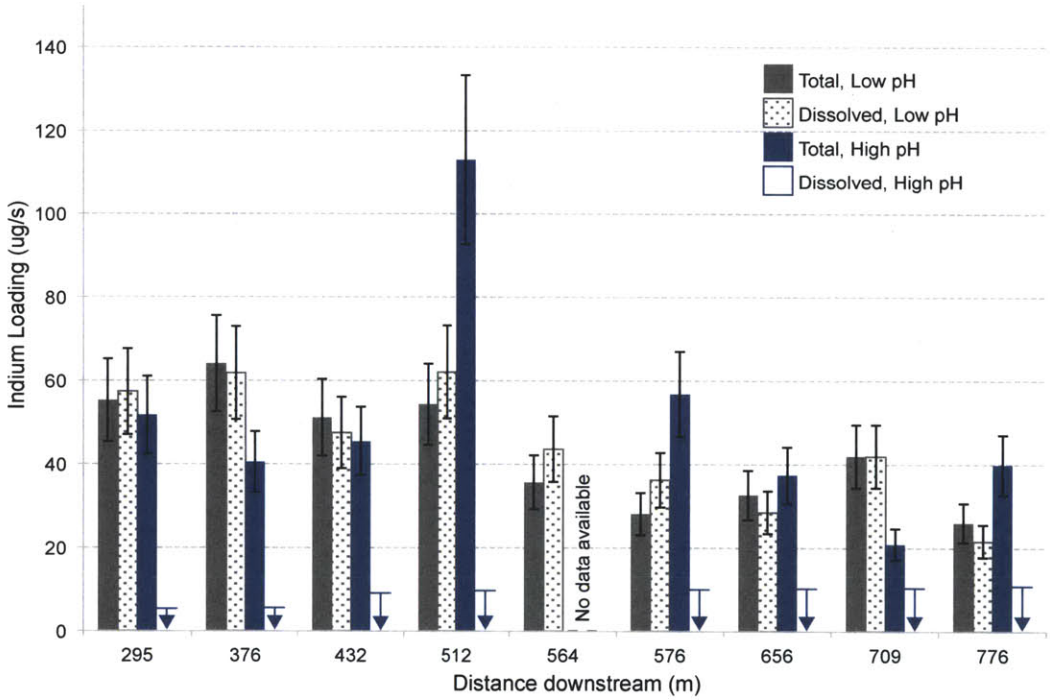

Figure 6-3: Indium mass loadings in existing low-pH conditions in Mineral Creek range from 24-46 μg/s, and are all dissolved. Upon raising the pH to greater than 8, indium associates completely with the suspended particulate phase, within the limits of analytical capability.

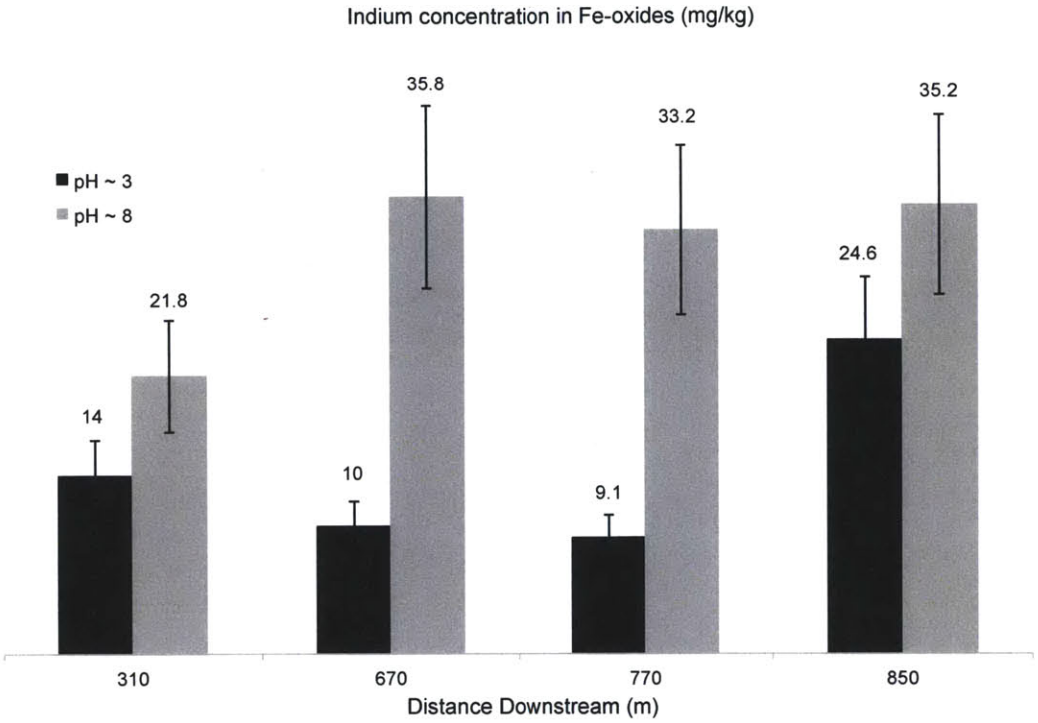

Figure 6-4: Indium concentrations of 9.1-24.6 mg/kg are associated with the Fe-oxides that coat the Mineral Creek streambed at existing low-pH conditions. Fe-oxide precipitates formed during experimental raising of the pH to above 8 have indium concentrations 43-73% higher than existing iron-oxides, suggesting that co-precipitation or sorption to Fe-oxides is a primary removal mechanism of indium from the dissolved phase. (Written communication, K. Walton-Day, US Geological Survey, 2011.)

modification on August 24th, beginning with sample site 512m. This increase is discussed in more detail below, and is thought to be due to unexplained changes in the metal loads from Koehler tunnel that occur on the scale of several hours and without a change in stream flow [Runkel et al., 2009a,b].

Sediment data shows that at existing conditions, indium concentrations associated with iron-oxide coatings on the stream bed are from 9.1-24.6 mg/kg. When the pH is raised, new iron-oxide precipitates contain 43-73% more indium, from 21.8-35.8 mg/kg (written communication, K. Walton-Day, US Geological Survey, 2011).

6.4 Discussion

6.4.1 Indium concentrations in Acid-Mine Drainage systems

At existing conditions of low pH in Mineral Creek, indium concentrations are 6 to 29 μg/L, 10^4 times higher than typical freshwater indium concentrations [White and Hemond, 2012]. At a pH of 3, 90% of the dissolved indium is expected to exist as free indium ion, In^{3+} [Wood and Samson, 2006]. Previous measurements of indium in polluted sites have found similar elevations in concentration in acid-mine drainage (0.53 and 6.7 μg/L; [Florence et al., 1974, Smith et al., 1978]). This clearly indicates the high potential for leaching of indium from mine wastes into freshwater systems.

At the existing low-pH conditions in Mineral Creek, indium exists completely in the dissolved form. This is the same as Al, Cd, Cu, Mn, and Zn in this system, but contrasts with Fe, As, and Pb, which have some solid-phase component even at a pH of 3 [Runkel et al., 2012]. The dissolved phase of a metal is typically thought to be more mobile and bioavailable than metals associated with a solid phase. Therefore acid-mine drainage systems that provide conditions in which indium exists in a dissolved form are a pathway for indium exposure to organisms.

6.4.2 Indium behavior with pH change

Upon raising the pH of the system to above 8, dissolved indium concentrations drop to below analytical detection limits of about 3 μg/L. This nearly 100% reduction in dissolved concentrations is seen for all of the other metals except Mn (83% reduction) in the upper reach of this system. Modeling by Runkel et al. [2012] shows that precipitation of Fe and Al-oxides, followed by sorption to Fe-oxides predicts the percent reduction of Al, As, Fe, and Pb concentrations well. Their model does not predict the extent of decrease, however, for Cd, Cu, Mn, or Zn concentrations. They attribute this discrepancy to an underestimate in the total amount of solid-phase Fe available to act as a sorbent, resulting in an underestimate of Cd, Cu, and Zn sorption and overestimate in their resulting dissolved concentrations [Runkel et al., 2012].

Two other possible removal mechanisms from this system are coprecipitation with Fe- or Al-oxides, or direct precipitation as an indium hydroxide. Coprecipitation is not a well-modeled process, but has been shown to enhance removal of metals from aqueous systems

beyond sorption [Crawford et al., 1993]. As may be expected, removal by coprecipitation and sorption differs depending on the metal ion and the sorbing surface. Crawford and colleagues, for example, showed that Cr(III) and Ni(II) removal from solution is significantly enhanced by coprecipitation with Fe-oxide when compared to adsorption alone to Fe-oxide colloids, while Zn(II) removal was not enhanced by coprecipitation. In practice, it is difficult to distinguish between coprecipitation and sorption except in well-controlled laboratory studies [Crawford et al., 1993], and it is unknown which processes are important for indium in this system.

In oxic waters, precipitation of indium is likely dominated by hydroxide species, and is not likely to occur below pH 3.5 except at concentrations of 10^{-5} or higher, based on the stability diagram presented in Wood and Samson [2006]. This stability diagram is based on best estimates of hydroxide complexation constants, and the solubility product for $In(OH)_3(s)$ of $10^{-36.9}$ [Wood and Samson, 2006]. The indium concentrations seen in this study were 5–35 μg/L ($10^{-7.4}$–$10^{-6.5}$ M), and would thus not precipitate in the existing conditions of low pH. When pH is raised, however, the conditions make precipitation possible. From pH 5.5-9, precipitation of $In(OH)_3(s)$ can occur when indium concentrations reach $10^{-7.3}$ M. Above a pH of 9, which is obtained in several of the samples in this study reach, lower concentrations are needed (as low as 10^{-6} at a pH of 11), and direct precipitation of $In(OH)_3$ may occur. It is likely, however, that sorption and coprecipitation of indium with Fe-oxides, which occurs at a lower pH, still dominates the removal of indium from the system.

Of note is that the complexation constants reported in Wood and Samson [2006] are not well-studied, and may have large uncertainties associated with them. Additionally, complexation and solubility constants for most other ligands have not been characterized for indium. This is an important research need in the future if indium's aqueous behavior in a wide range of systems is to be thoroughly understood.

The association of indium with Fe-oxides coating stream sediments, and the even higher indium concentrations found associated with Fe-oxide precipitates following a raise in pH supports the idea that sorption or coprecipitation with Fe-oxides is the main removal mechanism for indium in this system. The relative success of Runkel and colleagues in modeling the dissolved concentrations of other metals in this system using sorption to Fe-oxides as the main removal mechanism suggests that this will be a dominant mechanism for indium

removal as well. Coprecipitation, while difficult to model, may help to explain some of the metal concentrations that were not explained well by their model.

There is some question as to why total indium concentrations increase during the pH modification on August 24, particularly beginning with sample site 512m. If the increase were due only to different streamflow from one sample date to the next, the change should be reflected throughout the entire study reach. Instead, this increase is only seen beginning with the 512 m site. This is reflected in other metals as well [Runkel et al., 2009a,b], and is thought to be due to changes in the metal loads from Koehler tunnel that occur on the scale of several hours and without a change in stream flow. The processes that cause this type of short-term change are unknown at present, but can impact mass balance calculations that are based on the assumption of stream flow and chemical fluxes that are steady-state over the course of a day-long sampling campaign [Runkel et al., 2009a].

6.5 Conclusions

Indium occurs at concentrations of 6 - 29 μg/L in existing low pH conditions in Mineral Creek, CO. This is 10^4 times higher than natural freshwater concentrations of indium, and suggests that acid mine drainage from active and abandoned nonferrous mining operations contribute high levels of indium to aqueous systems via the leaching of primary ores and waste. Additionally, all of this indium exists in the filterable, 'dissolved' phase at low pH, meaning that it is highly mobile. Although the complexation of dissolved indium is not well studied, 90% of dissolved indium is expected to exist as the free ion, In^{3+}, at a pH of 3, suggesting that a majority is 'bioavailable'. Further study to quantify the extent of this leaching will be necessary to update our understanding of how much indium is mobilized from active and abandoned mining sites worldwide.

A pH modification experiment that raised Mineral Creek's pH from about 3 to above 8 caused all of the indium to associate with the suspended solid phase. Increases of indium concentrations by 43-73% in Fe-oxide precipitates before and after the pH modification suggest that sorption to or coprecipitation with Fe-oxides is the primary mechanism by which indium is removed from the dissolved phase. Modeling by USGS researchers of other metals in the system support sorption to Fe-oxides as the primary removal mechanism.

The behavior of indium in aqueous systems has not been well-studied. Future research

should focus on the determination of complexation constants of indium with a wide variety of inorganic and organic ligands, and of indium sorption constants to Fe-oxides. This information would allow indium to be added to modeling efforts in a system like this.

Additionally, a more thorough characterization of the whole system, including indium concentrations in primary ores and mine wastes present at the site, would allow an estimate of how indium moves through this system. This kind of knowledge could help in the determination of the global flux of indium to aqueous systems from current and abandoned mining sites.

6.6 Acknowledgments

We gratefully acknowledge Alan Shiller for alerting us to these interesting samples. Funding was provided by NSF Grant CBET-0853866 and an MIT Earth Systems Initiative Ignition Grant. Additional support was provided by an MIT Earth Systems Initiative Linden Graduate Fellowship and an MIT Energy Initiative Martin Family Graduate Fellowship for Sustainability to S.J.W., MIT Undergraduate Research Opportunities funding to F.A.H., and by the William E. Leonhard Professorship to H.F.H.

Table 6.1: Metal concentrations in existing conditions of low pH. Indium data is from this study. Other metal data is from Runkel et al. [2009b]

Distance Down-stream	pH	unfiltered Al mg/l	filtered Al mg/l	unfiltered Fe mg/l	filtered Fe mg/l	unfiltered Zn mg/l	filtered Zn mg/l	unfiltered Pb μg/l	filtered Pb μg/l	unfiltered As mg/l	filtered As mg/l	unfiltered In μg/L	filtered In μg/L
295	2.98	38.85	38.33	217.8	212.9	84.58	86.43	198.2	180.1	3.270	2.983	26	27
376	2.94	38.44	38.44	205.3	201.7	85.49	83.78	190.6	175.4	2.872	2.707	29	28
432	3.10	20.37	20.21	99.91	97.10	45.19	45.21	104.8	98.1	1.364	1.161	14	13
512	3.10	20.22	19.63	94.31	89.01	44.46	43.82	102.9	92.6	1.278	1.025	14	16
564	3.11	17.70	17.96	74.25	72.23	37.89	39.00	111.6	97.3	0.927	0.709	9	11
576	3.14	15.24	15.16	58.03	55.15	31.42	31.26	103.7	97.9	0.575	0.447	7	9
656	3.11	14.56	14.49	56.72	53.53	29.69	29.51	115.3	110.5	0.611	0.464	8	7
709	3.10	12.89	12.97	51.30	47.37	25.25	25.53	129.0	110.6	0.573	0.381	10	10
776	3.10	12.83	13.19	48.61	46.04	25.54	25.65	120.5	102.5	0.562	0.356	6	5

Table 6.2: Metal concentrations at experimentally raised, high pH. Indium data is from this study. Other metal data is from Runkel et al. [2009b]

Distance Down-stream	pH	unfiltered Al mg/l	filtered Al mg/l	unfiltered Fe mg/l	filtered Fe mg/l	unfiltered Zn mg/l	filtered Zn mg/l	unfiltered Pb μg/l	filtered Pb μg/l	unfiltered As mg/l	filtered As μg/l	unfiltered In μg/L	filtered In μg/L
295	11.76	40.14	14.73	219.6	0.029	81.64	0.079	214.1	<0.11	3.176	22.1	29	<3
376	11.64	34.87	13.21	183.3	<0.025	71.72	0.076	220.9	<0.11	2.253	17.7	22	<3
432	10.46	21.95	4.501	118.5	<0.025	48.85	<0.014	146.0	<0.11	1.547	8.09	15	<3
512	7.56	32.82	0.066	195.5	<0.025	71.75	0.520	147.1	<0.11	3.462	7.87	35	<3
564	-	-	-	-	-	-	-	-	-	-	-	25	<3
576	9.01	28.29	0.454	160.0	<0.025	63.21	0.025	124.6	<0.11	2.567	5.46	17	<3
656	9.51	20.96	1.693	127.8	<0.025	49.21	<0.014	171.7	<0.11	1.989	5.96	11	<3
709	9.31	16.07	1.509	105.9	<0.025	38.76	<0.014	198.2	<0.11	1.532	5.10	6	<3
776	8.44	17.68	0.807	109.3	<0.025	42.69	<0.014	178.9	<0.11	1.679	4.81	11	<3

Chapter 7

Summary and Conclusions

Indium is an important metal whose production is increasing dramatically due to new uses in the rapidly growing electronics, photovoltaic, and LED industries. Little is known, however, about the natural or industrial cycling of indium or its environmental behavior.

Industrial emissions of indium are already larger than natural emissions. A review of the literature suggests that metal smelting and coal burning are the primary industrial sources of indium to the environment, while releases from the semiconductor and electronics industries are small at present. This scenario may change with the rapid growth of indium use in the electronics and semiconductor industries.

Because atmospheric releases are thought to be large but are poorly quantified, and because inhalation is thought to be an important exposure pathway for indium, we have studied the cycling of indium in the atmosphere in the northeastern United States. These studies have shown that indium concentrations in 5 locations from Boston, MA to Rochester, NY vary from below detection limits to 8 pg/m^3. There are significant differences between samples from different locations and over the course of a year. Atmospheric back trajectories generated with NOAAs Hybrid Single-Particle Lagrangian Integrated Trajectory (HYSPLIT) model suggest that the highest indium concentrations come from the north, potentially from smelting operations, while lower concentrations are seen in air traveling from the midwestern US.

Historical atmospheric deposition over the past century was observed in a peat core from Thoreau's Bog, Concord, MA. Fluxes of indium to this region began increasing at least in the early 1900s, well before indium was used significantly in industry. This is likely due to

emissions from nonferrous smelting not associated with the production of indium, and from coal combustion. Fluxes peaked in the 1970s, and have been decreasing until the present, likely reflecting the advent of particulate emissions controls in the US and Canada.

Further work to constrain the source of indium to the atmosphere in the Northeastern United States has shown that air traveling from the north has a distinct chemical makeup than air traveling from the west, with higher In:other metal ratios. Particulate matter emitted from a hydrolometallurgical zinc smelter has indium concentrations 100 times higher than concentrations in coal fly ash. Receptor modeling suggests that sources high in nonferrous metals (Zn, Pb, Cu) peak on days when air is traveling from the north, suggesting that air from the north is indeed supplying metals associated with nonferrous smelting. However, the receptor modeling in this study has a high degree of uncertainty, and must be used cautiously.

Acid-mine drainage from an abandoned mining district in Colorado contributes indium concentrations 10^4 times higher than natural freshwaters to Mineral Creek, and all of this indium is in the dissolved phase. During an experimental raising of the pH of this system from 3 to >8, essentially all of the indium associates with the particulate phase. Sorption to iron-oxides is thought to be the primary removal mechanism of indium in this system, as evidenced by indium concentrations 40-70% higher in Fe-oxides collected after the pH modification than in those collected before the experiment. This is supported by modeling done by USGS researchers of the behavior of other metals in the system.

7.1 Future work

This work is only the beginning of an important characterization of the behavior and environmental cycling of indium. Future work could include the collection of air samples to compare present-day indium concentrations to those from 1995, and a survey of bogs, sediments, ice cores, corals, or other historical archives that span longer time periods and encompass a variety of geographical locations. More data can confirm trends that we have seen in this work, and variation in time and space may lead to insights on the source of indium to these samples.

It would be particularly useful to be able to better constrain the sources of indium to the environment. Measuring a larger number and variety of metals in the air samples

and peat samples discussed may help to constrain these sources. For example, further information about concentrations and fluxes of vanadium, a tracer for oil combustion, or selenium, a tracer for coal combustion, may shed light on how much these sources influence indium concentrations. A wider variety of metal concentrations may also be helpful in future attempts at receptor modeling. Additionally, isotopes can be instrumental in source tracking, as shown by Sturges & Barrie (discussed in Chapter 5). These authors used changes in Pb isotope ratios as a marker of the influence of smelter emissions, and showed that indium concentrations correlated with these Pb isotope changes. Therefore future work to analyze lead isotopes in air and peat samples may prove useful for more definitive source-tracking. Additionally, indium has two isotopes, ^{113}In and ^{115}In. The natural variation and fractionation of these isotopes is unknown, and future studies of the indium isotope system may prove useful for source tracking.

There is much work left to be done to characterize industrial emissions of indium. This may include a more detailed measurement of source emissions, particularly of nonferrous smelters. If access is possible, there would be great utility in a mass balance study of indium in smelting operations - what are the concentrations in the ore being smelted, what is the partitioning of indium during the smelting process, and how much indium is recovered or found in tailings, emissions, or fly ash collected by emissions controls? A mass balance of indium leaching from tailings piles would also be useful for understanding the releases of indium to aqueous systems from both active and abandoned mining and smelting operations. Lastly, investigation of the flow of indium through semiconductor manufacture and processing will be important for understanding the future releases of indium to the environment, as its use continues to increase in semiconductors and electronics.

The aqueous behavior of indium is poorly understood, and laboratory studies of indium's complexation and absorption would lead to a better understanding of its behavior, and the ability to model this behavior in natural systems.

A significant outstanding question is whether humans and other organisms are being exposed to significant levels of indium, and what the impacts of this exposure are. Future work may focus on exposure assessments for indium, determination of blood indium levels in the general population as compared with populations living near suspected sources such as smelters and how these body burdens have changed over time, or more detailed work on the effects of chronic exposure to environmentally-relevant levels of indium. This work can

be complemented by similar work in other organisms.

Lastly, an expansion of this work to other emerging metal contaminants is called for, as more and more elements of the periodic table are employed in industry without sufficient knowledge of their environmental behavior or impacts. The quest should continue to be able to predict the impacts of these metals. The determination of how industrial fluxes influence natural fluxes may have great utility in helping with this prediction, particularly if care is taken to understand the speciation of these metals and how this speciation affects transport and exposure. In order for detrimental effects to be prevented, this screening process must be rapid and accurate.

Appendix A

Electrochemical Technique for the Separation of Indium from Aqueous Samples

Authors: Laurie Kellndorfer, Sarah Jane O. White, Mansooreh Dehghani, Harold F. Hemond

A.1 Motivation & Objectives

Indium exists at extremely low concentrations (picomolar or about 0.1 ng/kg) in natural waters [White and Hemond, 2012]. The most sensitive analytical technique presently available to measure indium is Inductively-Coupled Plasma-Mass Spectrometry (ICP-MS), which has detection limits on the order of 10 ng/kg, 100 times higher than needed for these measurements.

Therefore, natural water samples must be pre-concentrated in order to be within a detectable range. Additionally, pre-concentration is important for removing other ions and dissolved organic matter, which can interfere with many analyses [White and Hemond, 2012]. The most common interferents for ICP-MS work are ^{113}Cd and $^{97}Mo^{16}O^{+}$ at Indium-113, and ^{115}Sn at Indium-115. For Graphite Furnace Atomic Absorption Spectrophotometry (GFAA), another sensitive analytical technique for trace metals, high salt concentrations are problematic, and sulfides have been implicated as interferents [White and Hemond, 2012]. For all analytical techniques, organic matter can interfere.

As discussed in White and Hemond [2012] and Chapter 2, preconcentration has been carried out in three main ways: (1) solvent extraction [e.g. Alibo et al., 1998]; (2) ion-exchange [e.g. Matthews and Riley, 1970a,b, Orians and Boyle, 1993, Tuzen and Soylak, 2006]; and (3) coprecipitation [e.g. Ueda and Mizui, 1988, Minamisawa et al., 2003].

The most widely-used concentration technique for environmental samples has been a solvent extraction technique that consists of chelation by HDEHP (bis(2-ethylhexyl) hydrogen phosphate) and H_2MEHP (2-ethylhexyl dihydrogen phosphate), extraction into heptane, then back extraction with HCl [Alibo et al., 1998]. Also used are ion-exchange schemes, including cation exchange using 8-hydroxyquinoline [e.g. Orians and Boyle, 1993, Mohammad et al., 1993] or Chelex-100 [e.g. Orians and Boyle, 1993], and anion exchange at either high pH [e.g. Chow and Snyder, 1969] or high chloride concentration [e.g. Matthews and Riley, 1970a]. Coprecipitation is less widely-used, but schemes such as precipitation with hafnium-hydroxide [Ueda and Mizui, 1988] or chitosan [Minamisawa et al., 2003] have been employed.

However, work in our laboratory with the solvent extraction technique of Alibo et al. [1998] and cation exchange using Chelex-100 has failed to achieve consistent recovery of indium from standards. This inconsistent recovery may be possible to overcome by use of isotope dilution with ^{113}In, for example, but the techniques must be tested further to determine whether they are selective enough to remove only indium, leaving behind interferents such as cadmium and tin.

A.2 Objectives

We have investigated electrochemistry as a consistent, simple method for pre-concentrating indium from solution and selectively separating it from other matrix constituents. In electrolysis, direct current flows through an ionic solution, supplying electrons that drive oxidation-reduction reactions within the solution. The current is usually supplied by an electropotential between two electrodes connected to a power supply and placed into the solution. In this electrochemical set-up, electrons flow through the cell in one direction, such that one electrode, called the cathode, supplies electrons, and the other electrode, or the anode, receives electrons and negatively charged particles. Oxidation of molecules within solution occurs on the anode and reduction occurs on the cathode, where electrons are in

excess.

Electrolytic refining has long been employed in metallurgical processes to purify indium metal [e.g. Alfantazi and Moskalyk, 2003, Zhou et al., 2004, 2005]. Indium has also been deposited electrolytically to make bearings [Walsh and Gabe, 1978] and semiconductors [Ho and Yen, 2006]. There have also been electrolytic techniques developed in order to measure indium analytically, albeit for concentrations well above those in natural waters [Kollock and Smith, 1910, Jaya et al., 1987, Sayun and Tsyb, 1959]. Electrodeposition has also been employed for other trace metal analytical work, for example, the plating of ^{226}Rn on steel disks for alpha counting for the dating of geologic materials [Benoit and Hemond, 1988].

Thus an electrolysis system has promise for use as a preconcentration technique for the analytical measurement of indium. Here we describe efforts to deposit indium on a cathode using a simple setup in lab, redissolve the indium into clean acid, and then analyze this clean solution using a graphite furnace atomic absorption spectrophotometer (GFAA). We present our efforts to optimize the deposition of indium on the cathode by varying the electrode material, voltage, current, and time duration of deposition, and our efforts to recover the deposited indium.

A.3 Experiments

The general setup for these electrochemical experiments consists of an electrochemical cell made up of a glass beaker with an indium solution in 2%HNO_3, with two electrodes (Figure A-1).

Alligator clips are connected to the electrodes, and the other end, bare wire, is screwed onto the power supply, to the 6+ connection and the COM connection. To keep electrodes from touching each other or the glass beaker during experiments, a piece of foam board with two slits for the electrodes was placed on top of the beaker. The electrodes were inserted into the slits, and positioned such that the alligator clips held them above the bottom of the beaker.

The standard reduction potential, E, for $In^{3+} + 3\ e = In$, is -0.3382 V [Deis, 2009]. The standard reduction potential for two important interferents, Cd^{2+} and Sn^{2+} are -0.4030 V and -0.1375 V, respectively [Deis, 2009].

Each experiment used 40 mL of a starting solution of 100 ppb In in 2% HNO_3. This

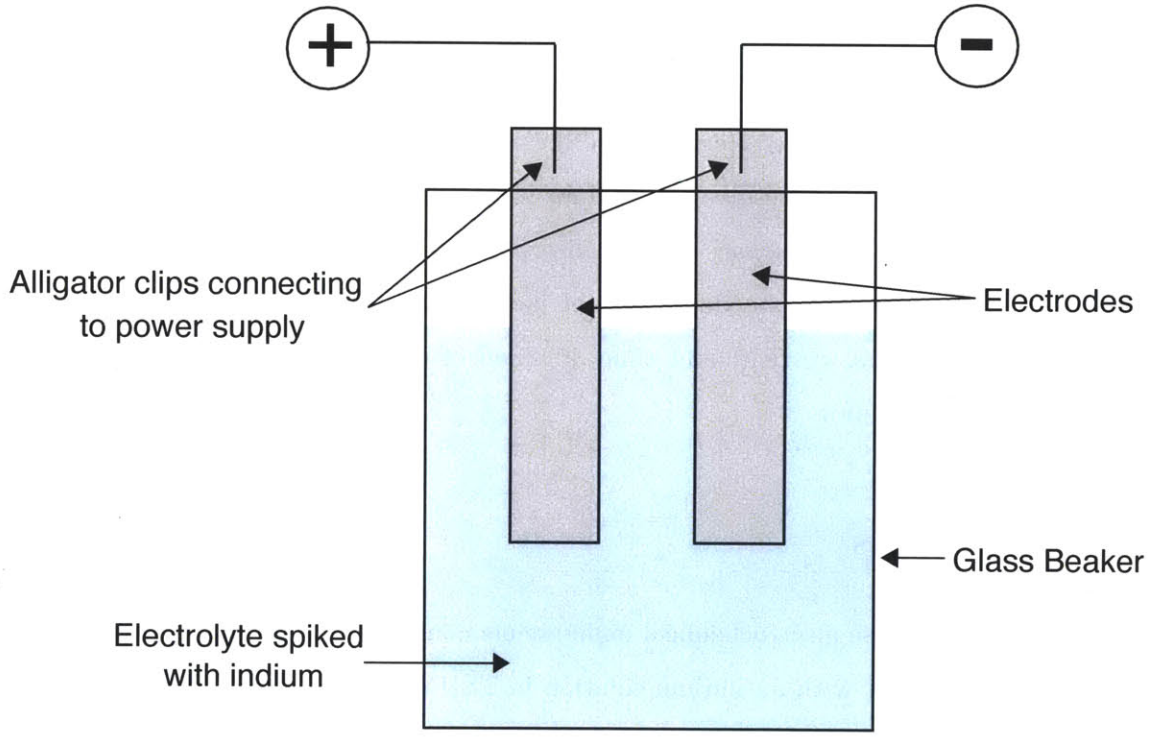

Figure A-1: Experimental setup for the electrochemical separation of indium from aqueous solution.

indium concentration was chosen to be easily measured using the GFAA, which has a detection limit of ~5 ppb indium. This starting concentration additionally allowed for the detection of losses of indium from solution up to 95%. The optimization of electrode material, current, voltage, and time of deposition are discussed subsequently.

During experiments, ~1 mm diameter bubbles rising from the anode were an indication of oxygen gas generation. This was confirmed by measurement of dissolved oxygen before and after experiments; oxygen concentrations began at saturation before applying current to the solution, and ended at higher than the oxygen probe maximum reading post-experiment. Additionally, if the voltage applied was 4.0 V or higher, bubbling also occurred at the cathode, indicating hydrogen gas generation. Lastly, many of the experiments in which stainless steel electrodes were used were accompanied by a warming of the solution and a color change from clear to light yellow. This color change may indicate oxidation and subsequent dissolution of the electrode material, perhaps chromium.

A.4 Graphite Furnace

Indium analyses were performed on samples using a PerkinElmer 4100-ZL Graphite Furnace Atomic Absorption Spectrophotometer (GFAA). An indium source lamp was used, and absorption at 325.6 nm with a slit width of 0.7 nm was measured. This instrument employs a Zeeman correction to correct for non-specific absorption by atoms other than the analyte of interest. A matrix modifier (0.005 mg Pd and 0.003 mg $Mg(NO_3)_2$ was used to assure uniform volatilization of indium at the atomization temperature of 2100°C. Standard curves with indium in 2% HNO_3 provided a benchmark detection limit of ~5 μg/L, and were linear up to 300 ppb. Integrated peak areas (PA) were measured for each sample and quantified with a six-point standard curve, which was run at several points during each GFAA run. The indium removed from solution was calculated by subtracting the concentration of indium left in solution after the experiment from the starting indium concentration of 100 ppb.

Blanks were run along with each experiment by placing 2% HNO_3 without indium into a second experimental setup and applying voltage. These blanks showed no detectable indium contamination. Controls run with 100 ppb indium but no voltage applied showed no detectable indium removal.

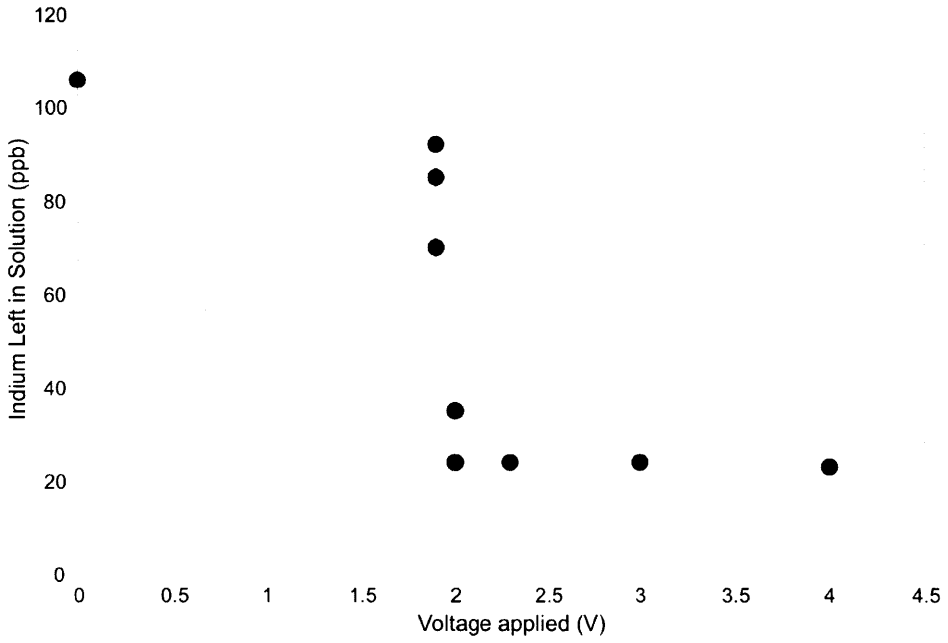

Figure A-2: Indium removal is close to its maximum at 2 V.

A.5 Optimizing Electrode Material, Current, Voltage, and Time

Stainless steel was used for most of the experiments due to its ease of use – it is cheap, easy to cut, and does not degrade in 2% HNO_3. Glassy graphite was tested, but it disintegrated when voltage was applied. Copper was also tested as an electrode material, but it corroded during the experiments and supplied a large background signal to the GFAA analyses. The electrolyte became bright blue during experiments with copper electrodes, and between 19-54% of the indium was removed from solution.

The optimal voltage was found to be 2.0–2.5 V, which resulted in an optimal current of 0.4–0.5 A (Figure A-2). The optimal deposition time was 30 min (Figure A-3). With stainless steel electrodes, and this voltage, current, and duration of time, up to 76% of indium could be removed from solution.

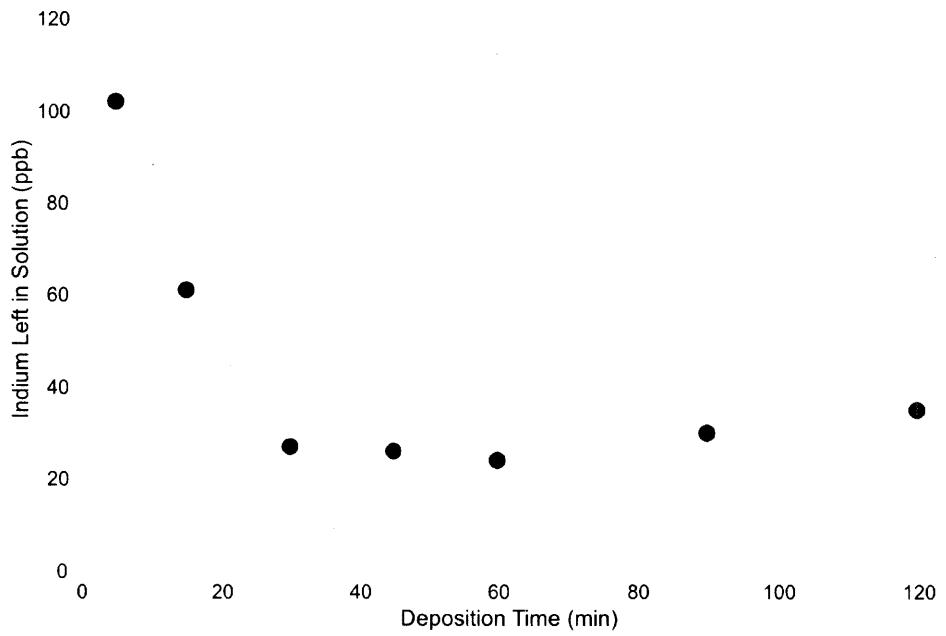

Figure A-3: Indium removal is close to its maximum by 30 minutes of deposition time.

A.6 Indium Recovery from Electrodes

In order to recover the deposited indium from stainless steel electrodes, the electrodes were soaked in 10% HNO_3 overnight to dissolve any deposited indium. This acid was then diluted to 2% HNO_3 and analyzed by GFAA. No indium was recovered from these electrodes. Dissolution using 70% HNO_3 overnight was also unsuccessful. After soaking, the acid was evaporated on a hotplate and indium was resuspended in 2% HNO_3. The solution was allowed to sit for one hour, mixed, then analyzed by GFAA. Again no indium was recovered.

Next, we attempted to reverse the direction of the current in the electrochemical cell to re-oxidize deposited indium to dissolved In^{3+}. In some cases, electrodes that had previously been run were set up to run in reverse in the electrochemical cell. In other cases, the forward experiment was immediately followed by a reversal of the current direction by reversing the leads. This type of experiment was repeated 11 times: detectable indium was recovered only one of those times, when 14% of the deposited indium was seen in solution.

Copper electrodes were re-tested, to determine whether the electrode material contributed to the poor indium recovery from the electrodes, perhaps to a chemical reaction

that formed highly stable, insoluble indium species. Soaking four copper electrodes that had been used for indium deposition in 2% or 10% HNO_3 resulted in at most a 10% recovery of the deposited indium. In addition, these solutions had a high background for the GFAA analysis. Stronger HNO_3 could not be used due to violent reaction upon contact with the copper electrodes; the solution rapidly bubbled, produced thick, brown NO_2 gas, and dissolved the electrode.

Experiments with higher concentrations of indium in the starting solution (as high as 10 ppm) were conducted in order to increase the likelihood of recovery, assuming a larger mass of indium deposited on the electrode. However, the deposition of indium in this experiment required a higher voltage and current (5 V and 2 A) for deposition to occur, and only resulted in a 10% removal of indium from solution. The mass of indium deposited was an order of magnitude larger than previous experiments despite the small relative removal, but recovery remained low, at about 1% of the deposited indium after soaking in concentrated nitric acid.

A.7 Indium Mass Balance

It is unclear why indium cannot be recovered from stainless steel or copper electrodes, either by soaking in nitric acid or by reversing the current of the electrochemical cell. The blanks discussed previously confirmed that indium was not adsorbing to the beaker walls, nor leaving solution unless a voltage was applied. In order to confirm that indium was being deposited on the cathode, the electrodes were analyzed with scanning electron microscopy and associated electron microprobe.

A.7.1 Confirming indium deposition on electrodes

To confirm that indium had been deposited on the cathodes during these experiments, a set of cathodes, anodes, and standards were analyzed qualitatively using a JEOL JXA-8200 WD/ED Combined Microanalyzer in the MIT Electron Microprobe Facility in the Department of Earth, Atmospheric and Planetary Sciences. Standards were made by evaporating a drop of indium solution on a piece of stainless steel on a hotplate. Interestingly, as the solution evaporated, the liquid formed a ring marking the diameter of the drop of original solution, depositing indium along the perimeter but not in the center. Based on this geom-

etry, ~50 g/cm^2 was deposited; this could easily be detected by the electron microprobe. However, no indium was detected on the experimental samples. This may simply be due to the expected 0.4 g/cm^2 indium deposited being below the instrument detection limits. More carefully made standards will be necessary to determine the instrumental detection limits for these electrodes.

Additionally, the electrodes from the high-indium experiments have not been analyzed by electron microprobe, but may be useful in determining whether indium is deposited on the cathode during these electrochemical experiments.

A.8 Generation of volatile indium?

If indium is not deposited on the cathode during these experiments, there is a possibility that it is volatilized and escapes to the atmosphere. Indium hydrides may exist as a gaseous species at low pH and low electropotential [Pourbaix, 1966], and hydride generation has been used to separate indium from solution previously [Busheina and Headridge, 1982, Yan et al., 1984, Castillo et al., 1988, Liao and Li, 1993, Matusiewicz and Krawczyk, 2007].

Work has begun in our lab to test for volatile indium species by running the electrochemical experiment in a closed system, with an airtight cap and an outlet for gases to be piped into the graphite furnace directly (Figure A-4). However, experiments thus far have produced peaks that are due to liquid from the experiment being able to travel to the graphite furnace along with the gases. The setup must therefore be modified to allow only gases to be transported, in order to determine whether volatile indium species are being formed.

The setup for hydride analysis is modeled after the hydride generation by Liao and Li [1993]. A small polypropylene sample bottle with an airtight cap is used. Four holes are drilled into the cap: two for wire leads connecting the electrodes to the power supply; one for a Teflon tube for argon inflow; and one for a fused silica tube for argon outflow. Epoxy holds the fused silica tube in place and forms an airtight seal. The Teflon tube and wires fit tightly such that epoxy is not necessary to prevent gas leaks. During an experiment, argon flows in through the teflon tube, and out through the silica tube, which is placed inside the sample injection hole in the graphite tube. Indium hydrides carried by this inert gas decompose in the graphite tube, which has been coated with a palladium and magnesium

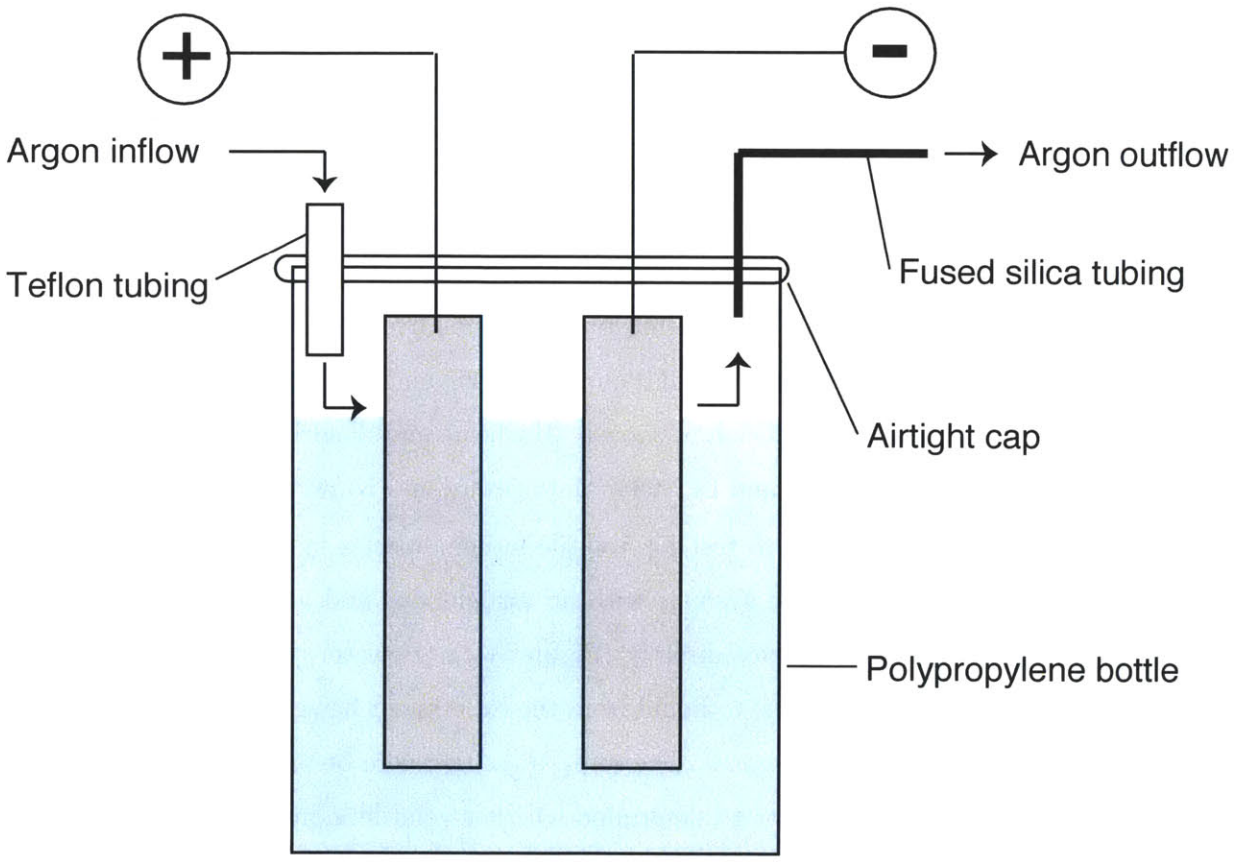

Figure A-4: Experimental setup for determination of the production of volatile indium species.

matrix modifier and heated to 360°C during injection (15 min).

A.9 Conclusions and Future Work

Using electrochemical techniques, indium can be removed from aqueous solution. The use of stainless steel electrodes, 2–2.5 V, 0.4–0.5 A, and a 30 min deposition time removed up to 76% of the mass from a 40 mL solution of 100 ppb indium in 2% HNO_3.

In order to then measure the mass of indium removed from solution, the deposited indium must be recovered from the cathode. A variety of techniques, including soaking the cathode in 2% and concentrated nitric acid, and reversing the direction of current in the electrochemical cell, failed to recover the indium from the cathode. It is unclear whether this failure is due to the deposited indium not redissolving under the conditions tested, or due to indium not being deposited on the electrode, perhaps due to volatilization.

Further experiments will focus on determining where the indium in solution has partitioned. More uniformly deposited standards can be prepared for the electron microprobe, in order to determine the true detection limits of the technique. At the same time, the mass of indium analyzed can be increased by analyzing electrodes from experiments with a higher starting concentration of indium. Additionally, more sensitive analytical techniques such as neutron activation analysis could be employed.

Further experiments to determine whether indium is being volatilized during these experiments will be key for understanding indium's behavior. The present setup for measuring volatile indium species must be modified to eliminate the transport of liquid to the graphite furnace. This could be accomplished through the addition of a condensation chamber—perhaps the simple addition of a wide piece of tubing prior to the silica tube. Additionally, since the technique of piping volatile indium through a silica tube into a graphite furnace is not well-tested, positive and negative controls must be carefully planned to assure that any volatile indium species created are actually able to travel through the silica tube, stick to the graphite tube, and subsequently be analyzed.

A.10 Acknowledgments

We gratefully acknowledge the assistance of Neil Chatterjee with the microprobe work. Funding was provided by NSF Grant CBET-0853866 and an MIT Earth Systems Initiative

Ignition Grant. Additional support was provided by an MIT Earth Systems Initiative Linden Graduate Fellowship and an MIT Energy Initiative Martin Family Graduate Fellowship for Sustainability to S.J.W., by MIT's Undergraduate Research Opportunities Program to L.K., and by the William E. Leonhard Professorship to H.F.H.

Bibliography

O. Acar, A. R. Turker, and Z. Kilic. Direct determination of bismuth, indium and lead in sea water by zeeman ETAAS using molybdenum containing chemical modifiers. *Talanta*, 49(1):135–142, 1999.

O. Acar, A. R. Turker, and Z. Kilic. Determination of bismuth, indium and lead in spiked sea water by electrothermal atomic absorption spectrometry using tungsten containing chemical modifiers. *Spectrochimica Acta Part B-Atomic Spectroscopy*, 55(10):1635–1641, 2000.

R. H. Adamson, G. P. Canellos, and S. M. Sieber. Studies on antitumor activity of gallium nitrate (NSC-15200) and other group IIIa metal-salts. *Cancer Chemotherapy Reports Part 1*, 59(3):599–610, 1975.

A. M. Alfantazi and R. R. Moskalyk. Processing of indium: a review. *Minerals Engineering*, 16(8):687–694, 2003.

D. S. Alibo, H. Amakawa, and Y. Nozaki. Determination of indium in natural waters by flow injection inductively coupled plasma mass spectrometry. *Proceedings of the Indian Academy of Sciences-Earth and Planetary Sciences*, 107(4):359–366, 1998.

D. S. Alibo, Y. Nozaki, and C. Jeandel. Indium and yttrium in north Atlantic and Mediterranean waters: Comparison to the Pacific data. *Geochimica et Cosmochimica Acta*, 63(13-14):1991–1999, 1999.

H. Amakawa, D. S. Alibo, and Y. Nozaki. Indium concentration in Pacific seawater. *Geophysical Research Letters*, 23(18):2473–2476, 1996.

American Conference of Governmental Industrial Hygienists. *2007 TLVs and BEIs: based on the documentation of the threshold limit values for chemical substances and physical*

agents & biological exposure indices. Paper presented at the American Conference of Governmental Industrial Hygienists, Cincinnati, Ohio, 2007.

M. R. Ames, G. Gullu, J. Beal, and I. Olmez. Receptor modeling for elemental source contributions to fine aerosols in New York State. *Journal of the Air & Waste Management Association*, 50(5):881–887, 2000.

Anonymous. Solar-cell efficiency reaches more than 40%, *Chemical and Engineering News*, 86, pg. 26, August 18 2008.

P. G. Appleby. *Chronostratigraphic Techniques in Recent Sediments*, pages 171–203. Tracking Environmental Change Using Lake Sediments, Volume 1: Basin Analysis, Coring, and Chronological Techniques. Kluwer Academic Publishers, Dordrecht, The Netherlands, 2001.

P. G. Appleby and F. Oldfield. The calculation of lead-210 dates assuming a constant rate of supply of unsupported ^{210}Pb to the sediment. *Catena*, 5:1–8, 1978.

P. G. Appleby, P. J. Nolan, F. Oldfield, N. Richardson, and S. R. Higgitt. Pb-210 dating of lake-sediments and ombrotrophic peats by gamma-essay. *Science of the Total Environment*, 69:157–177, 1988.

Y. Avnimelech, G. Ritvo, LE Meijer, and M. Kochba. Water content, organic carbon and dry bulk density in flooded sediments. *Aquacultural Engineering*, 25(1):25–33, 2001.

K. K. Banger. Indium: Organometallic chemistry. *Encyclopedia of Inorganic Chemistry*, pages 1–49, John Wiley & Sons,2006.

M. Baskaran. Po-210 and Pb-210 as atmospheric tracers and global atmospheric Pb-210 fallout: A review. *Journal of Environmental Radioactivity*, 102(12):501-513, 2011.

M. Bau and P. Dulski. Anthropogenic origin of positive gadolinium anomalies in river waters. *Earth and Planetary Science Letters*, 143(1-4):245–255, 1996.

G. Benoit and HF Hemond. Improved methods for the measurement of Po-210, Pb-210, and Ra-226. *Limnology and Oceanography*, 33(6):1618–1622, 1988.

S. R. Biegalski, S. Landsberger, and R. M. Hoff. Source-receptor modeling using trace metals in aerosols collected at three rural canadian great lakes sampling stations. *Journal of the Air & Waste Management Association*, 48(3):227–237, 1998.

C. Blaise, F. Gagne, J. F. Ferard, and P. Eullaffroy. Ecotoxicity of selected nano-materials to aquatic organisms. *Environmental Toxicology*, 23(5):591–598, 2008.

M. E. Blazka, D. Dixon, E. Haskins, and G. J. Rosenthal. Pulmonary toxicity to intratracheally administered indium trichloride in Fischer 344 rats. *Fundamental and Applied Toxicology,*, 22(2):231–239, 1994a.

M. E. Blazka, J. S. Tepper, D. Dixon, D. W. Winsett, R. W. Oconnor, and M. I. Luster. Pulmonary response of Fischer 344 rats to acute nose-only inhalation of indium trichloride. *Environmental Research,*, 67(1):68–83, 1994b.

C. Bodsworth. *The extraction and refining of metals.* CRC Press, Boca Raton, Fla., 1994.

A. Boughriet, N. Proix, G. Billon, P. Recourt, and B. Ouddane. Environmental impacts of heavy metal discharges from a smelter in Deule-Canal sediments (northern France): Concentration levels and chemical fractionation. *Water Air and Soil Pollution*, 180 (1-4):83–95, 2007.

P. H. Briggs. The determination of forty elements in geological and botanical samples by inductively coupled plasma-atomic emission spectrometry, *In* Taggart, J.E., ed., *Analytical Methods for Chemical Analysis of Geologic and Other Materials.* U.S. Geological Survey Open-File Report 02-223, Chapter G, 18 p., 2002.

P. H. Briggs and A. L. Meier. The determination of forty-two elements in geolocial materials by inductively coupled plasma-mass spectrometry, *In* Taggart, J.E., ed., *Analytical Methods for Chemical Analysis of Geologic and Other Materials.* U.S. Geological Survey Open-File Report 02-223, Chapter I, 16 p., 2002.

I. S. Busheina and J. B. Headridge. Determination of indium by hydride generation and atomic-absorption spectrometry. *Talanta*, 29(6):519–520, 1982.

J. R. Castillo, J. M. Mir, and M. T. Gomez. Some observations on the determination of indium by atomic-absorption spectrophotometry using the volatile covalent hydride technique. *Microchemical Journal*, 38(3):387–389, 1988.

F. P. Castronovo and H. N. Wagner. Comparative toxicity and pharmacodynamics of ionic indium chloride and hydrated indium oxide. *Journal of Nuclear Medicine*, 14(9): 677–682, 1973.

P. Chakrabarti, F. M. Hatcher, R. C. Blake, P. A. Ladd, and D. A. Blake. Enzyme-immunoassay to determine heavy-metals using antibodies to specific metal-EDTA complexes - optimization and validation of an immunoassay for soluble indium. *Analytical Biochemistry*, 217(1):70–75, 1994.

R. E. Chapin, M. W. Harris, E. S. Hunter, B. J. Davis, B. J. Collins, and A. C. Lockhart. The reproductive and developmental toxicity of indium in the Swiss mouse. *Fundamental and Applied Toxicology*, 27(1):140–148, 1995.

H. W. Chen. Gallium, indium, and arsenic pollution of groundwater from a semiconductor manufacturing area of Taiwan. *Bulletin of Environmental Contamination and Toxicology*, 77(2):289–296, 2006.

H.-W. Chen. Characteristics and risk assessment of trace metals in airborne particulates from a semiconductor industrial area of northern Taiwan. *Fresenius Environmental Bulletin*, 16(10):1288–1294, 2007.

S. Chibowski and J. Zygmunt. The influence of the sorptive properties of organic soils on the migration rate of Cs-137. *Journal of Environmental Radioactivity*, 61(2):213–223, 2002.

T. Chonan, O. Taguchi, and K. Omae. Interstitial pulmonary disorders in indium-processing workers. *European Respiratory Journal*, 29(2):317–324, 2007.

T. J. Chow and C. B. Snyder. Indium content of sea water. *Earth and Planetary Science Letters*, 7:221–223, 1969.

J. M. Cloy, J. G. Farmer, M. C. Graham, A. B. MacKenzie, and G. T. Cook. A comparison of antimony and lead profiles over the past 2500 years in Flanders moss ombrotrophic peat bog, Scotland. *Journal of Environmental Monitoring*, 7(12): 1137–1147, 2005.

J. M. Cloy, J. G. Farmer, M. C. Graham, and A. B. MacKenzie. Retention of As and Sb in ombrotrophic peat bogs: Records of As, Sb, and Pb deposition at four Scottish sites. *Environmental Science & Technology*, 43(6):1756–1762, 2009.

J. M. Cloy, J. G. Farmer, M. C. Graham, and A. B. MacKenzie. Scottish peat bog records of atmospheric vanadium deposition over the past 150 years: comparison with other records and emission trends. *Journal of Environmental Monitoring*, 13(1):58–65, 2011.

E. A. Conner, H. Yamauchi, B. A. Fowler, and M. Akkerman. Biological indicators for monitoring exposure toxicity from III-V semiconductors. *Journal of Exposure Analysis and Environmental Epidemiology*, 3(4):431–440, 1993.

E. A. Conner, H. Yamauchi, and B. A. Fowler. Alterations in the heme biosynthetic-pathway from the III-V semiconductor-metal, indium arsenide (InAs). *Chemico-biological Interactions*, 96(3):273–285, 1995.

C. T. Coulter. EPA-CMB8.2 Users Manual. Technical Report EPA-452/R-04-011, US Environmental Protection Agency, 2004.

R. J. Crawford, I. H. Harding, and D. E. Mainwaring. Adsorption and coprecipitation of single heavy-metal ions onto the hydrated oxides of iron and chromium. *Langmuir*, 9 (11):3050–3056, 1993.

S. P. Cuttle and D. C. Malcolm. Corer for taking undisturbed peat samples. *Plant and Soil*, 51(2):297–300, 1979.

R. Dams and R. Heindrycx. High-volume air sampling system for use with cellulose filters. *Atmospheric Environment*, 7(3):319–322, 1973.

K. David. Intel makes transistor breakthrough using new materials, 2005. Accessed December 3, 2011 at ftp://download.intel.com/technology/silicon/InSb_press_presentation.pdf.

L. F. Deis. *CRC handbook of chemistry and physics (89th edition)*. CRC Press, Cleveland, Ohio, 2009.

P. Sujatha Devi, M. Chatterjee, and D. Ganguli. Indium tin oxide nano-particles through an emulsion technique. *Materials Letters*, 55(4):205–210, 2002.

V. Diadiuk, MIT, Cambridge, MA. Personal communication, 2008.

C. A. DiFrancesco and M. George. Indium statistics, 2004. Accessed February 21, 2006 at http://minerals.usgs.gov/ds/2005/140/.

F. Douay, C. Pruvot, H. Roussel, H. Ciesielski, H. Fourrier, N. Proix, and C. Waterlot. Contamination of urban soils in an area of northern France polluted by dust emissions of two smelters. *Water Air and Soil Pollution*, 188(1-4):247–260, 2008.

R. R. Draxler. HYSPLIT4 user's guide. NOAA Tech Memo ERL ARL-230, NOAA Air Resources Laboratory, Silver Spring, MD, 1999.

R. R. Draxler and G. D. Hess. Description of the HYSPLIT4 modeling system. NOAA Tech. Memo ERL ARL-224, NOAA Air Resources Laboratory, Silver Spring, MD, 24 p., 1997.

R. R. Draxler and G. D. Hess. An overview of the HYSPLIT4 modeling system of trajectories, dispersion, and deposition. *Aust. Metor. Mag.*, 47:295–308, 1998.

R. R. Draxler and G. D. Rolph. HYSPLIT (HYbrid Single-Particle Lagrangian Integrated Trajectory) Model access via NOAA ARL READY Website (http://ready.arl.noaa.gov/HYSPLIT.php). NOAA Air Resources Laboratory, Silver Spring, MD, 2012.

J. Drukenbrod. 1970 - 2011 average annual emissions, all criteria pollutants in MS Excel - October 2011. http://www.epa.gov/ttnchie1/trends/, US Environmental Protection Agency, 2012a.

J. Drukenbrod. PM2.5 filterable and PM10 filterable emissions trends for electric generating utilities for 1970 to 2005 - August 2008. http://www.epa.gov/ttnchie1/trends/, US Environmental Protection Agency, 2012b.

D. A. Dzombak and F. M. M. Morel. *Surface Complexation Modeling: Hydrous Ferric Oxide.* John Wiley & Sons, New York, 1990.

Energy Information Administration. Table 1.1: World consumption of primary energy by energy type and selected country groups. International Energy Annual 2006, Energy Information Administration (EIA), 2008. Accessed May 2009, http://www.eia.doe.gov/iea/

Energy Information Administration. Short-term energy outlook. Energy Information Administration (EIA), May 8, 2012. Accessed May 2012, http://www.eia.gov/forecasts/steo/report/coal.cfm.

Environment Canada. National pollutant release inventory, 2012. Accessed 2012, www.ec.gc.ca/inrp-npri/.

EPA. National air pollutant emission estimates, 1900-1991. EPA Publication EPA-454/R-92-013, Office of Air Quality Planning and Standards, US Environmental Protection Agency, 1992.

EPA. National air pollutant emission trends, 1900-1998. EPA Report EPA-454/R-00-002, Office of Air Quality Planning and Standards, US Environmental Protection Agency, 2000.

EPA. SPECIATE version 4.3, 2011. Accessed 2012, www.epa.gov/ttnchie1/software/speciate/.

EPA. History of PM standards, 2012a. Accessed April 2012, epa.gov/pm/history.html.

EPA. History of the clean air act, 2012b. Accessed April 2012, epa.gov/oar/caa/caa_history.html.

Rhodes Whitmore Fairbridge. *The encyclopedia of geochemistry and environmental sciences*, volume IVA. Van Nostrand Reinhold Co, New York, 1972.

J. G. Farmer, M. C. Graham, C. Yafa, J. M. Cloy, A. J. Freeman, and A. B. MacKenzie. Use of Pb-206/Pb-207 ratios to investigate the surface integrity of peat cores used to study the recent depositional history and geochemical behaviour of inorganic elements in peat bogs. *Global and Planetary Change*, 53(4):240–248, 2006.

A. Finke, A. Kriele, W. Thumm, D. Bieniek, and A. Kettrup. Leaching tests with thin film solar cells based on copper indium diselenide (CIS). *Chemosphere*, 32(8):1633–1641, 1996.

T. M. Florence, G. E. Batley, and Y. J. Farrar. Determination of indium by anodic-stripping voltam-metry - application to natural-waters. *Journal of Electroanalytical Chemistry*, 56(2):301–309, 1974.

B. A. Fowler, E. A. Conner, and H. Yamauchi. Metabolomic and proteomic biomarkers for IIIV semiconductors: Chemical-specific porphyrinurias and proteinurias. *Toxicology and Applied Pharmacology*, 206(2):121–130, 2005.

R. M. Garrels, F. T. Mackenzie, and C. Hunt. *Chemical cycles and the global environment: assessing human influences.* W. Kaufmann, Los Altos, CA, 1975.

F. Geiger, C. A. Busse, and R. I. Loehrke. The vapor-pressure of indium, silver, gallium, copper, tin, and gold between 0.1-bar and 3.0-bar. *International Journal of Thermophysics*, 8(4):425–436, 1987.

S. H. Gilani and Y. Alibhai. Teratogenicity of metals to chick-embryos. *Journal of Toxicology and Environmental Health*, 30(1):23–31, 1990.

N. Givelet, G. Le Roux, A. Cheburkin, B. Chen, J. Frank, ME Goodsite, H. Kempter, M. Krachler, T. Noernberg, N. Rausch, S. Rheinberger, F. Roos-Barraclough, A. Sapkota, C. Scholz, and W. Shotyk. Suggested protocol for collecting, handling and preparing peat cores and peat samples for physical, chemical, mineralogical and isotopic analyses. *Journal of Environmental Monitoring*, 6(5):481–492, 2004.

B. C. Gottschling, R. R. Maronpot, J. R. Hailey, S. Peddada, C. R. Moomaw, J. E. Klaunig, and A. Nyska. The role of oxidative stress in indium phosphide-induced lung carcinogenesis in rats. *Toxicological Sciences*, 64(1):28–40, 2001.

E. Grahn, S. Karlsson, U. Karlsson, and A. Duker. Historical pollution of seldom monitored trace elements in sweden - part b: Sediment analysis of silver, antimony, thallium and indium. *Journal of Environmental Monitoring*, 8(7):732–744, 2006.

J. R. Graney, A. N. Halliday, G. J. Keeler, J. O. Nriagu, J. A. Robbins, and S. A. Norton. Isotopic record of lead pollution in lake-sediments from the northeastern United-States. *Geochimica et Cosmochimica Acta*, 59(9):1715–1728, 1995.

R. R. Greenberg. A study of trace elements emitted on particles from municipal incinerators, 1976. Doctoral dissertation, Environmental Sciences, University of Maryland.

R. R. Greenberg, G. E. Gordon, W. H. Zoller, R. B. Jacko, D. W. Neuendorf, and K. J. Yost. Composition of particles emitted from the Nicosia municipal incinerator. *Environmental Science & Technology*, 12(12):1329–1332, 1978a.

R. R. Greenberg, W. H. Zoller, and G. E. Gordon. Composition and size distributions of particles released in refuse incineration. *Environmental Science & Technology*, 12(5): 566–573, 1978b.

M. B. Griffith, S .B. Norton, L. C. Alexander, A. I. Pollard, and S. D. LeDuc. The effects of mountaintop mines and valley fills on the physicochemical quality of stream ecosystems in the central appalachians: A review. *Science of the Total Environment*, 417:1–12, 2012.

T. Hamaguchi, K. Omae, T. Takebayashi, Y. Kikuchi, N. Yoshioka, Y. Nishiwaki, A. Tanaka, M. Hirata, O. Taguchi, and T. Chonan. Exposure to hardly soluble indium compounds in ITO production and recycling plants is a new risk for interstitial lung damage. *Occupational and Environmental Medicine*, 65(1):51–55, 2008.

W. R. Harris and L. Messori. A comparative study of aluminum(III), gallium(III), indium(III), and thallium(III) binding to human serum transferrin. *Coordination Chemistry Reviews*, 228(2):237–262, 2002.

R. Heindryckx and R. Dams. Chemical-analysis of atmospheric aerosols by instrumental neutron-activation. *Progress in Nuclear Energy*, 3(3):219–252, 1979.

H. F. Hemond. Biogeochemistry of Thoreaus Bog, Concord, Massachusetts. *Ecological Monographs*, 50(4):507–526, 1980.

H. F. Hemond. The nitrogen budget of thoreau bog. *Ecology*, 64(1):99–109, 1983.

H. F. Hemond and E. J. Fechner-Levy. *Chemical fate and transport in the environment.* Academic Press, San Diego, CA, 2nd edition, 2000.

H. F. Hemond. Biogeochemistry of a New England *Sphagnum* bog. Ph.D. Dissertation, Civil and Environmental Engineering, Massachusetts Institute of Technology, Cambridge, MA, 1977.

T. Hinkley and A. Matsumoto. Mid-holocene change in types of degassing volcanoes, using indium in Antarctic ice as a tracer of volcanic source type. *Geophysical Research Letters*, 34:L17710, 2007.

T. K. Hinkley and A. Matsumoto. Atmospheric regime of dust and salt through 75,000 years of Taylor Dome ice core: Refinement by measurement of major, minor, and trace metal suites. *Journal of Geophysical Research-Atmospheres*, 106(D16):18487–18493, 2001.

T. K. Hinkley, M. F. Lecloarec, and G. Lambert. Fractionation of families of major, minor, and trace-metals across the melt vapor interface in volcanic exhalations. *Geochimica et Cosmochimica Acta*, 58(15):3255–3263, 1994.

T. K. Hinkley, P. J. Lamothe, S. A. Wilson, D. L. Finnegan, and T. M. Gerlach. Metal emissions from Kilauea, and a suggested revision of the estimated worldwide metal output by quiescent degassing of volcanoes. *Earth and Planetary Science Letters*, 170 (3):315–325, 1999.

W. H. Ho and S. K. Yen. Preparation and characterization of indium oxide film by electrochemical deposition. In *Thin Solid Films; 3rd Asian Conference on Chemical Vapor Deposition*, volume 498, pages 80–84, 2006.

W. Hoffmann. PV solar electricity industry: Market growth and perspective. *Solar Energy Materials and Solar Cells*, 90(18-19):3285–3311, 2006.

S. Homma, A. Miyamoto, S. Sakamoto, K. Kishi, N. Motoi, and K. Yoshimura. Pulmonary fibrosis in an individual occupationally exposed to inhaled indium-tin oxide. *European Respiratory Journal*, 25(1):200–204, 2005.

T. Homma, T. Ueno, K. Sekizawa, A. Tanaka, and M. Hirata. Interstitial pneumonia developed in a worker dealing with particles containing indium-tin oxide. *Journal of Occupational Health*, 45(3):137–139, 2003.

S. L. Huang, K. A. Rahn, and R. Arimoto. Testing and optimizing two factor-analysis techniques on aerosol at narragansett, Rhode Island. *Atmospheric Environment*, 33(14): 2169–2185, 1999.

S. Jaya, T. P. Rao, and G. P. Rao. Trace determination of indium by electrolytic preconcentration and open circuit stripping via localized galvanic cells. *Bulletin of the Chemical Society of Japan*, 60(8):3080–3082, 1987.

D. B. Johnson and K. B. Hallberg. Acid mine drainage remediation options: a review. *Science of the Total Environment*, 338(1-2):3–14, 2005.

J. D. Jorgenson and M. W. George. Indium. U.S. Geological Survey Open-File Report 2004-1300, pg. 1-20, 2005.

P. C. Jowsey. An improved peat sampler. *New Phytologist*, 65(2):245, 1966.

Matthew W. Kanan and Daniel G. Nocera. *In situ* formation of an oxygen-evolving catalyst in neutral water containing phosphate and Co_2^+. *Science*, 321(5892):1072–1075, 2008.

A. E. Kelly, M. K. Reuer, N. F. Goodkin, and E. A. Boyle. Lead concentrations and isotopes in corals and water near Bermuda, 1780-2000. *Earth and Planetary Science Letters*, 283(1-4):93–100, 2009.

T. D. Kelly and G. R. Matos. Historical statistics for mineral and material commodities in the United States: Indium statistics. U.S. Geological Survey Data Series 140, Reston VA: U.S. Geological Survey, 2008a. Retrieved from http://minerals.usgs.gov/ds/2005/140.

T. D. Kelly and G. R. Matos. Historical statistics for mineral and material commodities in the United States: Zinc statistics. U.S. Geological Survey Data Series 140, Reston, VA: U.S. Geological Survey, 2008b. Retrieved from http://minerals.usgs.gov/ds/2005/140.

T. D. Kelly and G. R. Matos. Historical statistics for mineral and material commodities in the United States: Lead statistics. U.S. Geological Survey Data Series 140, Reston, VA: U.S. Geological Survey, 2008c. Retrieved from http://minerals.usgs.gov/ds/2005/140.

B. A. Kimball, R. L. Runkel, K. Walton-Day, and K. E. Bencala. Assessment of metal loads in watersheds affected by acid mine drainage by using tracer injection and synoptic sampling: Cement Creek, Colorado, USA. *Applied Geochemistry*, 17(9): 1183–1207, 2002.

B. A. Kimball, K. Walton-Day, and R. L. Runkel. Quantification of metal loading by tracer injection and synoptic sampling, 1996-2000. Chapter E9, pp. 417-195, of "Integrated investigations of environmental effects of historical mining in the Animas River watershed, San Juan County, Colorado. Professional Paper 1651, Church, SE, von Guerard P, Finger SE (eds). US Geological Survey, 2007.

R. J. Klee and T. E. Graedel. Elemental cycles: A status report on human or natural dominance. *Annual Review of Environment and Resources*, 29:69–107, 2004.

L. G. Kollock and E. F. Smith. The determination of indium with the use of a mercury cathode. *Journal of the American Chemical Society*, 32:1248–1250, 1910.

M. Komarek, V. Ettler, V. Chrastny, and M. Mihaljevic. Lead isotopes in environmental sciences: A review. *Environment International*, 34(4):562–577, 2008.

M. E. Kylander, D. J. Weiss, and B. Kober. Two high resolution terrestrial records of atmospheric Pb deposition from New Brunswick, Canada, and Loch Laxford, Scotland. *Science of the Total Environment*, 407(5):1644–1657, 2009.

J. A. Lee and J. H. Tallis. Regional and historical aspects of lead pollution in Britain. *Nature*, 245(5422):216–218, 1973.

Y. P. Liao and A. M. Li. Indium hydride generation atomic-absorption spectrometry with *in-situ* preconcentration in a graphite-furnace coated with palladium. *Journal of Analytical Atomic Spectrometry*, 8(4):633–636, 1993.

A. L. Lima, B. A. Bergquist, E. A. Boyle, M. K. Reuer, F. O. Dudas, C. M. Reddy, and T. I. Eglinton. High-resolution historical records from Pettaquamscutt river basin sediments: 2. Pb isotopes reveal a potential new stratigraphic marker. *Geochimica et Cosmochimica Acta*, 69(7):1813–1824, 2005.

H. C. Lin and P. P. Hwang. Acute and chronic effects of indium chloride ($InCl_3$) on tilapia (*Oreochromis Mossambicus*) larvae. *Bulletin of environmental contamination and toxicology*, 61(1):123–128, 1998.

W. .P.linak. U.S. Environmental Protection Agency. Personal communication, 2008.

W. P. Linak and C. A. Miller. Comparison of particle size distributions and elemental partitioning from the combustion of pulverized coal and residual fuel oil. *Journal of the Air & Waste Management Association*, 50(8):1532–1544, 2000.

J. R. Loebenstein. The materials flow of arsenic in the United States. Information Circular IC 9382, US Bureau of Mines, US Department of the Interior, 1994.

B. G. Lottermoser. *Mine wastes : characterization, treatment and environmental impacts.* Springer, Berlin; New York, 2nd edition, 2007.

N. S. Macdonald, H. H. Neely, R. A. Wood, J. M. Takahashi, S. I. Wakakuwa, and R. L. Birdsall. Methods for compact cyclotron production of indium-111 for medical use. *International Journal of Applied Radiation and Isotopes*, 26(10):631–633, 1975.

A. B. MacKenzie, S. M. L. Hardie, J. G. Farmer, L. J. Eades, and I. D. Pulford. Analytical and sampling constraints in (210)Pb dating. *Science of the Total Environment*, 409(7):1298–1304, 2011.

W. Maenhaut and W. H. Zoller. Determination of chemical composition of South Pole aerosol by instrumental neutron-activation analysis. *Journal of Radioanalytical Chemistry*, 37(2):637–650, 1977.

A. E. Martell and R. M. Smith. *Critical stability constants*, volume 3: Other organic ligands. Plenum Press, New York, 1977.

A. Matsumoto and T. K. Hinkley. Trace metal suites in Antarctic pre-industrial ice are consistent with emissions from quiescent degassing of volcanoes worldwide. *Earth and Planetary Science Letters*, 186(1):33–43, 2001.

A. D. Matthews and J. P. Riley. The determination of indium in sea water. *Analytica Chimica Acta*, 51:287–294, 1970a.

A. D. Matthews and J. P. Riley. Occurrence of indium in seawater and some marine sediments. *Nature*, 225:1242, 1970b.

H. Matusiewicz and M. Krawczyk. Hydride generation-in situ trapping-flame atomic absorption spectrometry hybridization for indium and thallium determination. *Journal of the Brazilian Chemical Society*, 18(2):304–311, 2007.

T. M. Mighall, J. P. Grattan, S. Timberlake, J. A. Lees, and S. Forsyth. An atmospheric pollution history for lead-zinc mining from the Ystwyth Valley, Dyfed, mid-Wales, UK as recorded by an upland blanket peat. *Geochemistry: Exploration, Environment, Analysis*, 2:175–184, 2002.

H. Minamisawa, K. Murashima, M. Minamisawa, N. Arai, and T. Okutani. Determination of indium by graphite furnace atomic absorption spectrometry after coprecipitation with chitosan. *Analytical Sciences*, 19(3):401–404, 2003.

Minerals and Environment Canada Metals Division, National Office of Pollution Prevention. Multi-pollutant emission reduction analysis foundation (MERAF) for the base metals smelting sector. Final report, Environment Canada, 2002.

H. Mizuguchi, H. Atsumi, K. Hashimoto, Y. Shimada, Y. Kudo, M. Endo, F. Yokota, J. Shida, and T. Yotsuyanagi. Highly sensitive colour change system within slight differences in metal ion concentrations based on homo-binuclear complex formation equilibrium for visual threshold detection of trace metal ions. *Analytica Chimica Acta*, 527(2):131–138, 2004.

B. Mohammad, A. M. Ure, and D. Littlejohn. Online preconcentration of aluminum, gallium and indium with quinolin-8-ol for determination by atomic-absorption spectrometry. *Journal of Analytical Atomic Spectrometry*, 8(2):325–331, 1993.

D. L. Morgan, C. J. Shines, S. P. Jeter, R. E. Wilson, M. P. Elwell, H. C. Price, and P. D. Moskowitz. Acute pulmonary toxicity of copper gallium diselenide, copper indium diselenide, and cadmium telluride intratracheally instilled into rats. *Environmental Research*, 71(1):16–24, 1995.

D. L. Morgan, C. J. Shines, S. P. Jeter, M. E. Blazka, M. R. Elwell, R. E. Wilson, S. M. Ward, H. C. Price, and P. D. Moskowitz. Comparative pulmonary absorption, distribution, and toxicity of copper gallium diselenide, copper indium diselenide, and cadmium telluride in Sprague-Dawley rats. *Toxicology and Applied Pharmacology,*, 147 (2):399–410, 1997.

T. Murata, M. Kanao-Koshikawa, and T. Takamatsu. Effects of Pb, Cu, Sb, In and Ag contamination on the proliferation of soil bacterial colonies, soil dehydrogenase activity,

and phospholipid fatty acid profiles of soil microbial communities. *Water Air and Soil Pollution*, 164(1-4):103–118, 2005.

K. Nakajima, K. Yokoyama, K. Nakano, and T. Nagasaka. Substance flow analysis of indium for flat panel displays in Japan. *Materials Transactions*, 48(9):2365–2369, 2007a.

M. Nakajima, H. Takahashi, M. Sasaki, Y. Kobayashi, T. Awano, D. Irie, K. Sakemi, Y. Ohno, and M. Usami. Developmental toxicity of indium chloride by intravenous or oral administration in rats. *Teratogenesis Carcinogenesis and Mutagenesis*, 18(5): 231–238, 1998.

M. Nakajima, M. Sasaki, Y. Kobayashi, Y. Ohno, and M. Usami. Developmental toxicity of indium in cultured rat embryos. *Teratogenesis Carcinogenesis and Mutagenesis*, 19 (3):205–209, 1999.

M. Nakajima, H. Takahashi, M. Sasaki, Y. Kobayashi, Y. Ohno, and M. Usami. Comparative developmental toxicity study of indium in rats and mice. *Teratogenesis Carcinogenesis and Mutagenesis*, 20(4):219–227, 2000.

M. Nakajima, H. Takahashi, K. Nakazawa, and M. Usami. Fetal cartilage malformation by intravenous administration of indium trichloride to pregnant rats. *Reproductive Toxicology,*, 24(3-4):409–413, 2007b.

M. Nakajima, K. Mitsunaga, K. Nakazawa, and M. Usami. In vivo/in vitro study in rat embryos on indium-caused tail malformations. *Reproductive Toxicology*, 25(4):426–432, 2008.

S. Nakamura, T. Mukai, and M. Senoh. Candela-class high-brightness InGaN/AlGaN double-heterostructure blue-light-emitting diodes. *Applied Physics Letters*, 64(13): 1687–1689, 1994.

M. Nakano, K. Omae, A. Tanaka, M. Hirata, T. Michikawa, Y. Kikuchi, N. Yoshioka, Y. Nishiwakii, and T. Chonan. Causal relationship between indium compound inhalation and effects on the lungs. *Journal of Occupational Health*, 51(6):513–521, 2009.

National Institute of Occupational Safety and Health. *NIOSH recommendations for occupational safety and health: compendium of policy documents and statements (DHHS*

NIOSH Publication No. 92-100). U.S. Dept. of Health and Human Services, Cincinnati, Ohio, 1992. Retrieved from www.cdc.gov/niosh/92-100.html.

G. Norris, R. Vedentham, K. Wade, S. Brown, J. Prouty, and C. Foley. EPA Positive Matrix Factorization (PMF) 3.0 Fundamentals & User Guide. Technical Report EPA 600/R-08/108, US Environmental Protection Agency, 2008. Retrieved from http://www.epa.gov/heasd/products/pmf/pmf.html.

S. A. Norton, T. Wilson, M. Handley, and E. C. Osterberg. Atmospheric deposition of cadmium in the northeastern USA. *Applied Geochemistry*, 22(6):1217–1222, 2007.

M. Novak, L. Zemanova, P. Voldrichova, M. Stepanova, M. Adamova, P. Pacherova, A. Komarek, M. Krachler, and E. Prechova. Experimental evidence for mobility/immobility of metals in peat. *Environmental Science & Technology*, 45(17): 7180–7187, 2011.

Y. Nozaki, D. Lerche, D. S. Alibo, and A. Snidvongs. The estuarine geochemistry of rare earth elements and indium in the Chao Phraya River, Thailand. *Geochimica et Cosmochimica Acta*, 64(23):3983–3994, 2000a.

Y. Nozaki, D. Lerche, D. S. Alibo, and M. Tsutsumi. Dissolved indium and rare earth elements in three Japanese rivers and Tokyo Bay: Evidence for anthropogenic Gd and In. *Geochimica et Cosmochimica Acta*, 64(23):3975–3982, 2000b.

J. O. Nriagu. A history of global metal pollution. *Science*, 272(5259):223–224, 1996.

H. Obata, Y. Nozaki, D. S. Alibo, and Y. Yamamoto. Dissolved Al, In, and Ce in the eastern Indian ocean and the southeast asian seas in comparison with the radionuclides Pb-210 and Po-210. *Geochimica et Cosmochimica Acta*, 68(5):1035–1048, 2004.

H. Obata, D. S. Alibo, and Y. Nozaki. Dissolved aluminum, indium, and cerium in the sea of Japan and the sea of Okhotsk: Comparison to the marginal seas of the western north Pacific. *Journal of Geophysical Research-Oceans*, 112:C12003, 2007.

K. Oda. Toxicity of a low level of indium phosphide (InP) in rats after intratracheal instillation. *Industrial Health*, 35(1):61–68, 1997.

S. Ohkouchi, Y. Nakamura, H. Nakamura, and K. Asakawa. Indium nano-dot arrays formed by field-induced deposition with a nano-jet probe for site-controlled InAs/GaAs quantum dots. *Thin Solid Films*, 464-465:233–236, 2004.

F. Oldfield, P. G. Appleby, R. S. Cambray, J. D. Eakins, K. E. Barber, R. W. Battarbee, G. R. Pearson, and J. M. Williams. Pb-210, Cs-137 and Pu-239 profiles in ombrotrophic peat. *Oikos*, 33(1):40–45, 1979.

C. Olid, J. Garcia-Orellana, A. Martinez-Cortizas, P. Masque, E. Peiteado, and J.-A. Sanchez-Cabeza. Role of surface vegetation in (210)Pb-dating of peat cores. *Environmental Science & Technology*, 42(23):8858–8864, 2008.

I. Olmez, G. Gullu, M. Ames, X. Huang, S. Keskin, J. Che, A. Wakefield, J. K. Gone, and J. Beal. Upstate New York Trace Metals Program, vol. II "Trace Metals". Technical Report MITNRL-064, MIT Nuclear Reactor Laboratory, 1997.

M. Omura, M. Hirata, A. Tanaka, M. G. Zhao, Y. Makita, N. Inoue, K. Gotoh, and N. Ishinishi. Testicular toxicity evaluation of arsenic-containing binary compound semiconductors, gallium arsenide and indium arsenide, in hamsters. *Toxicology Letters*, 89(2):123–129, 1996a.

M. Omura, A. Tanaka, M. Hirata, M. G. Zhao, Y. Makita, N. Inoue, K. Gotoh, and N. Ishinishi. Testicular toxicity of gallium arsenide, indium arsenide, and arsenic oxide in rats by repetitive intratracheal instillation. *Fundamental and Applied Toxicology*, 32 (1):72–78, 1996b.

M. Omura, K. Yamazaki, A. Tanaka, M. Hirata, Y. Makita, and N. Inoue. Changes in the testicular damage caused by indium arsenide and indium phosphide in hamsters during two years after intratracheal instillations. *Journal of Occupational Health*, 42(4): 196–204, 2000.

M. Omura, A. Tanaka, M. Hirata, N. Inoue, T. Ueno, T. Homma, and K. Sekizawa. Testicular toxicity evaluation of indium-tin oxide. *Journal of Occupational Health*, 44 (2):105–107, 2002.

N. Onikura, A. Nakamura, and K. Kishi. Acute toxicity of thallium and indium toward

brackish-water and marine organisms. *Journal of the Faculty of Agriculture Kyushu University*, 53(2):467–469, 2008.

K. J. Orians and E. A. Boyle. Determination of picomolar concentrations of titanium, gallium and indium in sea-water by inductively-coupled plasma-mass spectrometry following an 8-hydroxyquinoline chelating resin preconcentration. *Analytica Chimica Acta*, 282(1):63–74, 1993.

K. J. Orians and K. W. Bruland. Dissolved aluminum in the central north Pacific. *Nature*, 316(6027):427–429, 1985.

P. Paatero and PK Hopke. Discarding or downweighting high-noise variables in factor analytic models. *Analytica Chimica Acta*, 490(1-2):277–289, 2003.

J. M. Pacyna. Emission factors of atmospheric trace elements. *Advances in Environmental Science and Technology*, 17:1–32, 1986.

J. M. Pacyna and E. G. Pacyna. An assessment of global and regional emissions of trace metals to the atmosphere from anthropogenic sources worldwide. *Environmental Reviews*, 9(4):269–298, 2001.

H. Palme and A. Jones. *Solar System Abundances of the Elements.* In H.D. Holland and K.K. Turekian (Eds.), *Treatise on Geochemistry*, (pp. 41–61). Elsevier/Pergamon, Amsterdam, the Netherlands, Boston, 2004.

I. Paolicchi, O. D. Renedo, M. A. A. Lomillo, and M. J. A. Martinez. Application of an optimization procedure in adsorptive stripping voltammetry for the determination of trace contaminant metals in aqueous medium. *Analytica Chimica Acta*, 511(2):223–229, 2004.

D. U. Pedersen, J. L. Durant, B. W. Penman, C. L. Crespi, H. F. Hemond, A. L. Lafleur, and G. R. Cass. Seasonal and spatial variations in human cell mutagenicity of respirable airborne particles in the northeastern United States. *Environmental Science & Technology*, 33(24):4407–4415, 1999.

AV Polissar, PK Hopke, and RL Poirot. Atmospheric aerosol over vermont: Chemical composition and sources. *Environmental Science & Technology*, 35(23):4604–4621, 2001.

Marcel Pourbaix. *Atlas of electrochemical equilibria in aqueous solutions.* Pergamon Press, Oxford, New York, 644 pp, 1966.

W. H. Press, S. A. Teukolsky, W. T. Vetterling, and B. R. Flannery. *Numerical Recipes in C*, 2nd Edition. Cambridge University Press, Cambridge, UK, 1992.

R. C. Ragaini, H. R. Ralston, and N. Roberts. Environmental trace metal contamination in Kellogg, Idaho, near a lead smelting complex. *Environmental Science & Technology*, 11(8):773–781, 1977.

K. A. Rahn and D. H. Lowenthal. Pollution aerosol in the northeast - northeastern-midwestern contributions. *Science*, 228(4697):275–284, 1985.

S. Rauch and H. F. Hemond. Sediment-based evidence of platinum concentration changes in an urban lake near Boston, Massachusetts. *Environmental Science & Technology*, 37 (15):3283–3288, 2003.

S. Rauch, H. F. Hemond, and B. Peucker-Ehrenbrink. Source characterisation of atmospheric platinum group element deposition into an ombrotrophic peat bog. *Journal of Environmental Monitoring*, 6(4):335–343, 2004.

A. Reff, P. V. Bhave, H. Simon, T. G. Pace, G. A. Pouliot, J. D. Mobley, and M. Houyoux. Emissions inventory of PM(2.5) trace elements across the United States. *Environmental Science & Technology*, 43(15):5790–5796, 2009.

M. K. Reuer, E. A. Boyle, and B. C. Grant. Lead isotope analysis of marine carbonates and seawater by multiple collector ICP-MS. *Chemical Geology*, 200(1-2):137–153, 2003.

J. B. T. Rocha, S. M. Tuerlinckx, M. R. C. Schetinger, and V. Folmer. Effect of group 13 metals on porphobilinogen synthase *in vitro*. *Toxicology and Applied Pharmacology*, 200 (3):169–176, 2004.

I. Roelandts and E. S. Gladney. Consensus values for NIST biological and environmental standard reference materials. In *Fresenius Journal of Analytical Chemistry; 7th International Symposium on Biological and Environmental Reference Materials (BERM-7)*, volume 360, pages 327–338, 1998.

G. D. Rolph. Real-time Environmental Applications and Display sYstem (READY) website (http://ready.arl.noaa.gov). NOAA Air Resources Laboratory, Silver Spring, MD, 2012.

R. L. Rudnick and S. Gao. *Composition of the Continental Crust*, volume 3 of *Treatise on Geochemistry*, chapter 3.01, pages 1–64. Elsevier/Pergamon, Amsterdam ; Boston, 1st edition, 2004.

R. L. Runkel and B. A. Kimball. Evaluating remedial alternatives for an acid mine drainage stream: Application of a reactive transport model. *Environmental Science & Technology*, 36(5):1093–1101, 2002.

R. L. Runkel, K. E. Bencala, B. A. Kimball, K. Walton-Day, and P. L. Verplanck. A comparison of pre- and post-remediation water quality, Mineral Creek, Colorado. *Hydrological Processes*, 23(23):3319–3333, 2009a.

R. L. Runkel, B. A. Kimball, J. I. Steiger, and K. Walton-Day. Geochemical data for upper Mineral Creek, Colorado, under existing ambient conditions and during and experimental pH modification, August 2005. U.S. Geological Survey Data Series 442, U.S. Geological Survey, 2009b.

R. L. Runkel, B. A. Kimball, K. Walton-Day, P. L. Verplanck, and R. E. Broshears. Evaluating remedial alternatives for an acid mine drainage stream: A model post audit. *Environmental Science & Technology*, 46(1):340–347, 2012.

L. G. Salmon, G. R. Cass, D. U. Pedersen, J. L. Durant, R. Gibb, A. Lunts, and M. Utell. Determination of fine particle and coarse particle concentration and chemical composition in the northeastern United States, 1995. Technical Report Report to the Northeast States for Coordinated Air Use Management (NESCAUM), 1999.

M. G. Sayun and P. P. Tsyb. The electrolytic separation of indium, thallium, zinc, and cadmium, and their determination on a single sample. *Industrial Laboratory*, 25(7): 819–821, 1959.

L. A. Schaider, D. B. Senn, D. J. Brabander, K. D. McCarthy, and J. P. Shine. Characterization of zinc, lead, and cadmium in mine waste: Implications for transport,

exposure, and bioavailability. *Environmental Science & Technology*, 41(11):4164–4171, 2007.

G. Schmalz, D. Arenholt-Bindslev, S. Pfuller, and H. Schweikl. Cytotoxicity of metal cations used in dental cast alloys. *Atla-Alternatives to Laboratory Animals*, 25(3): 323–330, 1997.

X. Q. Shan, Z. M. Ni, and Z. N. Yuan. Determination of indium in minerals, river sediments and coal fly-ash by electrothermal atomic-absorption spectrometry with palladium as a matrix modifier. *Analytica Chimica Acta*, 171:269–277, 1985.

D. M. Shaw. The geochemistry of indium. *Geochimica et Cosmochimica Acta*, 2:185–206, 1952.

W. Shotyk, D. Weiss, P. G. Appleby, A. K. Cheburkin, R. Frei, M. Gloor, J. D. Kramers, S. Reese, and W. O. Van der Knaap. History of atmospheric lead deposition since 12,370 C-14 yr bp from a peat bog, Jura mountains, Switzerland. *Science*, 281(5383): 1635–1640, 1998.

V. Singh, B. Saswat, and S. Kumar. Low temperature deposition of indium tin oxide (ITO) films on plastic substrates. In J.A. Theil, M. Bohm, D.S. Gardner, and T. Blalock, editors, *Materials, Integration and Technology for Monolithic Instruments,* volume 869, pages D2.9.1–D2.9.6, 2005.

I. C. Smith, B. L. Carson, and F. Hoffmeister. *Trace metals in the environment: Volume 5 - Indium.* Ann Arbor Science Publishers, Ann Arbor, Mich., 1978.

X. H. Song, A. V. Polissar, and P. .K Hopke. Sources of fine particle composition in the northeastern US. *Atmospheric Environment*, 35(31):5277–5286, 2001.

H. M. Spliethoff and H. F. Hemond. History of toxic metal discharge to surface waters of the Aberjona watershed. *Environmental Science & Technology*, 30(1):121–128, 1996.

E. Steinnes, T. Berg, and T. E. Sjobakk. Temporal trends in long-range atmospheric transport of heavy metals to Norway. *Journal De Physique IV*, 107:1271–1273, 2003.

T. Sterckeman, F. Douay, N. Proix, H. Fourrier, and E. Perdrix. Assessment of the

contamination of cultivated soils by eighteen trace elements around smelters in the north of France. *Water Air and Soil Pollution*, 135(1-4):173–194, 2002.

W. T. Sturges and L. A. Barrie. The use of stable lead 206/207 isotope ratios and elemental composition to discriminate the origins of lead in aerosols at a rural site in eastern Canada. *Atmospheric Environment*, 23(8):1645–1657, 1989.

A. Tanaka. Toxicity of indium arsenide, gallium arsenide, and aluminium gallium arsenide. *Toxicology and Applied Pharmacology*, 198(3):405–411, 2004.

A. Tanaka, A. Hisanaga, M. Hirata, M. Omura, N. Inoue, and N. Ishinishi. Pulmonary toxicity of indium arsenide and arsenic selenide following repeated intratracheal instillations to the lungs of hamsters. *Applied Organometallic Chemistry*, 8:265–271, 1994.

A. Tanaka, M. Hirata, M. Omura, N. Inoue, T. Ueno, T. Homma, and K. Sekizawa. Pulmonary toxicity of indium-tin oxide and indium phosphide after intratracheal instillations into the lung of hamsters. *Journal of Occupational Health*, 44(2):99–102, 2002.

A. Tanaka, M. Hirata, and M. Omura. Pulmonary squamous cyst induced by exposure to indium arsenide in hamsters. *Journal of Occupational Health*, 45(6):405–407, 2003.

K. H. Thompson and C. Orvig. Boon and bane of metal ions in medicine. *Science*, 300 (5621):936–939, 2003.

H. D. Thoreau. *Journals VI, X, XIII.* The Writing of Henry David Thoreau. Houghton Mifflin, Boston, MA, 1906.

A. C. Tolcin. Indium: Mineral commodity summaries. Reston, VA: US Geological Survey, 2009. Retrieved from http://minerals.usgs.gov/minerals/pubs/commodity/indium/

K. K. Turekian, L. K. Benninger, and E. P. Dion. Be-7 and Pb-210 total deposition fluxes at New Haven, Connecticut and at Bermuda. *Journal of Geophysical Research-Oceans and Atmospheres*, 88(C9):5411–5415, 1983.

M. Tuzen and M. Soylak. A solid phase extraction procedure for indium prior to its

graphite furnace atomic absorption spectrometric determination. *Journal of Hazardous Materials*, 129(1-3):179–185, 2006.

J. Ueda and C. Mizui. Preconcentration of gallium(III) and indium(III) by coprecipitation with hafnium hydroxide for electrothermal atomic-absorption spectrometry. *Analytical Sciences*, 4(4):417–421, 1988.

T. Uemura, K. Oda, K. Omae, T. Takebayashi, T. Nomiyama, C. Ishizuka, K. Hosoda, H. Sakurai, K. Yamazaki, and I. Kabe. Effects of intratracheally administered indium phosphide on male Fischer 344 rats. *Journal of Occupational Health*, 39(3):205–210, 1997.

G. Ungvary, E. Szakmary, E. Tatrai, A. Hudak, M. Naray, and V. Morvai. Embryotoxic and teratogenic effects of indium chloride in rats and rabbits. *Journal of Toxicology and Environmental Health-Part A*, 59(1):27–42, 2000.

G. Ungvary, E. Tatrai, E. Szakmary, and M. Naray. The effect of prenatal indium chloride exposure on chondrogenic ossification. *Journal of Toxicology and Environmental Health-Part A*, 62(5):387–396, 2001.

M. Van Hulle, K. De Cremer, R. Vanholder, and R. Cornelis. *In vivo* distribution and fractionation of indium in rats after subcutaneous and oral administration of [In-114m]InAs. *Journal of Environmental Monitoring*, 7(4):365–370, 2005.

F. C. Walsh and D. R. Gabe. Electrode-reactions during electrodeposition of indium from acid sulfate-solutions. *Surface Technology*, 6(6):425–436, 1978.

E. C. P. Wardenaar. A new hand tool for cutting peat profiles. *Canadian Journal of Botany-Revue Canadienne De Botanique*, 65(8):1772–1773, 1987.

J. G. Watson. Protocol for applying and validating the CMB model for PM2.5 and VOC. Technical Report EPA-451/R-04-001, US Environmental Protection Agency, 2004. Retrieved from http://www.epa.gov/ttn/scram/receptor_cmb.htm.

J. G. Watson, L. W. Anthony Chen, J. C. Chow, P. Doraiswamy, and D. H. Lowenthal. Source apportionment: Findings from the US Supersites program. *Journal of the Air & Waste Management Association*, 58(2):265–288, 2008.

K. H. Wedepohl. The composition of the continental-crust. *Geochimica et Cosmochimica Acta*, 59(7):1217–1232, 1995.

D. J. Weiss, N. Rausch, T. F. D. Mason, B. J. Coles, J. J. Wilkinson, L. Ukonmaanaho, T. Arnold, and T. M. Nieminen. Atmospheric deposition and isotope biogeochemistry of zinc in ombrotrophic peat. *Geochimica et Cosmochimica Acta*, 71(14):3498–3517, 2007.

R. G. Wetzel. *Limnology: lake and river ecosystems.* Academic Press, San Diego, 3rd edition, 2001.

T. Whitaker. LED market ready for accelerated growth in lighting, display backlights, and automotive applications, *LEDs Magazine 5-8*, March 2007.

S. J. O. White and H. F. Hemond. The anthrobiogeochemical cycle of indium: A review of the natural and anthropogenic cycling of indium in the environment. *Critical Reviews in Environmental Science & Technology*, 42:155–186, 2012.

Michael Whitfield and David R. Turner. *The role of particles in regulating the composition of seawater.* In W. Stumm (Ed.), *Aquatic Surface Chemistry: Chemical Processes at the Particle-Water Interface* (pp. 457-493). Wiley Interscience, New York, 1987.

S. A. Wood and I. M. Samson. The aqueous geochemistry of gallium, germanium, indium and scandium. *Ore Geology Reviews*, 28(1):57–102, 2006.

K. Yamazaki, A. Tanaka, M. Hirata, M. Omura, Y. Makita, N. Inoue, K. Sugio, and K. Sugimachi. Long term pulmonary toxicity of indium arsenide and indium phosphide instilled intratracheally in hamsters. *Journal of Occupational Health*, 42(4):169–178, 2000.

D. Yan, Z. Yan, G. S. Cheng, and A. M. Li. Determination of indium and thallium by hydride generation and atomic-absorption spectrometry. *Talanta*, 31(2):133–134, 1984.

T. Yeakley. Texas Instruments, Dallas, TX, personal communication, 2009.

W. Yi, A. N. Halliday, D. C. Lee, and J. N. Christensen. Indium and tin in basalts, sulfides, and the mantle. *Geochimica et Cosmochimica Acta*, 59(24):5081–5090, 1995.

P. Zamora. MIT, Cambridge, MA, personal communication, 2008.

J. Zhou. Indium tin oxide (ITO) deposition, patterning, and Schottky contact fabrication, 2005. Master's thesis, Microelectronic Engineering, Rochester Institute of Technology.

Z. H. Zhou, H. B. Mo, and D. M. Zeng. Preparation of high-purity indium by electrorefining. *Transactions of Nonferrous Metals Society of China*, 14(3):637–640, 2004.

Z. H. Zhou, J. M. Ruan, and H. B. Mo. Preparation of 6N high-purity indium by method of physical-chemical purification and electrorefining. *Journal of Materials Science*, 40 (24):6529–6533, 2005.

J. L. Zurita, A. Jos, A. del Peso, M. Salguero, A. M. Camean, M. Lopez-Artiguez, and G. Repetto. Toxicological assessment of indium nitrate on aquatic organisms and investigation of the effects on the PLHC-1 fish cell line. *Science of the Total Environment*, 387(1-3):155–165, 2007.